AD-A039 814 AIR FORCE FLIGHT DYNAMICS LAB WRIGHT-PATTERSON AFB OHIO F/G 20/11
THE DEVELOPMENT AND SOLUTION OF BOUNDARY INTEGRAL EQUATIONS FOR--ETC(U)
NOV 76 L T MONTULLI

UNCLASSIFIED AFFDL-TR-76-116 NL

1 OF 2
AD A039 814

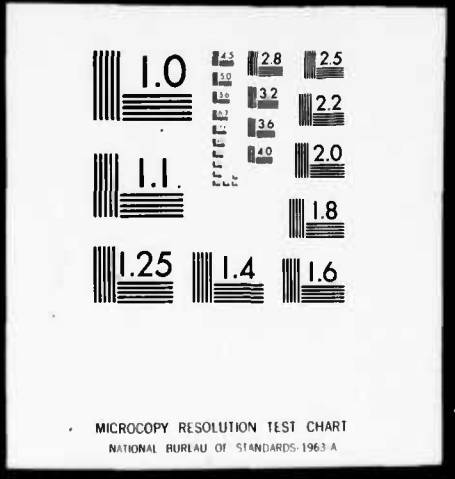

AFFDL-TR-76-116

THE DEVELOPMENT AND SOLUTION OF BOUNDARY INTEGRAL EQUATIONS FOR CRACK PROBLEMS IN FRACTURE MECHANICS

DEPT. OF MECHANICS AND ENGINEERING SYSTEMS
AIR FORCE INSTITUTE OF TECHNOLOGY

NOVEMBER 1976

TECHNICAL REPORT AFFDL-TR-76-116
FINAL REPORT FOR PERIOD JULY 1973 to JUNE 1975

AIR FORCE FLIGHT DYNAMICS LABORATORY
AIR FORCE SYSTEMS COMMAND
WRIGHT-PATTERSON AIR FORCE BASE, OHIO 45433

NOTICE

When Government drawings, specifications, or other data are used for any purpose other than in connection with a definitely related Government procurement operation, the United States Government thereby incurs no responsibility nor any obligation whatsoever; and the fact that the Government may have formulated, furnished, or in any way supplied the said drawings, specifications, or other data, is not to be regarded by implication or otherwise as in any manner licensing the holder or any other person or corporation, or conveying any rights or permission to manufacture, use, or sell any patented invention that may in any way be related thereto.

This report has been reviewed by the Office of Information (OI) and is releasable to the National Technical Information Service (NTIS). At NTIS, it will be available to the general public, including foreign nations.

This technical report has been reviewed and is approved for publication.

JOSEPH P. GALLAGHER,
Project Engineer

ROBERT M. BADER, Chief
Structural Integrity Br
Structural Mechanics Div

FOR THE COMMANDER

HOWARD L. FARMER, Col, USAF
Chief, Structural Mechanics Division

Copies of this report should not be returned unless return is required by security considerations, contractual obligations or notice on a specific document.

AIR FORCE - 16 MARCH 77 - 200

Unclassified
SECURITY CLASSIFICATION OF THIS PAGE (When Data Entered)

REPORT DOCUMENTATION PAGE

READ INSTRUCTIONS BEFORE COMPLETING FORM

1. REPORT NUMBER: AFFDL-TR-76-116	2. GOVT ACCESSION NO.
3. RECIPIENT'S CATALOG NUMBER	
4. TITLE (and Subtitle): THE DEVELOPMENT AND SOLUTION OF BOUNDARY INTEGRAL EQUATIONS FOR CRACK PROBLEMS IN FRACTURE MECHANICS	5. TYPE OF REPORT & PERIOD COVERED: Final Technical Report 1 Jul 1973-30 Jun 1975; 6. PERFORMING ORG. REPORT NUMBER
7. AUTHOR(s): Major Louis T. Montulli	8. CONTRACT OR GRANT NUMBER(s)
9. PERFORMING ORGANIZATION NAME AND ADDRESS: Dept. of Mechanics and Engr'g Systems, Air Force Institute of Technology, Dayton, Ohio	10. PROGRAM ELEMENT, PROJECT, TASK AREA & WORK UNIT NUMBERS: 136703, 13670324
11. CONTROLLING OFFICE NAME AND ADDRESS: Air Force Flight Dynamics Laboratory, Wright-Patterson Air Force Base, Ohio 45433	12. REPORT DATE: November 1976; 13. NUMBER OF PAGES: 170
14. MONITORING AGENCY NAME & ADDRESS (if different from Controlling Office): 179p.	15. SECURITY CLASS. (of this report): Unclassified; 15a. DECLASSIFICATION/DOWNGRADING SCHEDULE

16. DISTRIBUTION STATEMENT (of this Report)

DISTRIBUTION STATEMENT A
Approved for public release;
Distribution Unlimited

17. DISTRIBUTION STATEMENT (of the abstract entered in Block 20, if different from Report)

Approved for Public Release: Distribution Unlimited

18. SUPPLEMENTARY NOTES: 1367 03

19. KEY WORDS (Continue on reverse side if necessary and identify by block number)

- o Boundary Integral Equations
- o Linear Elastic Fracture Mechanics
- o Stress Intensity Factor

20. ABSTRACT (Continue on reverse side if necessary and identify by block number)

The elastostatic Boundary Integral Equation (B.I.E.) method is mathematically extended to include closed crack plane boundary value problems under general loading. The B.I.E. developed by Rizzo is formulated for a modified open crack geometry. By the

DD FORM 1 JAN 73 1473 EDITION OF 1 NOV 65 IS OBSOLETE

Unclassified
SECURITY CLASSIFICATION OF THIS PAGE (When Data Entered)

012070

formulation of a sum and difference state over the crack surfaces, a limit operation closing the crack is successfully performed. The resulting integral equation set is solved for two example problems possessing known solutions. The stress intensity factors, $K_{(I)}$, $K_{(II)}$, and $K_{(III)}$, and the resulting strain energy of the body are calculated and found to be accurate within 1% when compared to the analytical solution. The bent edge crack in a finite circular disk subject to mixed mode loading is investigated. Initial crack trajectories are predicted using the strain energy release rate criterion and compared to known results.

FOREWORD

The research reported herein was conducted by the Air Force Institute of Technology (AFIT) for the Structural Mechanics Division, Air Force Flight Dynamics Laboratory, Wright-Patterson Air Force Base, Ohio, under Project 1367, "Structural Integrity for Military Aerospace Vehicles", Task 136703, "Fatigue, Fracture and Reliability Analysis & Design Methods for Aerospace Vehicles." Dr. J. P. Gallagher of AFFDL/FBE was the project engineer.

The study was conducted during the period from 1 July 1973 to 30 June 1975. The principal investigator was Major Louis T. Montulli, Dept of Mechanics and Engineering Systems. Computer program assistance was accomplished by Capt Walter King, who was first a graduate student at AFIT and later on temporary assignment to AFFDL/FBE. This report was submitted by the author on 30 December 1975.

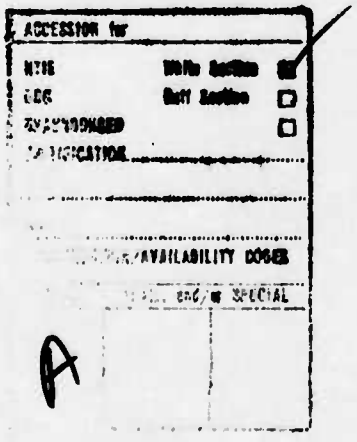

TABLE OF CONTENTS

	TITLE	PAGE
CHAPTER 1	INTRODUCTION	1
CHAPTER 2	MATHEMATICAL FORMULATION	8
	2.1 Basic Integral Equation Formulation	9
	2.2 Integral Equation Formulation for Cracked Plate Geometries	17
	2.3 The Plane Elastostatic Cracked Body Integral Equations	36
CHAPTER 3	MODE I AND II PROBLEM STATEMENT AND INTEGRAL REPRESENTATION	42
	3.1 Bent Crack Problem Formulation . . .	43
	3.2 Numerical Solution Technique	50
CHAPTER 4	NUMERICAL EXAMPLES AND DISCUSSION	56
	4.1 Numerical Verification Examples . . .	56
	4.2 Bent Crack Geometry Results	66
CHAPTER 5	CONCLUSIONS AND FUTURE APPLICATION	77
REFERENCES	. . . . .	81
APPENDIX A	GEOMETRIC KERNEL FUNCTIONS	86
APPENDIX B	GOVERNING B.I.E. FOR CLOSED BENT CRACK . .	110
	B.1 Full I.E. Set (System 3.2)	111
	B.2 Algebraic Insert Formula	139
	B.3 Forcing Functions	147
FIGURES	. . . . .	162

LIST OF ILLUSTRATIONS

Figure	TITLE	PAGE
1	General Elastic Closed Domain	162
2	Simple Anti-Plane Geometry	162
3	Modified Wedge Cracked Geometry	163
4a	General Cracked Body	163
4b	Modified Cracked Body	163
5	Bent Crack Geometry	164
6	Modified Bent Crack Geometry	165
7	Bent Crack Parametric Variable Definitions Normalized Geometry	166
8	Reference Point Locations for Bent Crack Geometry	167
9	Pressure Loaded Crack	168
10	Principle of Linear Superposition	169
11	Crack Branching Angle α as a Function of Load Orientation Angle β for Energy Criterion	170

LIST OF SYMBOLS

K_I	Stress intensity factor for Mode I loading
K_{II}	Stress intensity factor for Mode II loading
K_{III}	Stress intensity factor for Mode III loading
K_c	Critical stress intensity factor
λ,μ	Lame's elastic constants
u_i	Displacement in x_i direction
σ_{ij}	Stress tensor
t_j	Tractions in x_j direction
n	Unit normal vector
n_i	Component of n in x_i direction
x_i	Cartesian coordinates
C	Contour boundary of the domain D
D	Domain bounded by C
S	Arc length on C
r	Scalar distance
$p(\xi)$	Interior reference point in D
$P(\xi)$	Boundary reference point on C
$Q(x_i)$	Field point on boundary C
$M,K,\underline{\lambda}$	Elastic material constants dependent on λ, μ
(r,θ)	Polar coordinates
ρ	Non-dimensional coordinate
ϕ_j,ψ_j	Integral functions
U_{ij},T_{ij}	Tensor functions

(x,y,z)	Cartesian coordinates
u,v,w	Displacement in x,y,z direction
$K(\delta,\psi_o)$	Kernel functions
ψ_o	Crack opening angle
δ_o,θ_o	Polar coordinate reference point identifiers
C_i^u	Upper i^{th} crack surface
C_i^L	Lower i^{th} crack surface
Γ_i	Parametric surface identifier
$K_{IJ}(P,Q)$	Kernel functions
R_{JL}	Scalar distance functions
t_{xL}	Traction in x direction on L surface
t_{yL}	Traction in y direction on L surface
$[C]$	Geometric coefficient matrix
$\{u\}$	Displacement column matrix
$\{F\}$	Forcing function column matrix
$\underline{c}$	Length of bent crack
$\underline{C}$	Dimensionless length of bent crack
d	Length of parent crack
D	Dimensionless length of parent crack
R	Radius of circle
M1	Number of mesh points on $\underline{C}$
M2	Number of mesh points on D
M3	Number of mesh points on circle
H_1	Mesh spacing on $\underline{C}$
H_2	Mesh spacing on D

H_3	Mesh spacing on circle
α	Bent crack angle measured from x-axis
ρ	Load angle measured from x-axis
E_s	Strain energy
$\tilde{a}$	Total straight crack length $\underline{C}$ + D
$\underline{\alpha}$	Elastic material constants
α_c	Critical bent crack angle
E	Young's elastic modulus
ν	Poisson's ratio
Xl,	Field point variables
θ_o,B,B_2	Reference point variables
FAI	Forcing functions in A equation set
FBI	Forcing functions in B equation set

CHAPTER I

INTRODUCTION

Fracture mechanics, the study of failure mechanisms and the development of failure prediction criteria for engineering structures, focuses considerable attention on the stress distribution in the neighborhood of a crack embedded in an elastic body. The intensity of the elastic stress field around the tip of a sharp crack plays a dominant role in fracture analysis. Irwin (1) showed that the Griffith (2) fracture theory, originally based on energy considerations, is equivalent to an approach using the concept of crack-tip, stress intensity factors. The basic idea of the combined theory is that the crack propagates under static load when the stress intensity in the region near the crack tip reaches a certain critical value, say K_c. For a given material the combination of crack size and loading at incipient fracture results in a stress intensity factor equal to K_c. When the load or crack size is kept below this threshold point, the severity of the crack tip is measured by the "stress intensity factor" K which assumes the general form

$$K = \sigma_f \cdot \gamma \cdot \sqrt{\pi \hat{a}}$$

This K factor is a quantity determined analytically or

experimentally and varies as a function of the crack length $\tilde{a}$, the crack configuration and external geometry factor γ, and the manner in which the internal loads or far field stresses σ_f are applied. Successful application of the theory requires that the crack tip plastic zone size be small compared to the crack dimensions. This permits the use of elasticity theory to determine the stress intensity factors.

As a rule, the crack-tip stress state in a structural component must be described by at least two parameters, say K_I and K_{II}. K_I corresponds to Mode I loading which produces symmetric stress states near the crack tip and K_{II} stands for the amplitude of the skew-symmetric portion or Mode II loading. The criterion of fracture now requires a combination of K_I and K_{II} reaching some critical value, i.e.

$$F\ (K_I,\ K_{II}) = F_c$$

If the stress state is triaxial in nature, a third parameter K_{III} is usually required and the fracture criterion must be modified accordingly.

Common experience indicates that a crack follows a path in a structural component as dictated by the stress field. At each instant, the direction of crack propagation depends on the energy state and the material properties in a region ahead of the crack tip. It is of utmost importance

to be able to predict the direction of crack initiation.

One common method used to predict crack growth which may be useful in mixed mode problems is the criterion of maximum strain energy release rate. The strain energy release rate $\mathcal{G}$ represents the amount of energy released during an incremental increase in crack area. The critical strain energy release rate criterion and the K_c criterion can be related. For specimens subject to Mode I loading, $\mathcal{G}$ equals $C_1 \frac{K_I^2}{E}$ where C_1 is a constant depending on whether the body is in a state of plane stress or plane strain.

Analytical problems for the stress intensity factors are available for a number of crack geometries and boundary configurations (3-11). The largest class of solved problems apply to the conditions of Mode I and II loading for states of plane stress or plane strain. A large complement of mathematical methods have been used to seek solutions and are reviewed in (9,10). The major analysis techniques used for K calculations are complex variable, conformal mapping, Green's function, Riemann-Hilbert problem, Wiener-Hopf method, singular integral equations, and asymptotic approximations. Authors utilizing these methods have produced hundreds of solutions many of which are tabulated in (11). Analytical solutions for three-dimensional cracked bodies are more limited, generally restricted to the penny-shaped and elliptical crack geometry.

Analytical solutions for K factors, although large

in number, do not fully satisfy the designer's needs when analyzing complex structures. The presence of stiffeners, irregular geometries and complex boundary loadings often complicate the real problem. Thus considerable attention has been focused on numerical methods particularly finite element techniques.

Early studies of fracture mechanics problems involving the finite element method have been carried out by Swedlow(12), Tuba (13), and Watwood (14). They attempted a straightforward application of the technique with no special attention given to the stress singularity. The specimen was conceptually divided into finite elements with a relatively high element concentration near the crack tip. Computational experiments indicated the need to include a very large number of degrees of freedom in order to obtain reasonable accuracy (12-14). The numerical value of the stress intensity factor, determined in this manner, varies over a considerable range, depending upon which node is chosen for its calculation. Further study of this technique (15,16) concerns questions about its convergence, reliability, and convenience.

In an attempt to eliminate some of these undesirable features, an alternative approach has been developed by Wilson and others (15) and extended by Oglesby and Lomacky (16). They directly incorporated both the finite element method and the analytical crack tip expansions to form a

special singular crack tip element. This element centered at the crack tip, has the deformation field given by the elastic singular solution, with the stress intensity factors and crack tip displacement components as the parameters characterizing its behavior. The crack tip element is connected to standard elements along its boundary, by requiring the nodal displacement components on this interface to be consistent with the crack tip solution. Finite element results for complicated geometries using special cracked elements are believed to easily give accuracy within 2-3% (17).

Evaluation of stress-intensity factors will, in most cases require a numerical attack due to the complicating factor of geometry. The boundary integral equation (B.I.E.) technique is a numerical method particularly suited to the stress analysis of simply or multiply connected homogeneous, elastic bodies.

The method as developed by Rizzo(18) exploits the strong analogy between potential theory and classical elasticity theory. Unlike Jaswon(19) Rizzo's approach is not limited to two-dimensions and works directly with assigned boundary quantities instead of stress functions. This approach depends on the knowledge of the singular solution to the Navier-Cauchy elasticity equations in two-dimensions corresponding to a concentrated force. The singular solution gives rise to a vector identity similar

to Green's third identity for Laplace's equation. Taking the field point to lie on the boundary contour, a boundary formula is obtained which gives a relation between boundary displacements and corresponding boundary tractions. Since either of these boundary quantities, in principle, determines the other, the formula provides a constraint between them which generates a set of simultaneous integral equations involving the unknown boundary data. The reduction to a problem involving only the boundary surfaces reduces the dimensionality by one and has no requirement for discretization of the region contained within the boundary surface. This reduction in dimensionality significantly reduces the computational requirements.

This method has been extensively developed by Rizzo, Shippy, Cruse and Lee (20-28). They have applied the B.I.E. method to the following class of problems; 1) elasto-dynamics, 2) three-dimensional elasto-static, 3) elastic inclusion, and 4) anisotropic elastic boundary value problems . At the present time application to cracked bodies is restricted to symmetric geometries which allow the problem to be changed from a cracked body to a mixed boundary value problem with no cracks. The unsymmetrical crack problem is excluded in Rizzo's formulation due to regularity requirements on the boundary surfaces. These regularity conditions require that the body be finite, and smooth, and representable by unique parametric expressions.

Classical fracture problems require that the crack faces be defined to lie on the same contour and meet sharply at the crack tip. These conditions violate the regularity requirements upon which Rizzo's formulation relies.

It is the purpose of this thesis to extend the Rizzo technique to permit its application to those crack problems lacking symmetry. Chapter 2 presents the mathematical formulation of the B.I.E. for plane cracked bodies, while the solution technique is applied to a specific Mode I, Mode II problem in Chapter 3. Chapter 4 presents results and discussion for two sets of problems. The first set is for verification of the solution method and the second presents data for the bent crack. Finally, Chapter 5 is concerned with conclusions and applications of the developed method.

CHAPTER 2

MATHEMATICAL FORMULATION

Solutions of boundary value problems in fracture mechanics require the analysis of bodies containing mathematical models of crack-like flaws. The geometric modeling of these flaws generally result in configurations or geometries that are non-regular as defined in (29,30). The basic integral equation formulation developed by Rizzo (18) requires that the body under consideration be finite and bounded by a single smooth contour C, the contour satisfying certain regularity conditions (29). One regularity condition requires that contour C possess a unique representation in the parametric form $x_\alpha = x_\alpha(s)$. A second condition is imposed on the surface derivatives $x'_\alpha(s)$ which must be continuous. The two crack faces in classical fracture problems are defined to lie on the same contour; thus, unique parametric representation of the individual surfaces is excluded. The presence of a reentrant vertex at the crack tip, and the existence of sharp corners, where the crack intersects the outer boundary, violates the second regularity condition. Section 2.1 presents a summary of the Rizzo formulation considering C to be regular. This permits solution of a class of problems excluding the elastostatic crack problems arising in fracture

mechanics. The mathematical processes required to overcome these restrictions and to extend the B.I.E. method for solution of general crack problems are the subject of Section 2.2

2.1 Basic Integral Equation Formulation

The integral equation formulation presented in this section is restricted to the analysis of classical plane elastostatic problems for which the material may be taken to be isotropic and homogeneous[1,2]. The Navier displacement equations of equilibrium in the absence of body forces are given by

$$(\lambda + \mu)u_{\alpha,\alpha\beta} + \mu\, u_{\beta,\alpha\alpha} = 0 \quad (\alpha,\beta = 1,2) \tag{2.1}$$

where the displacement is denoted by $u_\beta\,(x_\alpha)$ while x_α are the orthogonal cartesian coordinates x_1, x_2 and λ, μ are the familiar Lamé constants. Eq. (2.1) formulated for problems of plane strain, may also embrace generalized plane stress with suitable exchange of material constants. The solution to this differential equation must also satisfy the boundary conditions for the displacements and

---

[1] A more general formulation for the 3-D elastic problem may be found in References 21,25,27.

[2] The formulation presented in this section is very similar to that of Rizzo(18). It is presented here because it is the foundation for mathematical extensions germane to this thesis.

tractions on the contour C , given by

$$u_\beta\ (x_\alpha) = q_\beta \qquad x_\alpha \in C^1$$

and

$$\sigma_{\alpha\beta} n_\alpha = t_\beta\ (x_\alpha) \qquad x_\alpha \in C^2 \qquad (2.2)$$

where C^1, C^2 are those portions of the contour subject to displacement-traction loading boundary conditions respectively. The unit vector n is the outward normal vector for the body D with components n_α.

The body under consideration will be assumed finite and bounded by a single smooth contour C, which, as described in (29), admits a unique representation in the parametric form $x_\alpha = x_\alpha(s)$. Further, the derivatives $x'_\alpha(s)$ are assumed to be continuous. The parameter S is the arc length along the contour from some arbitrary origin.

Figure 1 illustrates a simply connected body with closed contour C. For the body (D + C) under the action of boundary tractions t_α, the relation

$$t_\alpha = \lambda\, u_{\beta,\beta}\, n_\alpha + \mu n_\beta\, (u_{\alpha,\beta} + u_{\beta,\alpha}) \qquad (2.3)$$

must hold on C.

The distance between field points Q with coordinates

x_α and the source points p with coordinates ξ_α is given by

$$r = [(x_\alpha - \xi_\alpha)\ (x_\alpha - \xi_\alpha)]^{1/2} \qquad (2.4)$$

Then, concentrated forces of magnitude, $-4\pi\mu(\lambda + 2\mu)/(\lambda + 3\mu)$, are applied at points $p = p(\xi_\alpha)$ in the x_α directions respectively, giving rise to displacement vector u^*_β as defined by Love (31)

$$u^*_\beta = U_{\alpha\beta}\ e_\alpha = U_{1\beta} + U_{2\beta} \qquad (2.5)$$

where

$$U_{\alpha\beta} = \delta_{\alpha\beta} \mathrm{Ln}\ r + M\ r_{,\alpha}\ r_{,\beta}$$

and where e_α are unit base vectors. Eq. (2.5) satisfies Eqs. (2.1) in D, provided

$$r \neq 0, \quad M = -\frac{(\lambda + \mu)}{\lambda + 3\mu} \qquad (2.6)$$

In Eq. (2.5) and in what follows, all differentiation is with respect to the field point x. That is,

$$r_{,\alpha} = \frac{\partial r}{\partial x_\alpha} = \frac{1}{r}\ (x_\alpha - \xi_\alpha)$$

and

$$\frac{\partial r}{\partial n} = \frac{\partial r}{\partial x_\alpha}\eta_\alpha = \frac{1}{r}\ (x_\alpha - \xi_\alpha)\eta_\alpha$$

where the normal is evaluated at x_α also. The traction vectors t^*_β on C corresponding to u^*_β are computed from Eq.(2.3) and may be written

$$t^*_\beta = T_{\alpha\beta}\, e_\alpha = T_{1\beta} + T_{2\beta} \qquad (2.7)$$

where

$$T_{\alpha\beta} = \frac{\partial}{\partial n} \text{Ln } r \; [K\delta_{\alpha\beta} - 4\mu M r_{,\alpha}\, r_{,\beta}]$$
$$+ K\,[(\text{Ln } r)_{,\alpha}\, \eta_\beta - (\text{Ln } r)_{,\beta}\, \eta_\alpha]$$

and

$$K \equiv 2\mu^2/(\lambda + 3\mu)$$

The vectorial form of Betti's reciprocal work theorem may be written

$$\int_{C+m} (u_\alpha\, T_{\alpha\beta} - t_\alpha\, U_{\alpha\beta})\, dS = 0 \qquad (2.8)$$

where dS is an element of arc length at Q and where the point $p = p(\xi_\alpha)$ of D has been excluded by a small circle m of radius ρ because of the singular nature of U_α and $T_{\alpha\beta}$ for $r = 0$. The vectors and their derivatives are taken to be non-singular and sufficiently continuous for the usual validity of the theorem. These vectors correspond to an equilibrium stress state; body forces associated with $U_{\alpha\beta}$ and $T_{\alpha\beta}$ are taken as zero. It can be shown

(18) that

$$\lim_{\rho\to o} \int_m t_\alpha \, U_{\alpha\beta} \, dS = 0, \quad \lim_{\rho\to o} \int_m u_\alpha \, T_{\alpha\beta} \, dS = -\underline{\alpha}^{-1} u_{\beta(p)} \tag{2.9}$$

where

$$\underline{\alpha} = (\lambda+3\mu)/(4\pi\mu(\lambda+2\mu)).$$

Therefore, Eq. (2.8) yields

$$u_\beta(p) = \underline{\alpha} \int_C [u_\alpha(Q) \, T_{\alpha\beta}(p,Q) - t_\alpha(Q) \, U_{\alpha\beta}(p,Q)] \, dS_{(Q)} \tag{2.10}$$

which is the plane counterpart of Somigliana's identity (31) for the displacements inside the body, D, caused by surface tractions and displacements. Eq. (2.10) is analogous to Green's third identity of potential theory which expresses a harmonic function in terms of the boundary values of the function and its normal derivative. A parallel development using Green's third identity leads to the formulation of the Mode III problem.

The properties of the integrals in Eq. (2.10) as the boundary C is approached are necessary for the development of B.I.E. relating the displacements and tractions on C. The integrals present in Eq. (2.10) are

$$\phi_\beta(p) = \int_C t_\alpha(Q) \, U_{\alpha\beta}(p,Q) \, dS, \quad \psi_\beta(p) = \int_C u_\alpha(Q) \, T_{\alpha\beta}(p,Q) \, dS$$

The limits as $p \to P$ of $\phi_\beta(p)$ and $\psi_\beta(p)$ are obtained by assuming the point P lies on a smooth contour.

The second of these integrals yields

$$\lim_{p\to P} \psi_\beta(p) \equiv \psi_\beta(P) = \pi \cdot [K-2\mu M] u_\beta + \int_C u_\alpha (Q)\, T_{\alpha\beta}(P,Q)\, dS \tag{2.11}$$

This result is readily verified provided u_α is assumed to satisfy a Hölder condition on C and provided the singular integral is evaluated in the sense of a Cauchy Principal Value (32). A similar limiting procedure for the first integral gives

$$\lim_{p\to P} \phi_\beta(p) \equiv \phi_\beta (P) = \int_C t_\alpha(Q)\, U_{\alpha\beta}(P,Q)\, dS \tag{2.12}$$

The integral equations relating the surface tractions to surface displacements are found from Eq.(2.10), to (2.12). Since

$$u_{\beta(P)} = \underline{\alpha}[\psi_\beta (P) - \phi_\beta(P)] \tag{2.13}$$

and

$$\underline{\alpha}\pi\ (K - 2\mu M) = 1/2$$

it results that

$$u_\beta (P) - 2\,\underline{\alpha} \int_C u_\alpha (Q)\, T_{\alpha\beta}(P,Q)\, dS(Q)$$

$$= -2\,\underline{\alpha} \int_C t_\alpha (Q)\, U_{\alpha\beta}(P,Q)\, dS(Q) \tag{2.14}$$

As shown by Rizzo (18), Eq. (2.14) will be regular according to the classification of singular operators by Muskhelishvili (32) for values of Poisson's ratio $\upsilon \varepsilon [0,1/2)$. Given t_α on C, the traction problem, the two components of Eq. (2.14) form a simultaneous pair of integral equations for the unknown u_α. The rigid body displacement vector

$$u_\beta (P) = a_\beta + be_{\alpha\beta 3}\, \xi_\alpha(P)$$

satisfies the homogeneous form of these equations, i.e.,

$$u_\beta(P) - 2\, \underset{C}{\int} u_\alpha(Q)\; T_{\alpha\beta}(P,Q)\, dS(Q) = 0 \qquad (2.15)$$

where a_β and b are arbitrary constants. Application of the Fredholm alternative yields

$$\int_C t_\alpha(Q)\; dS(Q) = \int_C \varepsilon_{3\beta\alpha} x_\beta(Q)\; t_\alpha(Q)\; dS(Q) = 0 \qquad (2.16)$$

as the necessary and sufficient conditions for the solubility of Eq. (2.14). These are, of course, the conditions that the body be in equilibrium.

It should be noted that although the Fredholm alternative was employed above, Eq. (2.14) is not a Fredholm integral equation, since the term

$$T^*_{\alpha\beta} = K\left[(\text{Ln } r)_{,\alpha}\, \eta_\beta - (\text{Ln } r)_{,\beta}\, \eta_\alpha\right]$$

is present in the kernel function $T_{\alpha\beta}$. More precisely,

$$\lim_{Q \to P} \left| Q-P \right| T^{*}_{\alpha\beta}(P,Q) \neq 0$$

whereas a limit of zero is required for Fredholm kernels. Nevertheless, the index k in Muskhelishvili Chapter 19 (32) computed from $T_{\alpha\beta}$ equals zero and the Fredholm alternative is applicable.

Given the u_α on C, the displacement problem, the two components of Eq. (2.14) form a simultaneous pair of singular integral equations for the unknown t_α on C. Rizzo proved in (18) that the homogeneous equations

$$\int_C t_\alpha(Q)\ U_{\alpha\beta}(P,Q)\, dS(Q) = 0$$

has no nonzero solutions. Thus it may be expected that the displacement problem formulation of Eq. (2.14) results in unique solution t_α on C for arbitrary U_i on C.

With the knowledge of $u_\beta = u_\beta^{(1)}$ on part of C and $t_\alpha = t_\alpha^{(2)}$ on the remaining part (mixed problem), a set of four equations on the unknowns $u_\beta^{(2)}$ and $t_\alpha^{(1)}$ on C is obtained. The mixed-mixed boundary value problem may also be formulated by extension of the above reasoning. Evaluation of the displacement field (and subsequently the stress and strain fields) internal to the boundary C may be obtained through Eq. (2.10) from the boundary data given on all contours.

2.2 Integral Equation Formulation for Cracked Plate Geometrics

In this section, the Boundary Integral Equation (B.I.E.) formulation necessary to solve elastostatic, edge cracked plane problems is developed[3]. This formulation is restricted to traction loading, although displacement or mixed boundary conditions may be addressed with equal ease.

Direct formulation of the Boundary Integral Equation (2.14) applied to edge crack geometry leads to an incomplete problem statement. This shortcoming is caused by the inherent restriction that the complete contour of body D be described by a unique parametric representation $x_\beta = x_\beta(s)$. The upper and lower crack faces violate this condition. The other restriction on the continuity of $x'_\beta(s)$ must also be addressed since a discontinuous change in (s) occurs at the crack tip, and may occur at the crack corners.

The method is first illustrated for the case of a crack with Mode III loading, which is equivalent to the Dirichlet problem. This classical problem (30,33) is formulated beginning with Green's third identity yielding the governing integral equation

$$W(P) - \frac{1}{\pi} \int_C W(Q) \cdot K(Q,P)\, dS(Q) = F(P) \tag{2.17}$$

3. Throughout this thesis attention is restricted to edge crack problems. However, the method discussed is applicable to internal crack geometries by reformulating Eq.(2.14) to account for multiply connected regions.

where:

$$F_{(P)} = \frac{1}{2\pi}\int_C \frac{\partial w}{\partial n}(Q)\,\mathrm{Ln}\; r_o^2\, dS(Q)$$

$$K(Q,P) \equiv \frac{(x-x_o)\frac{\partial x}{\partial \bar{n}} + (y-y_o)\frac{\partial y}{\partial \bar{n}}}{r_o^2}$$

$$r_o^2 = [(x-x_o)^2 + (y-y_o)^2]$$

Eq. (2.17) relates the unknown displacement W in the z-direction to an applied shear load which is proportional to $\frac{\partial W}{\partial n}(Q)$ on the boundary C. Q and P are field and reference points on the boundary C, and n is the unit normal at point Q, and x,y are the usual cartesian coordinates. The derivation of Eq. (2.17) requires the same restrictions as imposed on Eq. (2.14) pertaining to unique parametric representation of C and continuous surface derivatives $x'_\alpha(s)$. Because the Mode III governing integral Eq. (2.17) is simple and has similar mathematical behavior to the Mode I and II formulation it is selected for initial investigation.

A simple Mode III B.V.P. is defined with geometry illustrated in Fig. 2. It consists of a right-circular cylinder of radius R with a sharp $2\psi_o$ wedge cut out beginning at the center line of the bar. The selection of an appropriate traction loading results in a closed form analytical solution suitable for comparison with the integral equation results. Analytical solution of the Mode III

problem begins with the definition of the usual cylindrical coordinates r,θ,z with origin at the bar's center. The governing differential equation is the classical

$$\nabla^2 W = 0$$

where $W = W(\rho,\theta)$, $\rho \equiv r/R$

$0 \leq \rho \leq 1$, $\psi_o \leq \theta \leq 2\pi-\psi_o$

The boundary conditions are defined as,

a) on the upper wedge face, $\theta = \psi_o$

$$\mu \frac{1}{\rho} \frac{\partial W}{\partial \theta} = T_z = 0$$

b) on the lower wedge face, $\theta = 2\pi - \psi_o$

$$\mu \frac{1}{\rho} \frac{\partial w}{\partial \theta} = T_z = 0$$

c) on the circular boundary, $\rho = 1$

$$\mu \left.\frac{\partial w}{\partial \rho}\right|_{\rho=1} = T_z = \frac{\mu B}{R} \cos\left\{\frac{\pi(\theta-\psi_o)}{2(\pi-\psi_o)}\right\}$$

Solution of the harmonic equation and satisfaction of the B.C. yields the following results for the boundary displacements

a) on $\theta = \psi_o$ $\quad W(\rho,\psi_o) = \rho^B$

b) on $\theta = 2\pi-\psi_o$ $\quad W(\rho,-\psi_o) = -\rho^B$

c) on $\rho = 1$ $\quad W(1,\theta) = \cos\left\{B(\theta-\psi_o)\right\}$

where $B = \pi/2(\pi-\psi_o)$

Integral Eq. (2.17) is formulated for a modified circular wedge geometry. The crack tip and crack corners are rounded with circular arcs of radius ε_i to insure starting with a contour C whose surface derivatives are continuous and ψ_o is assumed to be nonzero so the two crack faces are separate and distinct. This modified geometry shown in Fig. 3 meets all the restrictions imposed on Eq.(2.17).

The upper wedge surface is labeled C_1, the circular boundary C_2, the lower wedge surface C_3 and the crack tip and upper and lower corner contours C_4, C_5 amd C_6 respectively. Eq. (2.17) is applied to this modified geometry and the resulting equation separated into six parts. Each of the parts represents a unique portion of the I.E. for reference points located on individual contours C_i, i = 1 to 6. This yields:

$$W_i(P_i) - \frac{1}{\pi}\int_{C_1} W_1(Q_1)K_1(Q_1,P_i)dS_1(Q_1)$$
$$- \frac{1}{\pi}\int_{C_2} W_2(Q_2)K_2(Q_2P_i)dS_2(Q_2) - \frac{1}{\pi}\int_{C_3} W_3(Q_3)K_3(Q_3,P_i)dS_3(Q_3)$$
$$- \frac{1}{\pi}\int_{C_4} W_4(Q_4)K_4(Q_4,P_i)dS_4(Q_4) - \frac{1}{\pi}\int_{C_5} W_5(Q_5)K_5(Q_5,P_i)dS_5(Q_5)$$
$$- \frac{1}{\pi}\int_{C_6} W_6(Q_6)K_6(Q_6,P_i)dS_6(Q_6) = F_i(P_i) \quad i = 1,6$$

no sum on i

(2.18

where:

$$F_i(P_i) = \frac{-1}{2\pi}\int_{C_3}\frac{\partial W_3(Q_3)}{\partial n}\,\mathrm{Ln}\; r_{ij}^2\; dS_3(Q_3)$$

$$K_j(Q_j,P_i) = \frac{(x_j - x_{oi})\frac{\partial x_j}{\partial n} + (y_j - y_{oi})\frac{\partial y_j}{\partial n}}{r_{ij}^2}$$

$$r_{ij}^2 = \left\{(x_j - x_{oi})^2 + (y_j - y_{oi})^2\right\}$$

$w_i \equiv$ displacements on Γ_i

$P_i, Q_i \equiv$ field and reference points on Γ_i

Points P_i and Q_i include all points in the set which form the contour C_i; dS_i are incremental arcs on C_i for i=1 to 6. The operation limit $\epsilon_i \to 0$ is performed on Eq. (2.18). The integral over the surfaces C_4, C_5 and C_6 when i = 1,2, or 3 yields:

$$\lim_{\epsilon_1\to 0}\int_{C_4} W_4(Q_4)K_4(Q_4,P_i)\,dS_4(Q_4) = \lim_{\epsilon_2\to 0}\int_{C_5} W_5(Q_5,P_i)\,dS_5(Q_5)$$

$$= \lim_{\epsilon_3\to 0}\int_{C_6} W_6(Q_6)K_6(Q_6,P_i)\,dS_6(Q_6) = 0 \qquad i = 1,2,3$$

provided points $\bar{P}_K$ at the crack tip and each of the corners are excluded from the set of reference points P_i. The

exclusion of points $\bar{P}_K$ from Eq.(2.18) imposes no limitation on the eventual numerical solution of the equation set. This is an obvious result of the numerical solution technique which requires discretization of the equations with the accompanying freedom of selecting a finite number of reference points. The elimination of a small set of reference points $\bar{P}_K$ offers no special restriction nor any great inconvenience. The exclusion of points $\bar{P}_K$ also allows the remaining integral equations for i = 4,5 and 6 in the Eq.(2.18) system to be ignored. For, when the limit $\varepsilon_i \to 0$ is performed and the points P_K are excluded from the reference set, these equations are eliminated.

Equation (2.18) applied to the special right circular cylinder problem described above, now becomes,

$$W_1(\delta_o) - \frac{1}{\pi}\int_{\psi_o}^{2\pi-\psi_o} W_2(\theta)\left\{\frac{1-\delta_o\cos(\theta-\psi_o)}{1-2\delta_o\cdot\cos(\theta\cdot\psi_o)+\delta_o^2}\right\}d\theta$$

$$+\frac{1}{\pi}\int_0^1 W_3(\delta)\left\{\frac{\delta_o\sin(2\psi_o)}{\delta^2+\delta_o^2-2\delta\cdot\delta_o\cdot\cos 2\psi_o}\right\}d\delta$$

$$= \frac{-1}{4(\pi-\psi_o)}\int_{\psi_o}^{2\pi-\psi}\cos\frac{\pi(\theta-\psi_o)}{2(\pi-\psi_o)}\,\mathrm{Ln}\left[1-2\delta_o\cdot\cos(\theta-\psi_o)+\delta_o^2\right]d\theta \qquad (2.19a)$$

$$- \frac{1}{\pi} \int_0^1 W_1(\delta) \frac{\sin(\theta_o - \psi_o)}{\delta^2 - 2\delta \cdot \cos(\theta_o - \psi_o) + 1} \, dS + W_2(\theta_o)$$

$$- \frac{1}{\pi} \int_{\psi}^{2\pi - \psi_o} W_2(\theta) \cdot \frac{1}{2} \, d\theta + \frac{1}{\pi} \int_0^1 W_3(\delta) \frac{\sin(\theta_o + \psi_o)}{\delta^2 - 2\delta \cdot \cos(\theta_o + \psi_o) + 1} \, d\delta$$

$$= \frac{1}{4(\pi - \psi_o)} \int_0^{2\pi - \psi_o} \cos \frac{\pi(\theta - \psi_o)}{2(\pi - \psi_o)} \cdot \mathrm{Ln} \left[2 - 2\cos(\theta - \theta_o) \right] d\theta \qquad (2.19b)$$

$$\frac{1}{\pi} \int_0^1 W_1(\delta) \frac{\delta_o \sin 2\psi_o}{\delta^2 - 2\delta \, \delta_o \cos 2\psi_o + \delta_o^2} \, d\delta$$

$$- \frac{1}{\pi} \int_{\psi_o}^{2\pi - \psi_o} W_2(\theta) \frac{1 - \delta_o \cos(\theta + \psi_o)}{1 - 2\delta_o \cos(\theta + \psi_o) + \delta_o^2} \, d\theta + W_3(\delta_o)$$

$$= \frac{-1}{4(\pi - \psi_o)} \int_{\psi_o}^{2\pi - \psi_o} \cos \frac{\pi(\theta - \psi_o)}{2(\pi - \psi_o)} \, \mathrm{Ln} \left[1 - 2\delta_o \cdot \cos(\theta + \psi_o) + \delta_o^2 \right] d\theta \qquad (2.19c)$$

In Eq. (2.19) W_1, W_2, and W_3 are the unknown displacements in the z-direction for the surfaces C_1, C_2, and C_3 respectively, and $\delta, \delta_o, \theta, \theta_o$ are the remaining cylindrical coordinate variables for the field and reference points. The points $\delta_o = 1$, $\delta_o = 0$, $\theta_o = \psi_o$, and $\theta_o = 2\pi - \psi_o$ are inadmissible reference points in the Eq. (2.19), and $\psi_o \in (0, \pi)$.

Numerical solutions of the integral equations which arise in this paper require particular attention to those singular kernels whose integrals exist only in the sense of a Principal Value. Special techniques to account for the

effect of the singular stress field near crack tips and other critical points are also necessary for good numerical accuracy. Therefore, a major section in Chapter 3 is devoted to the discussion of these techniques, and numerical results pertinent to this chapter are presented without explanation of the numerical processes used to obtain them.

Eq. (2.19) is numerically solved for selected values of $0 \leq \psi_o \leq 90^o$. Displacement values along the wedge faces are of particular interest. A convenient parameter helpful to the evaluation of the numerical results is obtained by dividing the computed displacements along the wedge faces by the exact solution, and fitting a least squares straight line to this data. The intercept value for $\delta = 0$ is labeled NDP (Normalized Displacement Parameter). With the use of the parameter NDP, all problem solutions for $0 \leq \psi_o \leq 90^o$ will yield NDP equal to one if the numerical error is zero. Percent deviation of NDP from unity is thus a means of evaluating the numerical accuracy of the results. The results are tabulated in Table 2.1.

TABLE 2.1

Anti-Plane Wedge Problem Results

ψ_o	90^o	60^o	45^o	30^o	25^o	20^o	15^o	10^o	5^o
NDP	.998	.999	1.001	1.006	1.02	1.1	--	--	--
% Error	.2%	.1%	.1%	.6%	2%	10%	∿20%	∿30%	>50%

The results obtained for $\psi_o > 30^o$ clearly support the conclusion that the I.E. (2.19) is a proper representation of the sharp wedge problem and may be solved accurately. For values of $\Psi_o < 30^o$, the important displacement results near the crack tip develop significant errors as ψ_o approaches zero. These results are so badly behaved that they render NDP meaningless when $\psi_o \to 0$ and, the determination of the stress intensity factors for $\psi_o = 0$ is impossible by this formulation.

The requirement for a unique parametric representation of all boundary surfaces causes the computational difficulties experienced above. A direct limiting process executed on Eq. (2.19a) and Eq. (2.19c), taking special care with all Principal Value integrals, shows

$$\lim_{\psi_o \to 0} (\text{Eq. } 2.19a) = \lim_{\psi_o \to 0} (\text{Eq. } 2.19c)$$

This result is clearly manifested in the numerical example. The determinate of the linear algebraic equation set approaches zero as ψ_o approaches zero, confirming that Eq. (2.19) is incomplete in the limit $\psi_o \to 0$.

Before proceeding with the developments necessary to complete the I.E. it is convenient to rewrite Eq. (2.19) in

the following form,

$$W_1(s_1^o) - \frac{1}{\pi}\int_{\Gamma_1} W_1(s_1)\, K_{11}(s_1,s_1^o)\, ds_1 - \frac{1}{\pi}\int_{\Gamma_2} W_2(s_2) K_{21}(s_2,s_1^o) ds_2 - \frac{1}{\pi}\int_{\Gamma_3} W_3(s_3)\, K_{31}(s_3,s_1^o)\, ds_3 = F_1(s_1) \qquad (2.20a)$$

$$W_2(s_2) - \frac{1}{\pi}\int_{\Gamma_1} W_1(s_1)\, K_{12}(s_1,s_2^o)\, ds_1 - \frac{1}{\pi}\int_{\Gamma_2} W_2(s_2) K_{22}(s_2,s_2^o) ds_2 - \frac{1}{\pi}\int_{\Gamma_3} W_3(s_3)\, K_{32}(s_3,s_2^o)\, ds_3 = F_2(s_2^o) \qquad (2.20b)$$

$$W_3(s_3) - \frac{1}{\pi}\int_{\Gamma_1} W_1(s_1)\, K_{13}(s_1,s_3^o)\, ds_1 - \frac{1}{\pi}\int_{\Gamma_2} W_2(s_2) K_{23}(s_2,s_3^o) ds_2 - \frac{1}{\pi}\int_{\Gamma_3} W_3(s_3) K_{33}(s_3,s_3^o)\, ds_3 = F_3(s_3^o) \qquad (2.20c)$$

In Eq. (2.20) the symbols s_i and s_i^o, i = 1 to 3 represent field and source points on the domains Γ_i. The kernel functions appearing in Eq. (2.20) are identified from their counterparts in Eq. (2.19).

The influence coefficients corresponding to adjacent

source points on the upper and lower wedge faces are calculated from Eqs. (2.20a) and (2.20c). As $\psi \to 0$ the coefficients become equal, one approaching the limit value from above and the other from below. This suggests that if a sum and difference state relating adjoining wedge face source points is formed then higher order functions necessary to complete the governing I.E. may be identified. A scalar δ_o which measures the distance from the crack tip to the paired source points is introduced. The sum and difference state is achieved by first adding and then subtracting Eqs.(2.20a) and (2.20c) from each other with the result:

$$\left(W_1(\delta_o) + W_3(\delta_o)\right) - \frac{1}{\pi}\int_{\Gamma_1} W_1(s_1)\left[K_{11}(s_1\delta_o) + K_{13}(s_1,\delta_o)\right] ds_1$$

$$- \frac{1}{\pi}\int_{\Gamma_2} W_2(s_2)\left[K_{21}(s_2,\delta_o)+K_{23}(s_2,\delta_o)\right] ds_2$$

$$- \frac{1}{\pi}\int_{\Gamma_3} W_3(s_3)\left[K_{11}(s_3,\delta_o)+ K_{13}(s_3,\delta_o)\right] ds_3$$

$$= F_1(\delta_o) + F_3(\delta_o) \qquad (2.21a)$$

$$W_2(s_2^o) - \frac{1}{\pi}\int_{\Gamma_1} W_1(s_1)\left[K_{12}(s_1,s_2^o)\, ds_1 - \frac{1}{\pi}\int_{\Gamma_2} W_2(s_2)K_{22}(s_2,s_2^o) ds_2\right.$$

$$\left. - \frac{1}{\pi}\int_{\Gamma_3} W_3(s_3)K_{32}(s_3,s_2^o)\, ds_2 = F_2(s_2^o)\right.$$

(2.21b)

$$\left(W_1(\delta_o) - W_3(\delta_o)\right) - \frac{1}{\pi}\int_{\Gamma_1} W_1(s_1)\left[K_{11}(s_1,\delta_o)-K_{13}(s_1,\delta_o)\right] ds_1$$

$$- \frac{1}{\pi}\int_{\Gamma_2} W_2(s_2)\left[K_{21}(s_2,\delta_o)+K_{23}(s_2,\delta_o)\right]ds_2$$

$$- \frac{1}{\pi}\int_{\Gamma_3} W_3(s_3)\left[K_{31}(s_3,\delta_o)- K_{33}(s_3,\delta)\right]ds_3$$

$$= F_1(\delta_o) - F_3(\delta_o) \qquad (2.21c)$$

The operation Lim $\psi_0 \to 0$ performed on Eqs. (2.21a) and (2.19a) leads to identical equations. Taking the limit as $\psi_0 \to 0$ in Eq. (2.21c) results in the null identity. This limiting character of Eq. (2.21c) suggests the following assumption concerning the dependence of the integrals upon ψ_0. Assume,

$$\frac{1}{\pi}\int W_1(s_1)\left[K_{11}(s_1,\delta_o)- K_{13}(s_1,\delta_o)\right]ds_1 = W_1(\delta_o)+O\left[\psi_o^n f_1(\delta_o)\right]$$

$$n\geq 1 \text{ as } \psi_o \to 0$$

$$\frac{1}{\pi}\int W_2(s_2)\left[K_{21}(s_2,\delta_o)- K_{23}(s_2,\delta_o)\right]ds_2 = O\left[\psi_o^n f_2(\delta_o)\right]$$

$$n \geq 1 \text{ as } \psi_o \to 0$$

$$\frac{1}{\pi}\int W_3(s_3)\left[K_{31}(s_3,\delta_o)- K_{33}(s_3,\delta_o)\right]ds_3 = -W_3(\delta_o)+O\left[\psi_o^n f_3(\delta_o)\right]$$

$$n \geq 1 \text{ as } \psi_o \to 0$$

$$F_1(\delta_o,\psi_o)- F_3(\delta_o,\psi_o) = O\left[\psi_o^n F_{(\delta_o)}\right] \quad n \geq 1 \text{ as } \psi_o \to 0 \qquad (2.22)$$

Then Eq. (2.21c) assumes the form,

$$W_1(\delta_o) - W_3(\delta_o) - \left(W_1(\delta_o) + \psi_o^n f_1(\delta_o)\right) + \psi_o^n \cdot f_2(\delta_o) + \left(W_3(\delta_o) + \psi_o^n \cdot f_3(\delta_o)\right) = \psi_o^n \cdot \bar{F}(\delta_o) \tag{2.23}$$

and after simplifying (2.23) it follows that

$$\psi_o^n \left[-f_1(\delta_o) + f_2(\delta_o) + f_3(\delta_o) - \bar{F}(\delta_o)\right] = 0 \tag{2.24}$$

Eq. (2.24) may be satisfied if ψ_o equals zero or by the bracketed quantity vanishing.

In the following it is assumed that the bracketed expression equals zero, thus implying the existence of an additional constraint equation.

The arguments presented in Eqs.(2.22) to (2.24) do not provide a convenient method for extracting the necessary equation, although its existence is implied. Assuming n is integer, it is more convenient to differentiate n times and take the limit as $\psi_o \to 0$ thus arriving at the bracketed quantity directly. Application of the technique shows that only one differentiation is required for the problem considered here.

Returning to the notation of Eq. (2.19) this leads

to the simple process

$$\lim_{\psi_o \to 0} \frac{\partial}{\partial \psi_o} \left\{ \text{Eq.(2.19a)} - \text{Eq.(2.19c)} \right\} \equiv \lim_{\psi_o \to 0} \frac{\partial}{\partial \psi_o} \text{ [Eq.2.21c]} \tag{2.26}$$

Executing these operations yields

$$\begin{aligned}
&\lim_{\psi_o \to 0} \left\{ \frac{\partial W_1(\delta_o)}{\partial \psi_o} - \frac{1}{\pi} \frac{\partial}{\partial \psi_o} \int_1^1 W_1(\delta) \frac{\delta_o \cdot \sin 2\psi_o}{\delta^2 - 2\delta \cdot \delta_o \cdot \cos^2 \psi_o + \delta_o^2} \, d\delta \right. \\
&- \frac{1}{\pi} \frac{\partial}{\partial \psi_o} \int_{\psi_o}^{2\pi - \psi_o} W_2(\theta) \left[\frac{1 - \delta_o \cdot \cos(\theta - \psi_o)}{1 - 2\delta_o \cdot \cos(\theta - \psi_o) + \delta_o^2} - \frac{1 - \delta_o \cdot \cos(\theta + \psi_o)}{1 - 2\delta_o \cdot \cos(\theta - \psi_o) + \delta_o^2} \right] d\theta \\
&\left. - \frac{\partial W_3(\delta_o)}{\partial \psi_o} + \frac{1}{\pi} \cdot \frac{\partial}{\partial \psi_o} \int_1^1 W_3(\delta) \frac{\delta_o \sin 2\psi_o}{\delta^2 - 2\delta \cdot \delta_o \cdot \cos 2\psi_o + \delta_o^2} \, d\delta \right. \\
&= \frac{1}{2} \cdot \frac{\partial}{\partial \psi_o} \int_{\psi_0}^{2\pi - \psi_0} T_z \, \text{Ln} \left\{ \frac{1 - 2\delta_o \cdot \cos(\theta - \psi_o) + \delta_o^2}{1 - 2\delta_o \cdot \cos(\theta + \psi_o) + \delta_o^2} \right\} d\theta
\end{aligned} \tag{2.27}$$

Eq.(2.27) will be shown to provide the additional information necessary to complete the I.E. representation of the closed crack anti plane problem. In the following a numerical-analytical technique is developed to allow refomulation of Eq. (2.27) into a non-singular integral equation thereby permitting direct numerical solution. The technique begins by identifying those integrals which exist only in the principal value sense in the limit as $\psi \to 0$; in this case,the integrals over the crack faces containing $W_{1(\delta)}$ and $W_{3(\delta)}$. The Cauchy singular kernel in

the integral precludes interchanging the limit, differentiation, and integral operators. To proceed, the singular points in each P.V. integral are identified and the integrals separated into three integration domains as follows:

$$\text{P.V.}\int_0^1 W_1(\delta)\ \ K(\delta,\psi_o)\ d\delta = \int_0^{\delta-H} W_1(\delta)\ \ K(\delta,\psi_o)\ d\delta$$
$$+\text{P.V.}\int_{\delta-H}^{\delta+H} W_1(\delta)\ K(\delta,\psi_o)\ d\delta + \int_{\delta+H}^{1} W_1(\delta)\ \ K(\delta,\psi_o)\ d\delta \qquad (2.28)$$

For example, $K(\delta\ \psi_o)$ may have the form

$$K(\delta,\psi_o) \equiv \frac{\delta_o \cdot \sin 2\psi_o}{\delta^2 - 2\delta\cdot\delta_o\cdot\cos 2\psi_o + \delta_o{}^2}$$

$K(\delta,\psi_o)$ is singular for $\delta = \delta_o$ in the Lim $\psi_o \to 0$. The integrals

$$\int_0^{\delta-H} W_{1(\delta)}\ K(\delta,\psi_o)\ \ d\delta\ \ ,\ \ \int_{\delta+H}^{1} W_1(\delta)\ K\ (\delta,\psi_o)\ d\delta$$

are Riemann integrable and sufficiently well-behaved to permit interchange of differentiation and limit operations with the integral. The P.V. integral in Eq.(2.28) has been restricted to the domain of integration

$\delta_0 - H \leq \delta \leq \delta_o + H$. The value H is selected to be real and positive such that it is always less than or equal to the smallest value of δ_o. Since the numerical solution of the integral equations proceeds by the method of finite differences requiring satisfaction of the equations at a finite number of collocated points, H is conveniently chosen as the value of the division size.

Further analysis of the P.V. integral requires an approximation of the functional behavior of the displacements on the crack surfaces. The $\sqrt{\delta}$ functional dependence near the crack tip is well documented (34,35). A two term approximation for the crack tip displacements in the domain $\delta_o - H \leq \delta \leq \delta_o + H$ is selected which generally takes the form:

$$W_{1(\rho)} \doteq C_1 \delta^{\gamma} + C_2$$

For surfaces near the crack tip, a value of $\gamma = 1/2$ is used. The linear form $\gamma = 1$ is used for surfaces removed from the crack tip.

The constants C_1 and C_2 are dependent on the values of γ selected as well as the values of the unknown displacements evaluated at points $\delta = \delta_o - H$, δ_o, and $\delta_o + H$.

The Cauchy principal value integral may now be

approximated by

$$\text{P.V.} \int_{\delta_0-H}^{\delta_0+H} W_1 \cdot K(\delta,\psi_o)\, d\delta = C_1 \text{ P.V.} \int_{\delta_0-H}^{\delta_0+H} \delta^{\gamma} \cdot K(\delta,\psi_o)\, d\delta$$

$$+ C_2 \cdot \text{P.V.} \int_{\delta_0-H}^{\delta_0+H} K(\delta,\psi_o)\, d\delta \equiv C_1 \cdot J_1(\psi_o) + C_2 \cdot J_2(\psi_o)$$

The P.V. integrals $J_{1(\psi_o)}$ and $J_{2(\psi_o)}$ are analytically evaluated. Differentiation w.r.t. ψ_o followed by $\text{Lim}_{\psi_o \to 0}$ are operations easily performed on the resulting closed form expressions for $C_1 J_{1(\psi_o)} + C_2 J_{2(\psi_o)}$. Analytical expressions result which depend on the value of γ and are called insert functions. Performing the remaining operations in Eq.(2.27) yields the desired equation.

A system of integral equations which result from $\text{Lim}_{\psi_o \to 0}$ (Eq.2.21) may now be written. Using the detailed notation of Eq. (2.19) and completing the details for Eqs. (2.21a,b) yields

$$- W_1(\delta_o) + \frac{1}{\pi} \int_o^{2\pi} W_2(\theta) \frac{1-\delta_o \cdot \cos\theta}{1-2\delta_o \cdot \cos\theta + \delta_o^2}\, d\theta - W_3(\delta_o)$$

$$= \frac{1}{4\pi} \int_o^{2\pi} T_z(\theta) \cdot \text{Ln} \left\{ 1-2\delta_o \cdot \cos\theta + \delta_\ell^2 \right\}^2 d\theta .$$

(2.29a)

$$\frac{1}{\pi}\int_0^1 W_1(\delta)\left[\frac{\sin\theta_o}{\delta^2-2\delta\cdot\cos\theta_o+1}\right]d\theta \;-\; W_2(\theta_o)$$

$$+\frac{1}{\pi}\int_0^{2\pi} W_2(\theta)\,\frac{1}{2}\,d\theta \;-\; \frac{1}{\pi}\int_0^1 W_3\left[\frac{\cos\theta_o}{\delta^2-2\delta\cdot\cos\theta_o+1}\right]d\delta$$

$$=\frac{1}{4\pi}\int_0^{2\pi} T_z(\theta)\;\;\mathrm{Ln}\;\left\{2-2\cos(\theta-\theta_o)\right\}^2 d\theta \qquad (2.29b)$$

while from Eq. (2.21c) it follows that

$$\frac{1}{\pi}\int_0^{\delta_o-H} W_1(\delta)\left[\frac{2\delta_o}{(\delta-\delta_o)^2}\right]d\delta \;+\; \frac{1}{\pi}\int_{\delta_o+H}^1 W_1(\delta)\left[\frac{2\delta_o}{(\delta-\delta_o)^2}\right]d\delta$$

$$-\,W_1(\delta)\,\frac{1}{\pi}\,\frac{2\sqrt{\delta_o}}{H}\left(\sqrt{\delta_o+H}+\sqrt{\delta_o-H}\right)+\mathrm{Ln}\left[\frac{(\sqrt{\delta_o}-\sqrt{\delta_o-H})}{(\sqrt{\delta_o}+\sqrt{\delta_o-H})}\cdot\frac{(\sqrt{\delta_o}+\sqrt{\delta_o+H})}{(\sqrt{\delta_o+H}-\sqrt{\delta_o})}\right]$$

$$+\frac{1}{\pi}\int_0^{2\pi} W_2(\theta)\left[\frac{2\delta_o(1-\delta_o^2)\,\sin\theta}{(1-2\delta_o\cos\theta+\delta_o^2)}\right]d\theta$$

$$+\,W_3(\delta_o)\,\frac{1}{\pi}\,\frac{2\sqrt{\delta_o}}{H}\left(\sqrt{\delta_o+H}+\sqrt{\delta_o-H}\right)+\mathrm{Ln}\left[\frac{(\sqrt{\delta_o}-\sqrt{\delta_o-H})}{(\sqrt{\delta_o}+\sqrt{\delta_o-H})}\cdot\frac{(\sqrt{\delta_o}+\sqrt{\delta_o+H})}{(\sqrt{\delta_o+H}-\sqrt{\delta_o})}\right]$$

$$-\frac{1}{\pi}\int_0^{\delta_o-H} W_3(\delta)\left[\frac{2\delta_o}{(\delta-\delta_o)^2}\right]d\delta \;-\; \frac{1}{\pi}\int_{\delta_o+H}^1 W_3(\delta)\left[\frac{2\delta_o}{(\delta-\delta_o)^2}\right]d\delta$$

$$=-\frac{1}{\pi}\int_0^{2\pi} T_z(\theta)\left[\frac{2\delta_o\,\sin\theta}{1-2\delta_o\cos\theta+\delta_o^2}\right]d\theta \qquad (2.29c)$$

In the foregoing

$$\rho \varepsilon [0,1] \qquad \theta \varepsilon [0,2\pi]$$

$$\rho \varepsilon [0,1] \qquad \theta_0 \varepsilon [0,2\pi]$$

and T_z are normalized tractions prescribed on the circular boundary. Eq. (2.29c) incorporates the insert function assuming piecewise square root displacements on the crack surface, i.e. $\gamma = \frac{1}{2}$.

Investigation of the set of integral equations (2.29) shows them to be a quasi-regular system of Fredholm equations of the second kind as defined in Muskhelishivili, pp. 415-417 (32). This assures that a unique solution exists. It remains to show by example that this solution represents the cracked anti-plane boundary value problem of elasticity.

A numerical solution of Eq. (2.29) was obtained. The details of this numerical technique shall be discussed in a special section in Chapter 3. Comparison with the right circular cylinder ($\psi_o = 0$) problem discussed earlier, for loading $T_{z(\theta)} = \frac{1}{2} \cos \frac{\theta}{2}$ tractions, provides the necessary verification. The numerically determined displacement field on the boundary surfaces were accurate within 1% as compared to the analytical solution. These results confirm the limiting process developed for the anti-plane crack problem. Eq. (2.29) may now be assumed to be a complete formulation of the anti-plane cracked body

problem of elasticity.

2.3 The Plane Elastostatic Cracked Body Integral Equations

The plane elastostatic cracked body integral equations are developed by extension and generalization of the techniques used in the anti-plane problem. A traction loaded plane body with m number of edge cracks as shown in Fig.4a is considered. Fig. 4b illustrates the modified "open" crack geometry necessary to begin the analysis. This geometry retains the sharp crack tips and corner point description. Each open crack surface and all external boundaries are modeled by continuous parametric expressions which best lend themselves to the shape under consideration. A single parameter ψ_o is chosen which allows modeling the modified geometry of Fig. 4b and, for the $\lim_{\psi_o \to 0}$, yields the closed crack geometry of Fig. 4a. The Kth crack surfaces are labeled C_K^u, C_K^L where the upper (u) surface has been arbitrarily chosen to differentiate it from the opposite crack face, called the lower (L) face. The set of all crack surfaces $C_1^u + C_1^L + \cdots + C_K^u + C_K^L + \cdots + C_m^u + C_m^L$ is designated C. The external boundary is labeled S.

The plane elastostatic system of I.E. (2.14) applies directly to the modified geometry with the exclusion of crack tip and corner reference points. The exclusion of these points eliminates the need for rounding the corners which introduces additional complexities. As in the anti-plane problem no theoretical compromise or numerical

inconvenience occurs from this restriction.

This coupled pair of I.E. is separated into parts by writing individual equations for each crack surface and external boundary. Recalling Eqs. (2.5) and (2.7) for definitions of U_{ij} and T_{ij}, Eq. (2.14) assumes the form

$$
\begin{aligned}
&u_\beta(P_K^u) - 2\ \underline{\alpha} \int_{C_K^u} u_\alpha(Q_K^u)\ T_{\alpha\beta}(P_K^u, Q_K^u)\ dS(Q_K^u) \\
&- 2\ \underline{\alpha} \int_{C_K^L} u_\alpha(Q_K^L)\ T_{\alpha\beta}(P_K^L)\ dS(Q_K^L) \\
&- 2\ \underline{\alpha} \int_{C_1^u + C_2^u + C_{K-1}^u + C_{K+1}^u + \ldots C_M^u} u_\alpha(Q^u)\ T_{\alpha\beta}(P_K^u, Q)\, dS(Q^u) \\
&- 2\ \underline{\alpha} \int_{C_1^L + C_2^L + \ldots + C_{K-1}^u + C_{K+1}^u + \ldots C_M^u} u_\alpha(Q^L)\ T_{\alpha\beta}(P_K^u, Q)\ dS(Q^L) \\
&-2\ \underline{\alpha} \int_S u_\alpha(Q_S)\ T_{\alpha\beta}(P_K^u, Q)\ dS(Q_s) \\
&= -2\ \underline{\alpha} \int_{C+S} t_\alpha(Q)\ U_{\alpha\beta}(P_K^u, Q)\ dS(Q)
\end{aligned}
$$

(2.30β uK)

$$u_\beta(P_s) - 2\,\underline{\alpha}\int_C u_\alpha(Q)\; T_{\alpha\beta}(P_S,Q)\; dS(Q)$$

$$-2\,\underline{\alpha}\int_S u_\alpha(Q_s)\; T_{\alpha\beta}(P_s,Q_s)\; dS(Q_s)$$

$$= -2\,\underline{\alpha}\int_{C+S} t_\alpha(Q)\; U_{\alpha\beta}(P_s,Q)\; dS(Q)$$

(2.30βS)

$$u_\beta(P_K^L) - 2\,\underline{\alpha}\int_{C_K^u} u_\alpha(Q_K^L)\; T_{\alpha\beta}(P_K^L,Q_K^u)\; dS(Q_K^u)$$

$$-2\,\underline{\alpha}\int_{C_K^L} u_\alpha(Q_K^L)\; T_{\alpha\beta}(P_K^L,Q_K^L)\; dS(Q_K^L)$$

$$-2\,\underline{\alpha}\int_{C_1^u+C_2^u+\ldots+C_{K-1}^u+C_{K+1}^u+\ldots C_m^u} u_\alpha(Q^u)\; T_{\alpha\beta}(P_K^L,\,Q)\; dS(Q^u)$$

$$-2\,\underline{\alpha}\int_{C_1^L+C_2^L+\ldots+C_{K-1}^L+C_{K+1}^L+\ldots+C_m^L} u_\alpha(Q^L)\; T_{\alpha\beta}\;(P_K^u,Q)\; dS\;(Q^L)$$

$$-2\,\underline{\alpha}\int_S u_\alpha\;(Q_s)\,T_{\alpha\beta}(P_K^L,Q)\; dS(Q_s)$$

$$= -2\,\underline{\alpha}\int_{C+S} t_\alpha(Q)\,U_{\alpha\beta}(P_K^L,\,Q)\; ds\;(Q)$$

(2.30βLK)

where

$\alpha = 1,2 \qquad \beta = 1,2 \qquad K = 1,m$ (no sum on K)

Eqs. (2.30) may be considered as a system of coupled integral equations. The K index represents the decomposition of the I.E. over the selected crack faces. Eqs. (2.30βuK) represent the subset of equations whose reference points lie on upper crack surfaces, there being K = 1,2..m such equations, one for each crack. In like manner, Eq. (2.30βLK) represents m equations whose reference points lie on the lower surfaces. Eq. (2.30βS) is the remaining equation for reference points located on the external boundary S. As an example of this notation, the function $u_\beta(P_K^u)$ is interpreted as the displacements in the x_β direction for the set of points P_K^u which lie on the upper surface of the Kth crack. The kernel, $T_{\alpha\beta}(P_K^u, Q_K^L)$, is the function defined in Eq. (2.7) evaluated for reference points on the upper Kth crack surface (P_K^u) and field points on the lower Kth crack surface (Q_K^L). Integration variables containing sub or superscripts assume their normal meaning.

The rewriting of Eq.(2.14) as Eq. (2.30) permits the separation of the integrals into Cauchy principal value and Riemann integrals. In both Eq. (2.30βuK) and Eq. (2.30βLK), the P.V. integrals appear as the first two integrals in the equation, the remaining integrals being

Riemann integrals. In Eq. (2.30βS), the integrals over the boundary S exist only in the P.V. sense, all others are Riemann integrable.

The similarity of Eq. (2.30) to the governing I.E. for the anti-plane problem is evident. It may be shown that the kernel functions in Eq. (2.30) and those in the anti-plane representation, Eq. (2.19), have similar behavior. The kernels are still Cauchy singular although tne complexity of the kernel functions increases greatly. This result could be anticipated since both formulations rest upon the same mathematical development. Following a similar approach as in the Mode III problem a complete set of governing I.E. is formulated for Mode I and II problems. Proceeding as in the Mode III case, Eq. (2.30) is recombined and a $\lim_{\psi_o \to 0}$ operation performed in the following sequence.

$$\lim_{\psi_o \to 0} \left\{ \text{Eq. (2.24}\beta\text{uK)} + \text{Eq.(2.24}\beta\text{LK)} \right\} \tag{2.31a}$$

$$\lim_{\psi_o \to 0} \left\{ \text{Eq.(2.24}\beta\text{S)} \right\} \tag{2.31b}$$

$$\lim_{\psi_o \to 0} \frac{\partial}{\partial \psi_o} \left\{ \text{Eq.(2.24}\beta\text{uK)} - \text{Eq.(2.24}\beta\text{LK)} \right\} \tag{2.31c}$$

where $\beta = 1,2$, $K = 1,2 \ldots m$

The above operations are performed for each β, K

equation with special care exercised for those integrals which have Cauchy singularities. Eq. (2.30a) and (2.30c) each yield a minimum of 2m equations and Eq. (2.30b) yields a minimum of two more equations. Thus, a geometry with m external cracks requires a minimum system of 4m + 2 coupled integral equations. Complicated crack or external boundary shapes, requiring multiple parametric representation may require further decomposition of the equations with a commensurate increase in the system of governing equations.

An example problem is solved using the geometry of Fig. 2 for $\psi_o = 0$ and for surface tractions resulting in both Mode I and Mode II states. The detailed results are reported in the next chapter and compare within 1% to the exact analytical solution. The accuracy of the solution of Eq. (2.29) for the anti-plane Mode III example and Eq. (2.31) for the plane, Mode I, II case gives a numerical verification of the effectiveness of the method.

CHAPTER 3

MODE I AND II PROBLEM STATEMENT AND INTEGRAL REPRESENTATION

The solution technique for Mode I, II and III loading developed in Chapter 2 requires numerical verification. A circular disk with a simple edge crack is selected for study because it possesses a known closed form analytical solution for certain specific boundary conditions. This disk is in a state of plane strain and subjected to Mode I & II loading.

An accurate solution of this problem via Eqs. (2.31) serves as a numerical verification of the plane elastostatic solution method. A bent crack geometry which has drawn considerable attention [36,37] recently for application to mixed mode fracture is also considered to demonstrate the general applicability of the method. This geometry is asymetric and involves stress singularities at the bend vertex in addition to those at the crack tip. A limiting case of this geometry is the straight crack; therefore only the general bent crack formulation needs to be presented, since both straight crack and bent crack results follow. The bent crack problem statement and equation formulation is presented in Sec. 3.1, and the development of the numerical solution technique is discussed in Sec. 3.2. The mode III problem was extensively discussed in Sec. 2.2. It's numer-

ical solution is obtained by a similar process to that presented in Sec. 3.2 and need not be discussed further.

3.1 Bent Crack Problem Formulation

A cracked circular domain of radius R, as shown in Fig. 5, is considered. A cartesian coordinate system, xy, having its origin at the disk center,is employed. A straight crack of length d intersects the circular surface and lies on the x axis in the region $x\varepsilon[f,R]$. At x=f a secondary straight crack of length $\underline{c}$ emanates at an angle α to the x-axis. The values of $\underline{c}$, d, and α are restricted only by the requirement that the secondary crack must not penetrate the circular boundary S. Solutions for the traction boundary value problem for several loadings on the external surfaces are to be obtained numerically.

Analysis of this problem begins with the construction of the modified open crack geometry shown in fig. 6. The secondary crack is opened from the crack tip by an angle $2\psi_o$ so the primary crack has uniform separation $2g=2\underline{c}\cdot\cos\alpha\cdot\tan\psi_o$. The x-coordinate value of the crack tip is labeled e while the projection of $\underline{c}$ on x is denoted by $\underline{c}$. The individual surfaces forming the boundary are identified by Γ_i, i=1,2···5 (see Fig. 6). A normalized geometry, Fig. 7, is obtained by dividing all length variables by the radius R, capital letters denoting the normalized variables. On the bent crack surfaces Γ_1, Γ_5, the distance from the crack tip, ρ, locates field points, while B iden-

tifies source point locations. On the straight crack surfaces Γ_2, Γ_4, field points are located by the variable $\overline{x1}$ and source points by B_2, both measured from the coordinate origin . On the circular boundary Γ_3, the radian measure θ locates field points and θ_o the source points. As previously discussed the modified geometry needs no crack tip or corner rounding if the set of reference variables are restricted to an open set excluding these points.

The pair of coupled B.I.E. (2.14) apply directly to the modified bent crack geometry with crack tip and corner points excluded from the reference set. Eqs. (2.14) are separated into five parts by writing individual equations for reference points located on the discrete Γ_i boundaries. This decomposition permits examination of the P.V. integrals and allows application of the solution method discussed in Chapter 2. Thus, Eq. (2.14) yields.

$$\frac{-1}{\underline{\lambda}}\, u_J(P) + \int_0^{\underline{C}/\cos\psi_o} [u_1(\rho)\cdot KI_{J1}(P,\rho) + v_1(\rho)\cdot KII_{J1}]\,d\rho$$

$$+ \int_{F+C\cdot\tan\psi_o\cdot\tan\alpha}^{1} [u_2(\overline{x1})\, KI_{J2}(P,\overline{x1}) + v_2(\overline{x1})\cdot KII_{J2}]\, d\,\overline{x1}$$

$$+ \int_{C\cdot\tan\psi_o}^{2\pi-C\cdot\tan\psi_o} [u_3(\theta)\cdot KI_{J3}(P,\theta) + v_3(\theta)\cdot KII_{J3}]\,d\theta$$

$$+ \int_{F-C\cdot\tan\psi_o\cdot\tan\alpha}^{1} \left[u_4(\bar{x1}) \cdot KI_{J4}(P,\bar{x1}) + v_4(\bar{x1}) \cdot KII_{J4} \right] d\bar{x1}$$

$$+ \int_{0}^{\underline{C}/\cos\psi_o} \left[u_5(\rho) \cdot KI_{J5}(P,\rho) + v_5(\rho) \cdot KII_{J5} \right] d\rho$$

$$= F_J^A(P)$$

(3.1AJ)

$$-\frac{1}{\underline{\lambda}} v_J(P) + \int_{0}^{\underline{C}/\cos\psi_o} \left\{ u_1(\rho) \cdot KIII_{J1}(P,\rho) + v_1(\rho) \cdot KIV_{J1} \right\} d\rho$$

$$+ \int_{F+C\cdot\tan\psi_o\cdot\tan\alpha}^{1} \left\{ u_2(\bar{x1}) \cdot KIII_{J2}(P,\bar{x1}) + v_2(\bar{x1}) \cdot KIV_{J2} \right\} d\bar{x1}$$

$$+ \int_{C\tan\psi_o}^{2\pi-C\cdot\tan\psi_o} \left\{ u_3(\theta) \cdot KIII_{J3}(P,\theta_o) + v_3(\theta) \cdot KIV_{J3} \right\} d\theta$$

$$+ \int_{F-C\cdot\tan\psi_o\cdot\tan\alpha}^{1} \left\{ u_4(\bar{x1}) \cdot KIII_{J4}(P,\bar{x1}) + v_4(\bar{x1}) \cdot KIV_{J4} \right\} d\bar{x1}$$

$$+ \int_{0}^{\underline{C}/\cos\psi_o} \left[u_5(\rho) \cdot KIII_{J5}(P,\rho) + v_5(\rho) \cdot K\ IV_{J5} \right] d\rho$$

$$= F_J^B(P)$$

(3.1BJ)

where

$$KI_{JL}(P,Q) \equiv \left\{ K - 4 \cdot \mu \cdot M \cdot R_{JL,x} \right\} \frac{\partial Ln\ R_{JL}}{\partial n_L}$$

$$KII_{JL}(P,Q) \equiv \left\{ -4 \cdot \mu \cdot M \cdot R_{JL,y} \cdot R_{JL,x} \right\} \frac{\partial Ln R_{JL}}{\partial n_L}$$

$$+ K \cdot \left\{ (Ln\ R_{JL}),y\ \eta_x - (Ln\ R_{JL}),x\ \eta_y \right\}$$

$$KIII_{JL}(P,Q) \equiv \left\{ -4 \cdot \mu \cdot M \cdot R_{JL,y} \cdot R_{JL,x} \right\} \frac{\partial Ln R_{JL}}{\partial n_L}$$

$$-K \left\{ [(Ln\ R_{JL}),y\ \eta_x - (Ln\ R_{JL}),x\ \mu y] \right\}$$

$$KIV_{JL}(P,Q) \equiv \left\{ [K - 4 \cdot \mu \cdot M \cdot R_{JL,y}\ R_{JL,y}] \right\} \frac{\partial\ Ln\ R_{JL}}{\partial n_L}$$

$$F_J^A(P) \equiv \sum_{L=1}^{5} \frac{1}{\Delta} \int_{\Gamma_L} \{ t_{xL}(Q) \cdot (\tfrac{1}{2} \operatorname{Ln} R^2_{JL} + M \cdot R_{JL,x} R_{JL,x})$$

$$+ t_{yL}(Q) \cdot M \cdot R_{JL,x} \cdot R_{JL,y} \} \, dS_L(Q)$$

$$F_J^B(P) \equiv \sum_{L=1}^{5} \frac{1}{\Delta} \int_{\Gamma_L} \{ t_{yL}(Q) \cdot (\tfrac{1}{2} \operatorname{Ln} R^2_{JL} + M \cdot R_{JL,y} R_{JL,y}$$

$$+ t_{xL}(Q) \cdot M \cdot R_{JL,x} \cdot R_{JL,y} \} \, dS_L(Q)$$

J,L = 1,2, ... 5 no sum on repeated indices unless indicated

$$R_{JL} = \left\{ (X_J(Q) - X_L(P))^2 + (Y_J(Q) - Y_L(P))^2 \right\}^{\frac{1}{2}}$$

n_L = unit normal on surface Γ_L

$M \equiv -(\lambda+\mu)/(\lambda+3\mu)$

$K \equiv 2\mu^2/(-\lambda+3\mu)$

$\underline{\lambda} \equiv -(\lambda+3\mu)/2\pi\mu(\lambda+2\mu))$

μ,λ are Lamé's material constants.

In the notation of Eq. (3.1 AJ) and (3.1BJ), J takes on values from 1 to 5 creating a system of ten coupled equations. The reference point variable P is understood to have meaning B, B_2 or θ_0 depending on the Γ_i reference surface for which the equation applies. The kernel functions KI_{JL}, $KIII_{JL}$, $KIII_{JL}$, and KIV_{JL} defined in Eq. (3.1), are presented in algebraic detail in Appendix A. Kernels having repeated indices in Eq. (3.1 AJ) and (3.1 BJ) are singular in the lim $\psi_o \to 0$ and integrals containing such kernels exist only in the Principal Value sense.

To proceed, form a sum and difference state on those equations having source points on the crack surfaces. This is followed by the limiting operation lim $\psi_o \to 0$, after differentiation with respect to ψ_o in the case of the differen-

ce equations. These operations may be summarized as follows:

$$\lim_{\psi_0 \to 0} \{\text{Eq. (3.1 A 1)} + \text{Eq. (3.1 A 5)}\} \qquad (3.2\ \text{A 1})$$

$$\lim_{\psi_0 \to 0} \{\text{Eq. (3.1 A 2)} + \text{Eq. (3.1 A 4)}\} \qquad (3.2\ \text{A 2})$$

$$\lim_{\psi_0 \to 0} \{\text{Eq. (3.1 A 3)}\} \qquad (3.2\ \text{A 3})$$

$$\lim_{\psi_0 \to 0} \{\frac{\partial}{\partial \psi_0}[\text{Eq. (3.1 A 2)} - \text{Eq. (3.1 A 4)}]\} \qquad (3.2\ \text{A 4})$$

$$\lim_{\psi_0 \to 0} \{\frac{\partial}{\partial \psi_0}[\text{Eq. (3.1 A 1)} - \text{Eq. (3.1 A 5)}]\} \qquad (3.2\ \text{A 5})$$

$$\lim_{\psi_0 \to 0} \{\text{Eq. (3.1 B 1)} + \text{Eq. (3.1 B 5)}\} \qquad (3.2\ \text{B 1})$$

$$\lim_{\psi_0 \to 0} \{\text{Eq. (3.1 B 2)} + \text{Eq. (3.1 B 4)}\} \qquad (3.2\ \text{B 2})$$

$$\lim_{\psi_0 \to 0} \{\text{Eq. (3.1 B 3)}\} \qquad (3.2\ \text{B 3})$$

$$\lim_{\psi_0 \to 0} \frac{\partial}{\partial \psi_0}\{[\text{Eq. (3.1 B 2)} - \text{Eq. (3.1 B 4)}]\} \qquad (3.2\ \text{B 4})$$

$$\lim_{\psi_0 \to 0} \frac{\partial}{\partial \psi_0}\{[\text{Eq. (3.1 B 1)} - \text{Eq. (3.1 B 5)}]\} \qquad (3.2\ \text{B 5})$$

The mathematical operations indicated in equation (3.2) are performed using the techniques discussed in Section 2.2. The singularities are removed by assuming a piece-wise functional behavior for the unknown displace-

ments followed by analytical evaluation in the neighborhood of the singular point of each principal value integral. A key requirement for the successful performance of this analytical step is knowledge of the correct functional behavior of the unknown displacements. Fortunately, this behavior is well known.

In general a satisfactory representation is given by $u = C_1 \xi^{\gamma} + C_2$ where the selection of the parameter γ depends upon the surface in question. This selection of γ is treated in detail in Section 3.2. The analytical evaluation of the integrals in the neighborhood of the singular regions results in algebraic functions labeled insert functions. The equations which result are a coupled system of simultaneous non-singular integral equations of the second kind.

The completed equation set (3.2) is presented in Appendix B. Section B.1 contains the functional form of the integral equations, detailing the geometric kernel function. Section B.2 contains three sets of insert functions, one for each of three classes of assumed displacement functionals. Section B.3 presents the detailed forcing functions for general traction loading on all surfaces.

3.2 Numerical Solution Technique

The numerical solution of Eqs. (3.2) proceeds directly by employing the standard methods developed for non-singular Fredholm equations of the second kind. A finite

number of mesh points partition the boundaries Γ_i. The integrals in (3.2) are similarly partitioned and the unknown displacements approximated within these intervals. The integrals are numerically evaluated, resulting in a set of influence coefficients which operate on the unknown displacement vector evaluated at discrete mesh points. The continuous representation of Eqs. (3.2) is thus transformed into a linear system of algebraic equations.

The left side of Eqs. (3.2) shown in Section B.1 leads to the algebraically equivalent system involving the influence coefficient matrix and displacement column vector. The right side of (3.2) generates a column vector of forcing functions representing the traction loading.

$$[\ C\ ]\ \{\ u\ \} = \{\ F\ \} \qquad (3.3)$$

The resulting matrix equation (3.3) after row elimination or coefficient substitution for the supression of rigid body motion may be solved directly. Calculation of the influence coefficients forming the [C] matrix begins by partitioning the boundary as illustrated in Fig. 8. M1 points are located on Γ_1 and Γ_5 with equal spacing H1=C/(M1 + .5). The last reference point on Γ_1 or Γ_5 is located H1/2 distance from the bend vertex. Surface Γ_2 and Γ_4 contain M2 points spaced H2 = D/(M2 + .5) apart. The mesh point nearest the bend vertex is again spaced H2/2 from the bend point. A total of M3 reference points are equally spaced on Γ_3 with H3 = 2π/(M3 + 1). No reference points are located on the

crack tip, bend vertex, or crack corners.

The numerical evaluations of the integrals proceeds by employing the partition just described. The unknown displacements are approximated in a piecewise manner by the function

$$u \doteq A_n \, \xi^{\gamma} + C_n \qquad \gamma \varepsilon \, [\tfrac{1}{2}, 1] \tag{3.4}$$

where ξ is understood to be δ, $\overline{x1}$ or θ depending on the integration domain. A_n and C_n are coefficients involving the unknown displacements at the mesh points. Then, a typical integral term in (3.2) may be written as

$$\int_0^{B-H_1} u_1(\rho) \; K(\rho,\beta) \, d\rho = \sum_{n=0}^{N} \int_{n \cdot H_1}^{(n+1) \, H_1} u_1(\rho) \; K(\rho,\beta) \, d\rho$$

$$\doteq \sum_{n=o}^{N} A_n \int_{n \cdot H_1}^{(n+1) H_1} \rho^{\gamma} K(\rho,\beta) \, d\rho + C_n \int_{n \cdot H_1}^{(n+1) H_1} K(\rho,\beta) \, d\rho \tag{3.5}$$

The integrals appearing in Eq. (3.5) are further partitioned into an even number of M subintervals and numerically evaluated by Simpson's rule.

The insert functions discussed earlier and presented in App. B.2 contribute the dominant diagonal coefficients in the "C" matrix. These functions result from the analytical evaluation of the P.V. contribution and their accuracy is

directly dependent on the quality of the assumed unknown displacement function. The non-singular integrals in the near neighborhood of the singular points also result in large coefficients located in a band on either side of the diagonal elements. The accuracy of these coefficients is dependent on both the quality of the assumed displacement function and the accuracy of the numerical integration.

The functional behavior of the boundary displacement near the crack tip and bend vertex are well documented. [36, 38, 39]. The numerical analysis uses the square root functional, $\gamma=\frac{1}{2}$, for M1-2 partitions on Γ_1 and for M1-4 divisions on Γ_5. The bend corner formed by the common point on Γ_4 and Γ_5 is similar to a sharp wedge [39]. The displacement field in the neighborhood of the wedge vertex has the form (3.4) with γ determined from the first positive real root of the transcendental equation

$$\sin(\gamma[\pi+\alpha]) + \gamma\cdot\sin(\pi+\alpha) = 0 \qquad (3.6)$$

Values of $\alpha\varepsilon(0,\pi)$ result in $\gamma\varepsilon(\frac{1}{2},1)$.

This displacement approximation was employed for numerical integration of the non-singular integrals and for the analytical evaluation of the insert functions over a ten reference point domain. This domain includes 5 mesh points on Γ_4 and 5 points on Γ_5 surrounding the vertex surfaces. By restricting the bent crack angle α to be positive a linear displacement function suffices on the upper bend vertex. This is appropriate because under these conditions only the

lower surface possesses a singular behavior near the vertex [34,39,40]. On all of the remaining surfaces, the displacement components are modeled by piecewise linear functions. It should be noted that to insure compatibility of results similar displacement functions were assumed for both the analytically determined insert functions and the numerically integrated coefficients, depending on the surface of integration.

The accuracy of the numerical integration is ascertained by conducting numerical experiments on the most sensitive integrals. Taking advantage of the 16 digit accuracy of the CDC 6600 computer and using the simple Simpson's formula, most integrals are successfully evaluated ($<<1\%$ error) by a subpartition of $M = 20$. The most sensitive kernels require $M = 250$. In this manner the geometric influence coefficients forming [C] are calculated. The matrix [C] is full with the dominant influence coefficients banded along the diagonal.

Generation of the forcing function matrix proceeds by direct use of the Simpson approximation. Statement of the traction loading on each boundary completes the definition of the integrals shown in App. B.3 and evaluation proceeds by direct numerical integration. A partition of two-hundred evenly spaced points for each surface provides accurate results ($<1\%$ error).

This numerical reduction of the integral equations reduces Eqs. (3.2) to a system of $2\{\cdot 2\cdot(M1+M2) + M3\}$ algebraic equations in the same number of unknowns. Solution of this algebraic system by standard numerical methods then leads to the values of the displacement components at the mesh points.

The necessary computations for the examples presented herein were performed on a CDC 6600 computer. This computer features sixteen digit accuracy; thus, no special double precision operations were utilized. The program requirements dictated M1 = 8, M2 = 7, and M3 = 11 as minimum values for the general bent crack problem. The upper limit was established by accuracy requirements ($\sim$1%) and seldom exceeded 130 equations. This equation size required 130,000 memory units and sixty seconds to compute coefficients and solve the equations.

CHAPTER 4

NUMERICAL EXAMPLES AND DISCUSSION

Attention is now turned to two classes of problems. The first consists of two problems for which analytical solutions exist, thus permitting verification of the solution method. The second class of problems presents results for the bent crack as a function of crack angle and loading mode.

4.1 Numerical Verification Examples

EXAMPLE #1. The circular disk with a straight edge crack equal to the plate radius has an analytic closed form solution for specific traction loadings. This geometry is a special case of the bent crack shown in Fig. 5 with α equal to zero and c plus d equal to R. The governing biharmonic equation for the Airy stress function is solved using the technique developed by Williams (34,35). A traction loading, equivalent to the first term in the Williams' solution, is thus generated to develop a special problem possessing a closed form solution. A problem summary of the required traction loadings and the resulting displacements for each boundary surface follows using the notation in Chapter 3;

Traction Loading on Boundary Surfaces:

upper crack face Γ_1: $t_{x1} = t_{y1} = 0$

Γ_2: $t_{x2} = t_{y2} = 0$

lower crack face Γ_4: $t_{x4} = t_{y4} = 0$

Γ_5: $t_{x5} = t_{y5} = 0$

circular boundary Γ_3:

$$t_{x3} = \frac{K_I}{\sqrt{2\pi}} \sin\frac{\theta}{2}\left\{3\cdot\cos^2\left(\frac{\theta}{2}\right) - 1\right\} + \frac{K_{II}}{\sqrt{2\pi}} \cos\frac{\theta}{2}\left\{3\cos^2\left(\frac{\theta}{2}\right) - 1\right\}$$

$$t_{y3} = \frac{K_I}{\sqrt{2\pi}} \sin\frac{\theta}{2}\left\{\frac{3}{2}\sin\theta\right\} + \frac{K_{II}}{\sqrt{2\pi}} \sin\frac{\theta}{2}\left\{3\cos\left(\frac{\theta}{2}\right) - 1\right\}$$

Dimensionless Displacements in x-direction:

Γ_1: $u_{1(\rho)} = C_o\sqrt{\rho}\cdot K_{II}$

Γ_2: $u_{2(x1)} = C_o\sqrt{\bar{x}1}\, K_{II}$

Γ_4: $u_{4(x1)} = -C_o\sqrt{\bar{x}1}\, K_{II}$

Γ_5: $u_{5(\rho)} = -C_o\sqrt{\rho}\, K_{II}$

$$\Gamma_3: \quad u_3(\theta) = \frac{C_o}{2} K_I \left\{ \cos\theta \cdot \sin\left(\frac{\theta}{2}\right) \cdot \left(2(1-\nu) - \sin^2\frac{\theta}{2}\right) \right.$$

$$\left. - \sin\theta \cdot \cos\left(\frac{\theta}{2}\right) \left(\cos^2\left(\frac{\theta}{2}\right) + (1-2\nu)\right) \right\}$$

$$+ \frac{C_o}{2} K_{II} \left\{ \cos\theta \cdot \cos\frac{\theta}{2} \left(3 \cdot \cos^2\frac{\theta}{2}\right.\right.$$

$$\left. - (2\nu + 1)\right)$$

$$\left. - \sin\theta \cdot \sin\frac{\theta}{2} \left(3 \cdot \sin^2\frac{\theta}{2} + 2\nu - 4\right) \right\}$$

Dimensionless Displacements in the y-direction:

$$\Gamma_1: \quad v_1(\rho) = C_o \sqrt{\rho} \cdot K_I$$

$$\Gamma_2: \quad v_2(\overline{x1}) = C_o \sqrt{\overline{x1}} \; K_{II}$$

$$\Gamma_4: \quad v_4(\overline{x1}) = - C_o \sqrt{\overline{x1}} \; K_I$$

$$\Gamma_5: \quad v_5(\rho) = - C_o \sqrt{\rho} \cdot K_I$$

$$\Gamma_3: \quad v_3(\theta) = \frac{C_o}{2} K_I \left\{ \sin\theta \; \sin\frac{\theta}{2} \left(2(1-\nu) - \sin^2\frac{\theta}{2}\right) \right.$$

$$\left. + \cos\theta \; \cos\frac{\theta}{2} \left(\cos^2\frac{\theta}{2} + (1-2\nu)\right) \right\}$$

(Eq. continues on next page)

$$+ \frac{C_o}{2} K_{II} \Big\{ \sin\theta \cdot \cos\frac{\theta}{2} \left(3 \cdot \cos^2\frac{\theta}{2} - (2\nu + 1)\right) + \cos\theta \cdot \sin\frac{\theta}{2} \left(3 \cdot \sin^2\frac{\theta}{2} + 2(\nu-2)\right) \Big\} \tag{4.1}$$

where $C_o \equiv \frac{4(1-\nu^2)}{E\sqrt{2\pi}}$ and $\nu \equiv$ Poisson's ratio

$E \equiv$ Young's modulus

and u, v represent displacements in the x,y directions respectively.

The loading for this problem is confined to the circular boundary and generates both Mode I and Mode II states at the crack tip. The stress intensity factors K_I and K_{II} are explicitly represented in both traction and displacement equations in (4.1). K_I and K_{II} are arbitrary and may be set equal to unity in the traction equations above.

The B.I.E. (3.2) are solved for this geometry and traction loading stated in (4.1). The resulting displacement solutions are recorded and used to calculate the stress intensity factors and strain energy of the body. The stress intensity factors are analytically defined by the formula

$$K_I = \lim_{\rho \to 0} \frac{U_{n1}(\rho)}{C_o\sqrt{\rho}} = \lim_{\rho \to 0} \frac{U_{n5}(\rho)}{C_o\sqrt{\rho}}$$

$$K_{II} = \lim_{\rho \to 0} \frac{U_{t1}(\rho)}{C_o\sqrt{\rho}} = \lim_{\rho \to 0} \frac{U_{t5}(\rho)}{C_o\sqrt{\rho}} \qquad (4.2)$$

where U_n, U_t are normal and tangential displacements.

The numerical calculation of these factors proceeds by first forming the expressions

$$\bar{K}_{1(\rho)} = \frac{U_{n1}(\rho) - U_{n5}(\rho)}{2\ C_o\ \sqrt{\rho}}$$

$$\bar{K}_{2(\rho)} = \frac{U_{t1}(\rho) - U_{t5}(\rho)}{2\ C_o\ \sqrt{\rho}}$$

calculated for $\rho \in \Gamma_1, \Gamma_5$ and determining their values as $\rho \to 0$ by extrapolation. The calculated stress intensity factors then follow from (4.2):

$$K_I = \bar{K}_{1(0)}$$

$$K_{II} = \bar{K}_{2(0)} \qquad (4.3)$$

The strain energy is calculated from the boundary displacements and traction loading by use of Clapeyron's theorem(41),

$$E_s = \frac{1}{2} \int_{\Gamma} t_i\ u_i\ dS \qquad (4.4)$$

The displacements calculated at the mesh points are numerically integrated with the tractions using Simpson's

formula to complete the calculations.

EXAMPLE #1 - Results

The results for example #1 are summarized in Table 4.1 and 4.2. A parametric study is presented to test the sensitivity of mesh size and percent square root approximation on the accuracy of the numerical solution. Fifteen examples are cited for fixed C and D values (as a function of mesh size - M1, M2, and M3) and MT, the total number of equations in the matrix. The calculated values of K_I,K_{II}, and the strain energy ratio $\frac{E_s \text{ calculated}}{E_s \text{ Exact}}$ are compared to unity to assess the accuracy of the numerical solution. The maximum error in either K_I, K_{II} or E_s is listed in the last column.

Most of the results indicate less than 1% error for a wide range of mesh sizes. Errors over 1% are generally exhibited when the ratio of the partition sizes H_1 and H_2 on C and D, is greater than 3 to 1. The error sensitivity to the partition ratio of H_1/H_2 is understood by inspection of Eq. (3.2) which generates the influence coefficients. The dominant coefficients result from the kernel functions generated within and between the C and D crack faces, these exhibit a strong dependency on the values of $(\frac{1}{H_1})^2$ as compared to $(\frac{1}{H_2})^2$. Only off diagonal coefficients, small compared to the diagonals, are formed from the kernel functions interconnecting the circular surface and the crack.

In general these problems, and the bent crack geometries to be discussed later, require the restriction $1/3 \leq H_1/H_2 \leq 3$ to insure errors of less than one percent. This imposed restriction on the ratio of C/D which is important to the bent crack studies.

Table 4.2 presents example problem #1 results for varying partitions and increasing crack regions, on which the unknown displacement functions are represented by the square root functional form. One extreme, assuming linear displacement behavior over the complete crack boundary, shows an error of 35%. Rapid reduction in error (~2%) is achieved when the square root representation is utilized over four or more mesh points. These results confirm the importance of properly modeling the displacements near the crack tip and provide assurance that a reasonable number of mesh points leads to good accuracy.

The data in Tables 4.1 and 4.2 illustrate the relative insensitivity of the results upon mesh size provided certain guidelines are adhered to. This results from proper modeling of the unknown displacements and careful numerical integration of the known integrals on each partition. It is most important to model the square root behavior of the displacements in the neighborhood of the crack tip. The accuracy of the numerical integration scheme may be assured by successive refinement of the partitions or use of higher order integration techniques.

TABLE 4.1

No.Eq. MT	M1	M2	M3	K_I Cal.	K_{II} Cal.	$\frac{E_s \text{ Cal.}}{E_s \text{ Exact}}$	Max.% Error in K_I, K_{II}, or E_s
82	6	5	19	.9979	1.006	.9983	0.6
90	8	7	15	1.009	1.007	.9964	0.9
98	8	7	19	1.009	1.003	.9991	0.9
106	10	7	19	1.009	1.003	.9989	0.9
114	12	7	19	1.010	1.001	.9989	1.0
130	12	7	27	1.002	1.001	1.0006	0.2
138	10	7	35	.9988	1.002	1.001	0.2
138	12	7	31	1.000	1.001	1.001	0.1
138	16	7	23	1.006	1.001	1.001	0.6
138	10	13	23	1.010	.9991	1.003	1.0
138	14	13	15	.9992	1.006	.9944	0.6
138	12	11	23	1.016	.9993	1.0022	1.6
138	14	9	23	1.013	.9999	1.001	1.3
138	8	15	23	1.024	.9996	1.003	2.4

Note: 1) The values in this table were calculated for C = .625, D = .375, E_s exact = 1.561 #in/in.thickness

TABLE 4.2

%crack with $\sqrt{}$	No. Mesh pt $\sqrt{}$	M1	M2	M3	K_I	K_{II}	$\frac{E_s \text{ cal}}{E_s \text{ exact}}$	Max% Error in K_I, K_{II}, E_s
0	0	12	7	19	1.35	1.36	1.020	36%
3%	4	*6	29	23	1.042	1.018	1.001	4.2%
6%	4	**6	19	23	1.021	1.014	1.001	2.1%
20%	4	6	13	27	1.012	1.009	1.004	1.2%
30%	6	8	11	27	1.009	1.005	1.003	0.9%
40%	8	10	9	27	1.005	1.002	1.002	0.5%
50%	10	12	7	27	1.002	1.001	1.000	0.2%
60%	12	14	5	27	1.000	.9995	.9998	.05%

* $\underline{C}$ = .05 D = .950

** $\underline{C}$ = .1 D = .900

All other runs used constant $H_1 = H_2 = .05$ and $\underline{C} + D = 1.0$

After modeling the displacement behavior between mesh points, this study utilized a Simpson approximation coupled to an accuracy check to insure errors of less than 1%. Higher order integration techniques could have been selectively used to save modest amounts of computational time but were not attempted during this study.

EXAMPLE PROBLEM #2. The second example deals with the same circular geometry except that a variable length straight crack opened by a constant internal pressure p_o is considered. J. Tweed and D.P. Rooke (42) report results for a normalized disk of radius one and edge crack length $\tilde{a}$, where $\tilde{a}$ is allowed to vary between 0 and 1. This geometry is identical to that shown in Fig. 7 with $\alpha = 0$ and $\underline{C} + D = \tilde{a}$. The results are presented in Fig. 9 for values of $\tilde{a}$ between .025 and 1.9. Comparison with Tweed's data is possible in the range $\tilde{a} \epsilon (0,1)$ and shows less than a 1% deviation. The results of Gross et al (43) for stress intensity factors of a single edge notch specimen, modified to represent similar internal pressure loading are also shown for comparison purposes in the range $\tilde{a} \epsilon (1,1.8)$. As expected, due to the increased stiffness of the straight boundary surface vs. the curved surface of the disk geometry, the Gross results show lower K_I factors for $\tilde{a}$ values of 0 to 1.4. For values between 1.4 and 1.8, the results for the single edge notch specimen

and those presented here for the disk are similar.

The results of Example Problems #1 and #2 numerically confirm the solution method developed in Chapter 2 for plane elastostatic crack problems. In addition the numerical techniques necessary to obtain accurate solutions are established.

4.2 Bent Crack Geometry Results

The last example considers the bent crack ($\alpha > 0$) geometry of Fig. 7, and results from a parametric investigation of the geometry and loading are presented. The geometric parameters are restricted to values of $D = .5$ while $\underline{C} \in [.02, .3]$ and $\alpha \in [0, 85]$. A type of traction loading is examined which permits a continuous variation from tension to shear to be considered.

Before performing the bent crack study, a straight crack ($\alpha = 0$) with $\underline{C} + D = .6$ is investigated to determine the dependence of the error upon the ratio $\underline{C}/D$. Results of example problem #1 and #2 (not shown explicitly) are used to provide a comparison for values of $\underline{C}/D$ between .01 and .3. A partition size defined by M1 = 10, M2 = 19 and M3 = 27 is found to result in the lowest error for the widest range of $\underline{C}/D$. The results indicate errors of less than 1% for $\underline{C}/D \geq .05$, three percent error for $\underline{C}/D = .025$, and eight percent for $\underline{C}/D = .01$. This mesh size allows a square root approximation of the boundary displacements on six points in the neighborhood

of the crack tip. As discussed in section 3.2, the piecewise γ -displacement behavior is incorporated on 10 mesh points; 5 points on either side of the bend vertex on the lower crack surfaces.

A traction loading on the boundary surfaces which simulates a continuous variation between pure tension and pure shear on a straight cracked disk is desirable. This permits comparison of data with reported results for the bent crack in an unbounded medium subject to far field loading. This simulation is accomplished by loading the crack faces and retaining traction free boundary conditions on the circular domain. A superposition process illustrated in Fig. 10 helps to relate the problem with traction loading on the crack faces to one in which the circular boundary is loaded.

Begin by loading the circular boundaries of an uncracked disk with tractions $F(\beta)$, the details of this loading function need not be specified at this point. Assume that on the line, which will later become the crack, a constant traction of magnitude T and orientation β to the x- axis results from the applied load $F(\beta)$. Cutting this line, and forming a traction free crack results in a crack opening displacement. The crack face displacements are brought back to zero by the application of crack face tractions $-\bar{T}$. Fig. 10a shows the results of this process, while Fig. 10b illustrates a similar cracked body

with crack face tractions $\bar{T}$ applied. Superposition of the two problems in Fig. 10a,b result in the problem indicated by Fig. 10c. The stress intensity calculated for the geometry of Fig. 10a is zero, thus the stress intensities for the geometry and loadings of Fig. 10b and 10c are identical. The strain energy release rates which may be calculated from the stress intensity factors will also be similar for the geometries of Fig. 10b,c.

Consider a pure Mode I loading by defining $F(\beta)$ to be a constant set of tractions with magnitude T and orientation $\beta = 90^{o}$. Constant tractions T applied to the faces of a straight crack (Fig. 10b) leads to the desired formulation. Pure Mode II loading requires $F(\beta)$ to be taken as a set of tractions $T_r = T \cos (2\theta - \frac{\pi}{2})$ and $T_\theta = T \ \mathrm{Sin}(2\theta + \frac{\pi}{2})$ where θ is measured from the x-axis. This results in a loading for the problem shown in Fig. 10b defined by constant tractions T applied parallel ($\beta = 0$) to the crack faces, and opposite in direction on opposing faces. Constant loading on the crack faces for the geometry of Fig. (10b) applied at angles $0 < \beta < 90^{o}$ result in mixed mode loading.

The geometry and loading of Fig. 10b offer further advantages in conducting the numerical operations. The higher concentration of mesh points on the crack surfaces compared to the circular domain, coupled with the simple loading, produces accurate results for the strain energy,

which is important for the calculation of the strain energy release rate. As a check of this point, a series of straight crack geometries under Example #2 loading are solved for crack lengths of .5, .510, .525, and .550. The strain energy release rate, calculated using the .5 crack length as the standard is used to predict the K_I factor. The stress intensity factor calculated in this manner from the strain energy release rate is accurate within 1% when compared with that from the crack face displacement calculation. This calculation requires accuracy in the strain energy results to four significant figures; this is easily achieved for all of the check problems considered.

Results

The geometry and loading of Fig. 10b is investigated for values of α between 0^o and 80^o in 5^o increments and β between 0^o and 180^o in 15^o increments. In all cases considered in the following, the magnitude of T is set equal to unity. Table 4.3 presents the calculated values of K_I, K_{II} and the strain energy E_s for $\underline{C}$ = 0.25 and D = .50. The last column presents results for a straight crack length $\underline{C}$ + D = .5 which is taken as the initial crack length. The expected increase or decrease in K_I and K_{II} as a function of α and β is produced. For example, at β = 0 which represents pure shear loading, the crack at α = 0 begins with K_I = 0 and K_{II} = 1.30. As the crack

TABLE 4.3

BENT CRACK RESULTS

β \ α	0°	5°	10°	20°	30°
0	.402879 0 1.3	.38513 .25 1.02	.371933 .49 .82	.372538 .65 .72	.373799 .79 .59
15	.439216 .613 1.25	.431000 .75 1.00	.420990 .91 .81	.423354 1.05 .68	.426216 1.16 .51
30	.538535 1.18 1.12	.530070 1.22 .93	.522079 1.26 .74	.525241 1.37 .57	.528815 1.47 .40
45	.674223 1.67 .92	.66113 1.59 .55	.648113 1.52 .63	.650899 1.61 .45	.654104 1.67 .26
60	.809923 2.05 .65	.78532 1.89 .55	.765322 1.69 .47	.766658 1.73 .28	.768513 1.76 .10
75	.909274 2.28 .33	.872300 2.00 .30	.842301 1.73 .27	.841501 1.74 .10	.841386 1.73 -.05
90	.945655 2.36 0	.898400 1.92 0	.858421 1.67 .05	.855373 1.62 -.08	.853196 1.58 0.21
105	.909318 2.28 -.33	.86241 1.83 -.08	.809365 1.48 -.15	.804558 1.4 -.26	.800780 1.32 -.35
120	.810000 2.05 -.65	.77108 1.64 -.50	.708276 1.19 -.35	.702671 1.07 -.42	.698181 .98 -.48
135	.674312 1.67 -.92	.65234 1.20 -.71	.582242 .83 -.54	.577013 .70 -.56	.572892 .56 -.56
150	.538612 1.18 -1.12	.50214 .81 -.88	.465032 .41 -.68	.461253 .25 -.66	.458483 .02 -.61
165	.439261 61 -1.25	.40256 .35 -.98	.388054 -.04 -.78	.386411 -.20 -.70	.385610 -.34 -.62
180	.402879 0 -1.30	.35813 -.25 -1.02	.371933 -.49 -.82	.372538 -.65 -.72	.373799 -.79 -.59

Key: $E_s \times 10^{-7}$ K_I K_{II}

$E_s \equiv$ Strain energy lb-in/in.thick

K_I, $K_{II} \sim$ psi $\sqrt{\text{in.}}$ $E = 10^7$ psi

$D = .50$ $C = .025$ $\nu = .25$

TABLE 4.3 (cont.)

β= \ α=	40°	50°	60°	70°	**0°
0	.375510 .92 .43	.377763 1.04 .25	.381188 1.15 .02	.408756 1.32 -.28	.362732 0 1.1
15	.429538 1.27 .34	.433796 1.38 .14	.440637 1.50 -.11	.457678 1.66 -.52	.381135 .56 1.1
30	.533054 1.55 .21	.538938 1.64 0	.559288 1.72 -.27	.576983 1.90 -.71	.467012 1.1 1.0
45	.658319 1.73 .06	.665017 1.78 0.14	.678028 1.84 -.40	.724704 2.0 -.88	.584382 1.5 .82
60	.771771 1.78 -.07	.778250 1.8 -.26	.792361 1.84 -.51	.833938 1.97 -.97	.701686 1.9 .58
75	.843008 1.71 -.21	.848296 1.69 -.37	.861652 1.71 -.59	.902737 1.81 -1.01	.787603 2.1 .3
90	.852944 1.52 -.32	.856387 1.47 -.46	.867334 1.45 -.61	.902666 1.52 -.97	.819071 2.2 0
105	.793915 1.23 -.44	.800355 1.16 -.50	.807885 1.11 -.61	.833744 1.13 -.86	.787602 2.1 .3
120	.695400 .85 -.50	.695213 .76 -.52	.699234 .68 -.55	.714439 .66 -.72	.701870 1.9 -.58
135	.570134 .42 -.55	.569134 .31 -.50	.570494 .21 -.46	.576718 .14 -.48	.584450 1.5 -.82
150	.456683 -.04 -.55	.455901 -.17 -.46	.456161 -.28 -.35	.457484 -.38 -.24	.467106 1.1 -.10
165	.385445 -.49 -.50	.385854 -.61 -.36	.386870 -.74 -.21	.388685 -.88 0	.381189 .56 -1.1
180	.375510 -.92 -.43	.377763 -1.04 -.25	.381188 -1.15 -.02	.388756 -1.32 -.28	.362732 0 -1.1

** $\underline{C}$ = .05, D = .45

bends with increasing α the K_I factor increases as K_{II} is seen to decrease. At $\beta = 90^o$, the load is applied normal to the straight crack and, as expected at $\alpha = 0$, $K_I = 2.36$ and $K_{II} = 0$. Increasing the bend angle α results in decreased values of K_I with commensurate increases in K_{II}. The results for a constant bend angle α, say 30^o, as a function of loading angle β, are also of interest. As the load approaches the neighborhood of perpendicular alignment with the bent crack, for example $\beta = 60^o$ for $\alpha = 30^o$, the K_I factor and the strain energy release rate reach local maxima. As the load angle β sweeps past this neighborhood and becomes parallel to the bent crack, crack closure occurs as indicated by negative K_I values. For $\alpha = 30^o$, this first occurs between $\beta = 150^o$ and 165^o. The model developed in this study includes no provision for crack surface contact under compressive loads; thus, the results for negative K_I are of little interest.

A careful examination of the strain energy data in Table 4.3 for $\beta > 120^o$ and $\alpha > 5^o$ indicates <u>lower</u> calculated values than the corresponding strain energy for the straight reference crack $\alpha = 0$. This indicates a negative strain energy release rate contradicting the physics of the problem. It is noted that in all cases where this contradiction occurs the strain energy differences are quite small. The error study performed for ratios of C/D = .05 indicates that a 3% error might be expected in

the results of Table 4.3. All of the questionable data in Table 4.3 can result in a zero or slightly positive strain energy release rate when a 2.5% or less correction factor is applied. The results would then be consistent with the expected physical behavior.

An analysis of the data to predict the initial direction of crack growth as a function of load is readily performed using an energy criterion. Given a fixed α for $\underline{C}$ = .025 and D = .50, the resulting strain energy as a function of β is compared to the results for the straight crack when $\underline{C}$ + D = .5 for the same β load. The maximum strain energy release rate is used as the criterion for determining direction of crack growth. The results are shown at 10^{o} increments in Fig. 11, along with the results for a bent crack geometry in an infinite medium reported by K. Palaniswamy (36). The change in strain energy as a function of α and β is found to have a relatively flat maximum extending over a range of 10 to 15°. The sharpest maxima occur for values of α near zero and β near 90^{o}. The data in Fig.11 have bars indicating an estimate of the error incorporated in numerically selecting the critical values. These flat maxima have been studied by J. Swedlow (45) for similar problems of interest. He appropriately concluded that small changes in local microstructure could strongly influence the growth direction

making experimental study difficult. He presents both analytical and experimental evidence to confirm this behavior.

The numerical results for the bent crack problem indicate the presence of a critical angle α_c. This critical angle manifests itself through the geometric influence coefficient matrix [C] which develops a zero determinant for $\alpha = \alpha_c$ and results in large values of K_I, K_{II} and E_s as α_c is approached. The geometry reported in Table 4.3, representing a C/D ratio of .05, shows that α_c equals 78^o (to the nearest degree). Lower values of C/D lead to similar results while larger C/D values produce lower critical angles. These results are summarized below.

C	D	C/D	α_c
.015	.50	.03	78^o
.020	.50	.04	78
.025	.50	.05	78
.050	.50	.10	63
.100	.50	.20	58
.150	.50	.30	46
.200	.50	.40	42
.300	.50	.60	38
.400	.50	.80	35

It should be noted that the numerical value of the determinant for all problems is quite large (10^{25} to 10^{50}). This determinant remains relatively constant for values of $\alpha < (\alpha_c - 5^o)$, then decreases rapidly. Once past the

critical angle α_c the determinant assumes large negative values. The K_I calculated for $\alpha > \alpha_c$ becomes negative, thus the results for K_I, K_{II} and E_s, for $\alpha > \alpha_c$ are invalid.

As background to this problem recall the work of Sternberg and Koiter (39). Their studies for an open wedge geometry subjected to a concentrated moment at the tip focuses on the break down of the solution for wedge angles of 257.45 degrees (this corresponds to $\alpha = 77.45^\circ$ for the bent crack geometry). Westmann (40) showed that, at $\alpha = 77.45^\circ$, a second singular contribution may enter the analysis while only one singularity exists for $\alpha > 77.45$. His work centers on the geometric effects in adhesive joints and illustrates the importance of this second singularity for both the development and elimination of stress intensity factors at the wedge vertex. K. Palaniswamy (36) discusses the existence of a critical angle for Mode II loading and reports a value of 77.4°. He does not enter into detailed discussion but indicates the existence of qualitative experimental results taken in the neighborhood of α_c.

Certainly, the existence of α_c as at least a mathematical phenomenon is well documented. However, the work of Westmann, Palaniswamy and experimental observations for Mode II loaded cracks leave open to question whether α_c is indeed a physically real limit upon the crack growth direction.

The resulting lower values indicated for α_c as the bent crack $\underline{C}$ extends, are in contrast with Palaniswamy's results. Since he reports in Fig. 12 of (36) increasingly permissible bend angles for increased values of $\underline{C}$, the bent crack length. The results presented in (35) are obtained for a bent crack in an unbounded domain while the problem considered here is for a bent edge crack in a finite disk. The contrasting differences in the two results may be caused by crack tip interaction with the boundary and severe bending induced for larger $\underline{C}/D$ ratios, features not present in the problem considered by Palaniswamy.

CHAPTER 5

CONCLUSIONS AND FUTURE APPLICATIONS

The results presented herein demonstrate the application of integral equation analysis to two-dimensional elastostatic fracture mechanics problems. A solution method is developed for analysis of general closed edge cracked bodies subject to traction loading. This method is demonstrated using example problems with known solutions, the results for K_I, K_{II}, and E_s being accurate within one percent. The bent crack geometry illustrates the application of the method to an asymmetric complex domain which incorporates the effects of singularities at the bend vertex.

The application of this solution method to more general two-dimensional edge cracked problems is possible. However, the practical limitations of the method should be clarified. Section 2.3 discusses the solution for a general plane cracked body. In the closing portion of Section 2.3 it was implied that a body, with m external cracks and N parametric relationships describing them, will require a (4N + 2) system of coupled integral equations to be analyzed and solved. Therefore, the bent crack requires ten such equations. Geometries with non-circular outer boundaries requiring multiple parametric representation (say N_2) lead to further expansion of the equation set.

The formula determining the size of the equation set now becomes $4N + 2N_2$. For example, the simple rectangular plate with one bent edge crack requires five parametric expressions for the outer boundary and two for the crack faces; a system of 18 coupled equations results. Thus, analysis of complex geometries by the method represented herein may require manual manipulation exceeding the practical value of the solution. Future developments in computer software technology may alleviate this difficulty. It is currently possible to construct programs such that the geometric coefficients resulting from most of the equations are automatically calculated from simple boundary surface data. The computer derivation of the equations resulting from the limiting process, $\psi_o \to 0$ and differentiation, w.r.t. ψ_o is beyond the current computer software technology. Successful development of this technology will permit practical application of this method to complex geometries without extensive problem preparation.

For the present, analysis of complex structures using finite elements is possible. This method incorporates special singular elements adjacent to the crack tip and provides the analyst with an accurate tool for the determination of stress intensity factors in complex geometries (17,46-50). The circular element with bent crack developed in this study may possibly be incorporated as the special

element enclosing the crack tip. This will allow study of complex geometries with bent cracks,and at the same time incorporate all of the advantages of the finite element method.

The success achieved using integral equations in the analysis of two-dimensional elastostatic problems led Cruse (21,22,51) to the natural extension of the solution capability to three-dimensional problems. In (51) he presents the B.I.E. for three-dimensional problems valid for reference points P(x) not located at an edge or corner. His equation (14) yielded:

$$\frac{1}{2}\, u_j(P) + \int_S u_i(Q)\, \bar{T}_{ji}(Q,P)\, dS = \int_S t_{i(Q)} \bar{U}_{ij}(Q,P) ds(Q) \qquad (5.1)$$

where:

$$\bar{U}_{ij} = \frac{1}{4\pi\mu} \frac{1}{r} \left[\frac{3 - 4\nu}{4(1-\nu)} \delta_{ij} + \frac{1}{4(1-\nu)} r_{,i} r_{,j} \right]$$

$$\bar{K} = (1 - 2\nu)/2(1-\nu)$$

$$\bar{T}_{ij} = -\frac{\bar{K}}{4\pi} \frac{1}{r^2} \frac{\partial r\sigma}{\partial n} \left(\delta_{ij} + \frac{3}{1-2\nu} r_{,i} r_{,j} \right) - n_j r_{,j} + n_j r_{,j}$$

where the integrals are interpreted in the sense of the Cauchy principal value and the notation is similar to that in Chapter 2. Eq. (5.1) can be viewed as the governing equation relating surface tractions to surface displacements. Eqs. (2.14) present the equations for the two-

dimensional problem. The mathematical character of Eqs. (2.14) and (5.1) is similar, leading to the speculation that the solution method developed and verified for anti-plane and plane two-dimensional problems can be extended to three dimensions.

In summary, this work extends the B.I.E. developed by Rizzo to the application of closed crack geometries. It demonstrates that accurate numerical solutions can be obtained by this method for finite, asymmetrical cracked bodies.

REFERENCES

1. Irwin, G.R., "Fracture," Encyclopedia of Physics, Vol.6, Springer Verlag, Berlin, Germany, 1958, pp. 551-590.

2. Griffith, A.A., "The Phenomena of Rupture and Flow in Solids," Proceedings of the Royal Society, A, Vol. 221, 1920, pp. 163-198.

3. Westergaard, H.M., "Bearing Pressures and Cracks," Journal of Applied Mechanics, June 1939, pp. A49-A53.

4. Sih, G.C., et al, "Crack-Tip, Stress-Intensity Factors for Plane Extension and Plate Bending Problems," Journal of Applied Mechanics, Vol. 29, Trans. ASME, Vol. 84, Series E, 1962, pp. 306-312.

5. Sih, G.C., "Strength of Stress Singularities at Crack Tips for Flexural and Torsional Problems," Journal of Applied Mechanics, Vol. 30, Trans. ASME, Vol. 85, Series E, 1963, pp. 419-425.

6. Koiter, W.T., "An Infinite Row of Collinear Cracks in an Infinite Elastic Sheet," Ingenieur-Archiv, Vol. 28, 1959, pp. 168-172.

7. Koiter, W.T., "An Infinite Row of Parallel Cracks in an Infinite Elastic Sheet," Problems of Continuum Mechanics: Contributions in Honor of the 70th Birthday of N.I. Muskhelishvili, (English Edition), The Society for Industrial and Applied Mathematics, Philadelphia, Pa., 1961, pp. 146-159.

8. Bowie, O. L., "Analysis of an Infinite Plate Containing Radial Cracks Originating at the Boundary of an Internal Circular Hole," Journal of Mathematics and Physics, Vol. 25, 1956, pp. 60-71.

9. Sih, G.C., Editor, Mechanics of Fracture 1, Methods of Analysis and Solutions of Crack Problems, P. Noordhoff, Groningen, The Netherlands, 1974.

10. Sih, G.C., Handbook of Stress Intensity Factors, Institute of Fracture and Solid Mechanics, Lehigh University, P. Noordhoff, Groningen, The Netherlands, 1974.

11. Tada, H., P.C. Paris, and G. R. Irwin, The Stress Analysis of Cracks Handbook, Del Research Corp., Hellertown, Pa., 1974.

12. Swedlow, J.L., The Thickness Effect and Plastic Flow in Cracked Plates, Ph.D. dissertation, Graduate Aeronautical Laboratory, California Institute of Technology, Pasadena, California, 1965.

13. Chan, S.K., I. S. Tuba, and W. Wilson, "On the Finite Element Method in Linear Fracture Mechanics," Engrg. Fracture Mech., Vol. 2, No. 1, 1970, pp. 1-17.

14. Watwood, V.B., "The Finite Element Method for Prediction of Crack Behavior," Nuclear Engineering Design, Vol. 2, 1969, pp. 323-332.

15. Wilson, W.K., "Crack Tip Finite Elements for Plane Elasticity," Westinghouse, Pittsburgh, Pa., Report 71-1E7-FMPWR-P2, June 1971.

16. Oglesby, J.J., O. Lomacky, "An Evaluation of Finite Element Methods for the Computation of Elastic Stress Intensity Factors," NSRDS, Washington, D.C., Report No. 3751, 1972.

17. Byskov, E., "The Calculation of Stress Intensity Factors Using the Finite Element Method with Cracked Elements," International Journal of Fracture Mechanics, Vol. 6, No. 2, June 1970, pp. 159-167.

18. Rizzo, F.J., "An Integral Equation Approach to Boundary Value Problems of Classical Elastostatics," Quarterly of Applied Mathematics, Vol. 25, No. 1, 1967, pp. 83-95.

19. Jaswon, M.A.," Integral Equation Methods in Potential Theory I," Proceedings of the Royal Society, A, Vol. 275, 1963, pp. 23-32.

20. Cruse, T.A., "Lateral Constraint in a Cracked, Three-Dimensional Elastic Body," Department of Mechanical Engineering, Carnegie Institute of Technology, Pittsburgh, Pa., Report SM-36, July, 1970.

21. Cruse, T.A., "Elastic Fracture Mechanics Analysis for Three-Dimensional Cracks," Invited paper for Advanced Analysis Methods for Fracture Mechanics, ASCE, National Structural Engineering Meeting, New Orleans, La., April, 1975.

22. Cruse, T.A., and W. Van Buren, "Three-Dimensional Elastic Stress Analysis of a Fracture Specimen with an Edge Crack," International Journal of Fracture Mechanics, Vol. 7, No. 1, March 1971, pp. 1-15.

23. Cruse, T.A., "Lateral Constraint in a Cracked, Three-Dimensional Elastic Body, " Department of Mechanical Engineering, Carnegie-Mellon University, Pittsburgh, Pa., Report SM-36, July, 1970.

24. Rizzo, F.J., and D.J. Shippy, "A Method for Stress Determination in Plane Anisotropic Elastic Bodies," Journal of Composite Materials, Vol. 4, January 1970, pp. 36-61.

25. Cruse, T.A.," A Direct Formulation and Numerical Solution of the General Transient Elastodynamic Problem II," Journal of Mathematical Analysis and Application, Vol. 22, No. 2, May, 1968, pp. 341-355.

26. Rizzo, F.J., and D.J. Shippy, "A Formulation and Solution Procedure for the General Non-Homogeneous Elastic Inclusion Problem," International Journal of Solids and Structures, Vol. 4, 1968, pp. 1161-1179.

27. Cruse, T.A., "The Direct Potential Method in Three-Dimensional Elastostatics," Department of Mechanical Engineering, Carnegie Institute of Technology, Pittsburgh, Pa., Report SM-13, June, 1968.

28. Lee, K.J.,"An Integral Equation Method for Stress Analyses of Anisotropic Elastic Media," Rockwell International, Los Angeles, Cal., TFD-74-1175-No.30, 1974.

29. Muskhelishvili, N.I., Some Basic Problems of the Mathematical Theory of Elasticity, P. Noordhoff, Groningen, The Netherlands, 1953.

30. Kellogg, O.D., Foundations of Potential Theory, Frederick Ungar Pub. Co., New York, 1929.

31. Love, A.E.H., A Treatise on the Mathematical Theory of Elasticity, Dover, New York, 1944.

32. Muskhelishvili, N.I., Singular Integral Equations, P. Noordhoff,Groningen, The Netherlands, 1946.

33. Tricomi, E.G., Integral Equations, Interscience Publishers, Inc., New York, 1957.

34. Williams, M.L., "Stress Singularities Resulting from Various Boundary Conditions in Angular Corners of Plates in Extension," Journal of Applied Mechanics, Vol. 19, Trans. ASME, Vol. 74, 1952, pp. 526-528.

35. Williams, M.L., "On the Stress Distribution at the Base of a Stationary Crack," Journal of Applied Mechanics, Vol. 24, Trans. ASME, Vol. 79, 1957, pp. 109-114.

36. Palaniswamy, K., and W.G. Knauss, "On the Problem of Crack Extension in Brittle Solids Under General Loading," Graduate Aeronautical Laboratories, California Institute of Technology, Pasadena, Cal., Report SM 74-8, 1974.

37. Williams, J.G., and P.D. Ewing, " Fracture Under Complex Stress - - The Angled Crack Problem," International Journal of Fracture Mechanics, Vol. 8, December 1972, pp. 441-447.

38. Muki, R., and R.A. Westmann, "Crack Emanating from an Open Notch, " Journal of Elasticity, Vol. 4, No. 3, September 1974, pp. 1-14.

39. Sternberg, E., and W.T. Koiter, "The Wedge Under a Concentrated Couple: A Paradox in the Two-Dimensional Theory of Elasticity," Journal of Applied Mechanical Science, December 1958, p. 575.

40. Westmann, R.A., "Geometrical Effects in Adhesive Joints, IJES to be published.

41. Sokolnikoff, I.E., Mathematical Theory of Elasticity, McGraw-Hill, New York, N.Y., 1956.

42. Tweed, J., and D.P. Rooke, "The Stress Intensity Factor of an Edge Crack in a Finite Disc," International Journal of Engineering Science, Vol. II, 1973, pp. 65-73.

43. Gross, B., et al, "Stress Intensity Functions for a Single Edge Notch Specimen by Boundary Collocation of a Stress Function,"NASA, Houston, Texas, TND-2395, 1964.

44. Hussain, M.A., S.L. Pu, and J. Underwood, "Strain Energy Release Rate for a Crack Under Combined Mode I and Mode II," Report from Benet Weapons Laboratory, Watervliet Arsenal, Watervliet, N.Y., February 1973.

45. Swedlow, J.L., Private Conversations at WPAFB, February-April, 1975. Results to be published.

46. Tong, P., and T.H.H. Pian, "On the Convergence of the Finite Element Method for Problems with Singularity," International Journal of Solids and Structures, Vol. 9, 1973, pp. 313-321.

47. Anderson, G., V.L. Ruggles, and G. S. Stibor, "Use of Finite Element Computer Programs in Fracture Mechanics," International Journal of Fracture Mechanics, Vol. 7, No. 1, March 1971, pp. 63-76.

48. Wilson, W.K., and D.G. Thompson, "On the Finite Element Method for Calculating Stress Intensity Factors for Cracked Plates in Bending," Engineering Fracture Mechanics, Vol. 3, 1971, pp. 97-102.

49. Leverenz, R.K., "A Finite Element Stress Analysis of a Crack in a Bi-Material Plate," International Journal of Fracture Mechanics, Vol. 8, No. 3, September 1972, pp. 311-324.

50. Jordan, S., et al, "Development and Application of Improved Analytical Techniques for Fracture Analysis Using Magic III," Bell Aerospace Company, Batelle, Columbus Laboratories, Columbus, Ohio, TR AFFDL-TR-73-61, June 1973.

51. Cruse, T.A., "Numerical Solution in Three-Dimensional Elastostatics," International Journal of Solids and Structures, Vol. 5, 1969, pp. 1259-1274.

APPENDIX A

GEOMETRIC KERNEL FUNCTIONS

This appendix presents the geometric kernel functions for Eq. set (3.1) which apply to the geometry of Fig. 7. The one hundred kernels are presented in twenty-five sets of four. Each set has a heading Ker L M where L, M have values 1 to 5. The L index defines the reference surface Γ_L and the M index defines the field surface Γ_M to which the kernel corresponds.

AD-A039 814 AIR FORCE FLIGHT DYNAMICS LAB WRIGHT-PATTERSON AFB OHIO F/G 20/11
THE DEVELOPMENT AND SOLUTION OF BOUNDARY INTEGRAL EQUATIONS FOR--ETC(U)
NOV 76 L T MONTULLI

UNCLASSIFIED AFFDL-TR-76-116 NL

2 OF 2
ADA039 814

END

DATE FILMED
6-77

2 OF 2

ADA039 814

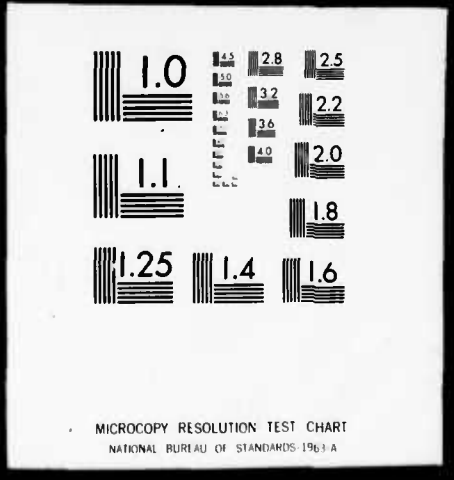

Ker 11 $\quad \underset{\neg}{R}_{11}^2 \equiv (\rho - B)^2$

$$KI_{11} = 0, \quad KII_{11} = \frac{K}{\rho - B}$$

$$KIII_{11} = \frac{-K}{\rho - B}, \quad KIV_{11} = 0$$

Ker 12

$$\underset{\neg}{R}_{12}^2 \equiv \left[\overline{X1} - E - B\cdot\cos(\alpha-\psi_0)\right]^2 + \left[C\cdot\tan\psi_0 - C\cdot\tan\alpha + B\cdot\sin(\alpha-\psi_0)\right]^2$$

$$KI_{12} = \left\{ \left[K - \frac{M\cdot 4\cdot\mu(\overline{X1} - E - B\cdot\cos(\alpha-\psi_0)^2}{\underset{\neg}{R}_{12}^2} \right] \left[\frac{C\cdot\tan\alpha - C\cdot\tan\psi_0 - B\cdot\sin(\alpha-\psi_0)}{\underset{\neg}{R}_{12}^2} \right] \right\}$$

$$KII_{12} = \left\{ M\cdot 4\cdot\mu \left[\frac{\overline{X1} - E - B\cdot\cos(\alpha-\psi_0)\right]\left[C\cdot\tan\psi_0 - C\cdot\tan\alpha + B\cdot\sin(\alpha-\psi_0)\right]^2}{\underset{\neg}{R}_{12}^4} \right. \right.$$

$$\left. \left. + K \cdot \left[\overline{X1} - E - B\cdot\cos(\alpha-\psi_0)\right] / \underset{\neg}{R}_{12}^2 \right\} \right.$$

$$KIII_{12} = \left\{ M\cdot 4\cdot\mu \left[\frac{\overline{X1} - E - B\cdot\cos(\alpha-\psi_0)\right]\left[C\cdot\tan\psi_0 - C\cdot\tan\alpha + B\cdot\sin(\alpha-\psi_0)\right]^2}{\underset{\neg}{R}_{12}^4} \right. \right.$$

$$\left. \left. - K \cdot \left[\overline{X1} - E - B\cdot\cos(\alpha-\psi_0)\right] / \underset{\neg}{R}_{12}^2 \right\} \right.$$

$$KIV_{12} = \left\{ \left[K - M\cdot 4\cdot\mu \frac{\left[C\cdot\tan\psi_0 - C\cdot\tan\alpha + B\cdot\sin(\alpha-\psi_0)\right]^2}{\underset{\neg}{R}_{12}^2} \right] \right.$$

$$\left. \cdot \frac{\left[-C\cdot\tan\psi_0 + C\cdot\tan\alpha - B\cdot\sin(\alpha-\psi_0)\right]}{\underset{\neg}{R}_{12}^2} \right\}$$

Ker 13

$$\underline{R}_{13}^2 \equiv \left[\cos\theta - E - B\cdot\cos(\alpha-\psi_0)\right]^2 + \left[\sin\theta - C\cdot\tan\alpha + B\cdot\sin(\alpha-\psi_0)\right]^2$$

$$KI_{13} = \left\{\left[K - M\cdot 4\cdot\mu\frac{\left[\cos\theta - E - B\cdot\cos(\alpha-\psi_0)\right]^2}{\underline{R}_{13}^2}\right]\left[1 - E\cdot\cos\theta - C\cdot\tan\alpha\cdot\sin\theta - B\cdot\cos(\theta+\alpha-\psi_0)\right]/\underline{R}_{13}^2\right\}$$

$$KII_{13} = \left\{-M\cdot 4\cdot\mu\left[\cos\theta - E - B\cdot\cos(\alpha-\psi_0)\right]\left[\sin\theta - C\cdot\tan\alpha + B\cdot\sin(\alpha-\psi_0)\right]\cdot\left[1 - E\cdot\cos\theta - C\cdot\tan\alpha\cdot\sin\theta - B\cdot\cos(\theta+\alpha-\psi_0)\right]/\underline{R}_{13}^4 + K\cdot\left[E\cdot\sin\theta - C\cdot\tan\alpha\cdot\cos\theta + B\cdot\sin(\theta+\alpha-\psi_0)\right]/\underline{R}_{13}^2\right\}$$

$$KIII_{13} = \left\{-M\cdot 4\cdot\mu\left[\cos\theta - E - B\cdot\cos(\alpha-\psi_0)\right]\left[\sin\theta - C\cdot\tan\alpha + B\cdot\sin(\alpha-\psi_0)\right]\cdot\left[1 - E\cdot\cos\theta - C\cdot\tan\alpha\cdot\sin\theta - B\cdot\cos(\theta+\alpha-\psi_0)\right]/\underline{R}_{13}^4 - K\left[E\cdot\sin\theta - C\cdot\tan\alpha\cdot\cos\theta + B\cdot\sin(\theta+\alpha-\psi_0)\right]/\underline{R}_{13}^2\right\}$$

$$KIV_{13} = \left\{\left[K - M\cdot 4\cdot\mu\frac{\left[\sin\theta - C\cdot\tan\alpha + B\cdot\sin(\alpha-\psi_0)\right]^2}{\underline{R}_{13}^2}\right]\cdot\left\{\left[1 - E\cdot\cos\theta - C\cdot\tan\alpha\cdot\sin\theta - B\cdot\cos(\theta+\alpha-\psi_0)\right]/\underline{R}_{13}^2\right\}\right\}$$

Ker 14

$$\underline{R}^2_{14} \equiv \left[\overline{Xl}-E-B\cdot\cos(\alpha-\psi_0)\right]^2+\left[-C\cdot\tan\psi_0-C\cdot\tan\alpha+B\cdot\sin(\alpha-\psi_0)\right]^2$$

$$KI_{14}=\left\{\left[K-M\cdot 4\cdot\mu\frac{\left[\overline{XI}-E-B\cdot\cos(\alpha-\psi_0)\right]^2}{\underline{R}^2_{14}}\right]\cdot\left[-C\cdot\tan\psi_0+B\cdot\sin(\alpha-\psi_0)-C\cdot\tan\alpha\right]/\underline{R}^2_{14}\right\}$$

$$KII_{14}=\left\{-M\cdot 4\cdot\mu\frac{\left[\overline{Xl}-E-B\cdot\cos(\alpha-\psi_0)\right]\left[-C\cdot\tan\psi_0+B\cdot\sin(\alpha-\psi_0)-C\cdot\tan\alpha\right]^2}{\underline{R}^4_{14}}-K\cdot\left[\overline{Xl}-E-B\cdot\cos(\alpha-\psi_0)\right]/\underline{R}^2_{14}\right\}$$

$$KIII_{14}=\left\{-M\cdot 4\cdot\mu\frac{\left[\overline{Xl}-E-B\cdot\cos(\alpha-\psi_0)\right]\left[-C\cdot\tan\psi_0+B.\sin(\alpha-\psi_0)-C\cdot\tan\alpha\right]^2}{\underline{R}^4_{14}}+K\cdot\left[\overline{Xl}-E-B\cdot\cos(\alpha-\psi_0)\right]/\underline{R}^2_{14}\right\}$$

$$KIV_{14}=\left\{\left[K-M\cdot 4\cdot\mu\frac{\left[-C\cdot\tan\psi_0+B\cdot\sin(\alpha-\psi_0)-C\cdot\tan\alpha\right]^2}{\underline{R}^2_{14}}\right]\cdot\left\{\left[-C\cdot\tan\psi_0+B\cdot\sin(\alpha-\psi_0)-C\cdot\tan\alpha\right]/\underline{R}^2_{14}\right\}\right\}$$

Ker 15

$$\underset{\neg 15}{R^2} \equiv \rho^2 + B^2 - 2\cdot\rho\cdot B.\cos 2\cdot\psi_0$$

$$KI_{15} = \left\{ \left[K - M\cdot 4\cdot\mu \cdot \frac{\left[\rho\cdot\cos(\alpha+\psi_0) - B\cdot\cos(\alpha-\psi_0)\right]^2}{\underset{\neg 15}{R^2}} \right] \cdot \left[\frac{-B\cdot\sin 2\psi_0}{\underset{\neg 15}{R^2}} \right] \right\}$$

$$KII_{15} = \left\{ +M\cdot 4\cdot\mu \cdot \left[\rho\cdot\cos(\alpha+\psi_0) - B\cdot\cos(\alpha-\psi_0)\right]\left[+\rho\cdot\sin(\alpha+\psi_0) - B\cdot\sin(\alpha-\psi_0)\right] \cdot \left[-B\cdot\sin 2\psi_0\right]/\underset{\neg 15}{R^4} + K \frac{\left[-\rho + B\cdot\cos 2\psi_0\right]}{\underset{\neg 15}{R^2}} \right\}$$

$$KIII_{15} = \left\{ +M\cdot 4\cdot\mu\left[\rho\cdot\cos(\alpha+\psi_0) - B\cdot\cos(\alpha-\psi_0)\right]\left[+\rho\cdot\sin(\alpha+\psi_0) - B\cdot\sin(\alpha-\psi_0)\right] \cdot \left[-B\cdot\sin 2\alpha\right]/\underset{\neg 15}{R^4} - K\frac{\left[-\rho + B\cdot\cos 2\psi_0\right]}{\underset{\neg 15}{R^2}} \right\}$$

$$KIV_{15} = \left\{ \left[K - M\cdot 4\cdot\mu \frac{\left[\rho\cdot\sin(\alpha+\psi_0) - B\cdot\sin(\alpha-\psi_0)\right]^2}{\underset{\neg 15}{R^2}} \right] \cdot \left[\frac{-B\cdot\sin 2\psi_0}{\underset{\neg 15}{R^2}} \right] \right\}$$

Ker 21

$$\underset{21}{R^2} = \left\{(E+\rho\cdot\cos(\alpha-\psi_0)-B_2)^2+(C\cdot\tan\alpha-\rho\cdot\sin(\alpha-\psi_0)-C\cdot\tan\psi_o)^2\right\}$$

$$KI_{21}= \left\{\left[K-M\cdot 4\cdot\mu\ \frac{(E+\rho\cdot\cos(\alpha-\psi_0)-B_2)^2}{\underset{21}{R^2}}\right]\left[(E+\rho\cdot\cos(\alpha-\psi_0)-B_2)(-\sin(\alpha-\psi_0))\right.\right.$$

$$\left.\left.+(C\cdot\tan\alpha-\rho\cdot\sin(\alpha-\psi_0)-C\cdot\tan\psi_0)(-\cos(\alpha-\psi_0))\right]/\underset{21}{R^2}\right\}$$

$$KII_{21}= \left\{-M\cdot 4\cdot\mu\left[E+\rho\cdot\cos(\alpha-\psi_0)-B_2\right]\left[C\cdot\tan\alpha-\rho\cdot\sin(\alpha-\psi_0)-C\cdot\tan\psi_0\right]\cdot\right.$$

$$\left[(E+\rho\cdot\cos(\alpha-\psi_0)-B_2)(-\sin(\alpha-\psi_0))\right.$$

$$\left.+(C\cdot\tan\alpha-\rho\cdot\sin(\alpha-\psi_0)-C\cdot\tan\psi_0)(-\cos(\alpha-\psi_0))\right]/\underset{21}{R^4}$$

$$+\frac{K}{\underset{21}{R^2}}\left[(E+\rho\cos(\alpha-\psi_0)-B_2)(\cos(\alpha-\psi_0))\right.$$

$$\left.\left.+(C\cdot\tan\alpha-\rho\sin(\alpha-\psi_0)-C\cdot\tan\psi_0)(-\sin(\alpha-\psi_0))\right]\right\}$$

$$KIII_{21}= \left\{-M\cdot 4\cdot\mu\left[E+\rho\cdot\cos(\alpha-\psi_0)-B_2\right]\left[C\cdot\tan\alpha-\rho\cdot\sin(\alpha-\psi_0)-C\cdot\tan\psi_0\right]\cdot\right.$$

$$\left[(E+\rho\cdot\cos(\alpha-\psi_0)-B_2)(-\sin(\alpha-\psi_0))\right.$$

$$\left.+(C\cdot\tan\alpha-\rho\cdot\sin(\alpha-\psi_0)-C\cdot\tan\psi_0)(-\cos(\alpha-\psi_0))\right]/\underset{21}{R^4}$$

$$-\frac{K}{\underset{21}{R^2}}\left[(E+\rho\cos(\alpha-\psi_0)-B_2)(\cos(\alpha-\psi_0))\right.$$

$$\left.\left.+(C\cdot\tan\alpha-\rho\sin(\alpha-\psi_0)-C\cdot\tan\psi_0)(-\sin(\alpha-\psi_0))\right]\right\}$$

$$KIV_{21}= \left\{\left[K-M\cdot 4\cdot\mu\ \frac{(C\cdot\tan\alpha-\rho\cdot\sin(\alpha-\psi_0)-C\cdot\tan\psi_0)^2}{\underset{21}{R^2}}\right]\right.$$

$$\cdot\left[(E+\rho\cdot\cos(\alpha-\psi_0)-B_2)(-\sin(\alpha-\psi_0))\right.$$

$$\left.\left.+(C\cdot\tan\alpha-\rho\cdot\sin(\alpha-\psi_0)-C\cdot\tan\psi_0)(-\cos(\alpha-\psi_0))\right]/\underset{21}{R^2}\right\}$$

Ker 22

$$\underline{R}^2_{22} = (\overline{X1}-B_2)^2$$

$$KI_{22} = 0$$

$$KII_{22} = \frac{K}{\overline{X1}-B_2}$$

$$KIII_{22} = -\frac{K}{\overline{X1}-B_2}$$

$$KIV_{22} = 0$$

Ker 23

$$\underline{R}_{23}^2 = (\cos\Theta - B_2)^2 + (\sin\Theta - C\cdot\tan\psi_0)^2$$

$$KI_{23} = \left\{ \left[K - \frac{M\cdot 4\cdot\mu(\cos\Theta - B_2)^2}{\underline{R}_{23}^2} \right] \left[\frac{1 - B_2\cdot\cos\Theta - C\cdot\tan\psi_0\cdot\sin\Theta}{\underline{R}_{23}^2} \right] \right\}$$

$$KII_{23} = \left\{ -M\cdot 4\cdot\mu\left[\cos\Theta - B_2\right]\left[\sin\Theta - C\cdot\tan\psi_0\right] \left[\frac{1 - B_2\cdot\cos\Theta - C\cdot\tan\psi_0\cdot\sin\Theta}{\underline{R}_{23}^4} \right] + K\cdot\left[B_2\cdot\sin\Theta - C\cdot\tan\psi_0\cdot\cos\Theta\right]/\underline{R}_{23}^2 \right\}$$

$$KIII_{23} = \left\{ -M\cdot 4\cdot\mu\left[\cos\Theta - B_2\right]\left[\sin\Theta - C\cdot\tan\psi_0\right] \left[\frac{1 - B_2\cdot\cos\Theta - C\cdot\tan\psi_0\cdot\sin\Theta}{\underline{R}_{23}^4} \right] - K\cdot\left[B_2\cdot\sin\Theta - C\cdot\tan\psi_0\cdot\cos\Theta\right]/\underline{R}_{23}^2 \right\}$$

$$KIV_{23} = \left\{ \left[K - M\cdot 4\cdot\mu \frac{(\sin\Theta - C\cdot\tan\psi_0)^2}{\underline{R}_{23}^2} \right] \left[\frac{1 - B_2\cdot\cos\Theta - C\cdot\tan\psi_0\cdot\sin\Theta}{\underline{R}_{23}^2} \right] \right\}$$

Ker 24

$$\underline{R}_{24}^2 = \left\{ (\overline{X1}-B_2)^2 + (-2\cdot C\cdot \tan\psi_0)^2 \right\}$$

$$KI_{24} = \left\{ \left[K - M\cdot 4\cdot \mu \frac{(\overline{X1}-B_2)^2}{\underline{R}_{24}^2} \right] \left[\frac{-2\cdot C\cdot \tan\psi_0}{\underline{R}_{24}^2} \right] \right\}$$

$$KII_{24} = \left\{ -M\cdot 4\cdot \mu \left[\overline{X1}-B_2\right] \left[-2\cdot C\cdot \tan\psi_0\right]^2 / \underline{R}_{24}^4 - K\left[\frac{+(\overline{X1}-B_2)}{\underline{R}_{24}^2} \right] \right\}$$

$$KIII_{24} = \left\{ -M\cdot 4\cdot \mu \left[\overline{X1}-B_2\right] \left[-2\cdot C\cdot \tan\psi_0\right]^2 / \underline{R}_{24}^4 + K\left[\frac{\overline{X1}-B_2}{\underline{R}_{24}^2} \right] \right\}$$

$$KIV_{24} = \left\{ \left[K - \frac{M\cdot 4\cdot \mu (2\cdot C\cdot \tan\psi_0)^2}{\underline{R}_{24}^2} \right] \left[\frac{-2\cdot C\cdot \tan\psi_0}{\underline{R}_{24}^2} \right] \right\}$$

Ker 25

$$\underline{R}_{25}^2 = (E+\rho\cdot\cos(\alpha+\psi_0)-B_2)^2 + (C\cdot\tan\alpha-\rho\cdot\sin(\alpha+\psi_0)-C\cdot\tan\psi_0)^2$$

$$KI_{25}= \left\{\left[K- \frac{M\cdot 4\cdot\mu\ (E+\rho(\cos(\alpha+\psi_0)-B_2)^2}{\underline{R}_{25}^2}\right]\left[(E+\rho\cdot\cos(\alpha+\psi_0)-B_2)\ \sin(\alpha+\psi_0)\right.\right.$$

$$\left.\left. + (C\cdot\tan\alpha-\rho\cdot\sin(\alpha+\psi_0)-C\cdot\tan\psi_0)\ \cos(\alpha+\psi_0)\right]/\underline{R}_{25}^2\right\}$$

$$KII_{25}= \left\{-M\cdot 4\mu\left[E+\rho\cdot\cos(\alpha+\psi_0)-B_2\right]\left[C\cdot\tan\alpha-\rho\cdot\sin(\alpha+\psi_0)-C\cdot\tan\psi_0\right]\right.$$

$$\cdot\left[(E+\rho\cdot\cos(\alpha+\psi_0)-B_2)\ \sin(\alpha+\psi_0)\right.$$

$$\left. + C\cdot\tan\alpha-\rho\cdot\sin(\alpha+\psi_0)-C\cdot\tan\psi_0\right]\left[\cos(\alpha+\psi_0)\right]/\underline{R}_{25}^4$$

$$+ \frac{K}{\underline{R}_{25}^2}\left[(E+\rho\cdot\cos(\alpha+\psi_0)-B_2)(-\cos(\alpha+\psi_0))\right.$$

$$\left.\left. +(C\cdot\tan\alpha-\rho\cdot\sin(\alpha+\psi_0)-C\cdot\tan\psi_0)\sin(\alpha+\psi_0)\right]\right\}$$

$$KIII_{25}= \left\{-M\cdot 4\cdot\mu\left[E+\rho\cdot\cos(\alpha+\psi_0)-B_2\right]\left[C\cdot\tan\alpha-\rho\cdot\sin(\alpha+\psi_0)-C\cdot\tan\psi_0\right]\right.$$

$$\cdot\left[(E+\rho\cdot\cos(\alpha+\psi_0)-B_2)\ \sin(\alpha+\psi_0)\right.$$

$$\left. + C\cdot\tan\alpha-\rho\cdot\sin(\alpha+\psi_0)-C\cdot\tan\psi_0\right]\left[\cos(\alpha+\psi_0)\right]/\underline{R}_{25}^4$$

$$- \frac{K}{\underline{R}_{25}^2}\left[(E+\rho\cdot\cos(\alpha+\psi_0)-B_2)(-\cos(\alpha+\psi_0))\right.$$

$$\left.\left. +(C\cdot\tan\alpha-\rho\cdot\sin(\alpha+\psi_0)-C\cdot\tan\psi_0)\sin(\alpha+\psi_0)\right]\right\}$$

$$KIV_{25} = \left\{\left[K- \frac{M\cdot 4\cdot\mu(C\cdot\tan\alpha-\rho\cdot\sin(\alpha+\psi_0)-C\cdot\tan\psi_0)^2}{\underline{R}_{25}^2}\right]\right.$$

$$\left[(E+\rho\cdot\cos(\alpha+\psi_0)-B_2)\sin(\alpha+\psi_0)\right.$$

$$\left.\left. +(C\cdot\tan\alpha-\rho\cdot\sin(\alpha+\psi_0)-C\cdot\tan\psi_0)\cos(\alpha+\psi_0)\right]/\underline{R}_{25}^2\right\}$$

Ker 31

$$\underline{R}_{31}^2 = \left\{ (E+\rho\cdot\cos(\alpha-\psi_0)-\cos\theta_0)^2 + (C\cdot\tan\alpha-\rho\cdot\sin(\alpha-\psi_0)-\sin\theta_o)^2 \right\}$$

$$KI_{31} = \left\{ \left[K-M\cdot 4\cdot\mu\frac{(E+\rho\cdot\cos(\alpha-\psi_0)-\cos\theta_0)^2}{\underline{R}_{31}^2} \right] \cdot\left[-E\cdot\sin(\alpha-\psi_0)-C\cdot\tan\alpha\cdot\cos(\alpha-\psi_0)+\sin(\theta_0+\alpha-\psi_0)\right]/\underline{R}_{31}^2 \right\}$$

$$KII_{31} = \left\{ -M\cdot 4\cdot\mu\left[E+\rho\cdot\cos(\alpha-\psi_0)-\cos\theta_0\right]\left[C\cdot\tan\alpha-\rho\cdot\sin(\alpha-\psi_0)-\sin\theta_0\right] \cdot\left[-E\cdot\sin(\alpha-\psi_0)-C\cdot\tan\alpha\cdot\cos(\alpha-\psi_0)+\sin(\theta_0+\alpha-\psi_0)\right]/\underline{R}_{31}^4 + K\cdot\left[E\cdot\cos(\alpha-\psi_0)-C\cdot\tan\alpha\cdot\sin(\alpha-\psi_0)+\rho-\cos(\theta_0+\alpha-\psi_0)\right]/\underline{R}_{31}^2 \right\}$$

$$KIII_{31} = \left\{ -M\cdot 4\cdot\mu\left[E+\rho\cdot\cos(\alpha-\psi_0)-\cos\theta_0\right]\left[C\cdot\tan\alpha-\rho\cdot\sin(\alpha-\psi_0)-\sin\theta_0\right] \cdot\left[-E\cdot\sin(\alpha-\psi_0)-C\cdot\tan\alpha\cdot\cos(\alpha-\psi_0)+\sin(\theta_0+\alpha-\psi_0)\right]/\underline{R}_{31}^4 - K\cdot\left[E\cdot\cos(\alpha-\psi_0)-C\cdot\tan\alpha\cdot\sin(\alpha-\psi_0)+\rho-\cos(\theta_0+\alpha-\psi_0)\right]/\underline{R}_{31}^2 \right\}$$

$$KIV_{31} = \left\{ \left[K-M\cdot 4\cdot\mu\frac{(C\cdot\tan\alpha-\rho\cdot\sin(\alpha-\psi_0)-\sin\theta_0)^2}{\underline{R}_{31}^2} \right] \cdot\left[-E\cdot\sin(\alpha-\psi_0)-C\cdot\tan\alpha\cdot\cos(\alpha-\psi_0)+\sin(\theta_0+\alpha-\psi_0)\right]/\underline{R}_{31}^2 \right\}$$

Ker 32

$$\underline{R}_{32}^2 = (\overline{X1}-\cos\Theta_0)^2 + (C\cdot\tan\psi_0-\sin\Theta_0)^2$$

$$KI_{32} = \left\{\left[K-\frac{M\cdot 4\cdot\mu(\overline{X1}-\cos\Theta_0)^2}{\underline{R}_{32}^2}\right]\left[\frac{\sin\Theta_0-C\cdot\tan\psi_0}{\underline{R}_{32}^2}\right]\right\}$$

$$KII_{32} = \left\{+M\cdot 4\cdot\mu\left[\overline{X1}-\cos\Theta_0\right]\left[C\cdot\tan\psi_0-\sin\Theta_0\right]^2/\underline{R}_{32}^4 + K\cdot\left[\overline{X1}-\cos\Theta_0\right]/\underline{R}_{32}^2\right\}$$

$$KIII_{32} = \left\{M\cdot 4\cdot\mu\left[\overline{X1}-\cos\Theta_0\right]\left[C\cdot\tan\psi_0-\sin\Theta_0\right]^2/\underline{R}_{32}^4 - K\cdot\left[\overline{X1}-\cos\Theta_0\right]/\underline{R}_{32}^2\right\}$$

$$KIV_{32} = \left\{\left[K-M\cdot 4\cdot\mu\frac{(C\cdot\tan\psi_0-\sin\Theta_0)^2}{\underline{R}_{32}^2}\right]\left[\frac{\sin\Theta_0-C\cdot\tan\psi_0}{\underline{R}_{32}^2}\right]\right\}$$

Ker 33

$$\underline{R}^2_{33} = 2 \cdot (1-\cos(\theta-\theta_0))$$

$$KI_{33} = \left\{ \left[K - M \cdot 4 \cdot \mu \frac{(\cos\theta - \cos\theta_0)^2}{\underline{R}^2_{33}} \right] \left[\frac{1}{2} \right] \right.$$

$$= \left\{ \frac{K}{2} - \frac{M \cdot 4 \cdot \mu}{2} \cdot \sin^2 \left(\frac{\theta+\theta_0}{2} \right) \right\}$$

$$KII_{33} = \left\{ + \frac{M \cdot 4 \cdot \mu}{4} \left[\sin(\theta+\theta_0) \right] + \frac{K}{2} \cdot \frac{\cos\left(\frac{\theta-\theta_0}{2} \right)}{\sin\left(\frac{\theta-\theta_0}{2} \right)} \right\}$$

$$KIII_{33} = \left\{ + \frac{M \cdot 4 \cdot \mu}{4} \cdot \sin(\theta+\theta_0) - \frac{K}{2} \cdot \frac{\cos\left(\frac{\theta-\theta_0}{2} \right)}{\sin\left(\frac{\theta-\theta_0}{2} \right)} \right\}$$

$$KIV_{33} = \left\{ \frac{K}{2} - \frac{M \cdot 4 \cdot \mu}{2} \cdot \cos^2 \left(\frac{\theta+\theta_0}{2} \right) \right\}$$

Ker 34

$$\underline{R}_{34}^2 = (\overline{Xl}-\cos\theta_0)^2 + (-C\cdot\tan\psi_0-\sin\theta_0)^2$$

$$KI_{34} = \left\{\left[K-M\cdot 4\cdot\mu\frac{(\overline{Xl}-\cos\theta_0)^2}{\underline{R}_{34}^2}\right]\left[\frac{-\sin\theta_0-C\cdot\tan\psi_0}{\underline{R}_{34}^2}\right]\right\}$$

$$KII_{34} = \left\{-M\cdot 4\cdot\mu\left[\overline{Xl}-\cos\theta_0\right]\left[C\cdot\tan\psi_0+\sin\theta_0\right]^2/\underline{R}_{34}^4 + K\cdot\left[\cos\theta_0-\overline{Xl}\right]/\underline{R}_{34}^2\right\}$$

$$KIII_{34} = \left\{-M\cdot 4\cdot\mu\left[\overline{Xl}-\cos\theta_0\right]\left[C\cdot\tan\psi_0+\sin\theta_0\right]^2/\underline{R}_{34}^4 - K\cdot\left[\cos\theta_0-\overline{Xl}\right]/\underline{R}_{34}^2\right\}$$

$$KIV_{34} = \left\{\left[K-M\cdot 4\cdot\mu\frac{(C\cdot\tan\psi_0+\sin\theta_0)^2}{\underline{R}_{34}^2}\right]\left[\frac{-C\cdot\tan\psi_0-\sin\theta_0}{\underline{R}_{34}^2}\right]\right\}$$

Ker 35

$$\underline{R}_{35}^2 = (E+\rho\cdot\cos(\alpha+\psi_0)-\cos\theta_0)^2 + (C\cdot\tan\alpha-\rho\cdot\sin(\alpha+\psi_0)-\sin\theta_0)^2$$

$$KI_{35} = \left\{\left[K-M\cdot 4\cdot\mu\ \frac{(E+\rho\cdot\cos(\alpha+\psi_0)-\cos\theta_0)^2}{\underline{R}_{35}^2}\right]\cdot\left[E\cdot\sin(\alpha+\psi_0)+C\cdot\tan\alpha\cos(\alpha+\psi_0)-\sin(\alpha+\psi_0+\theta_0)\right]/\underline{R}_{35}^2\right\}$$

$$KII_{35} = \left\{-M\cdot 4\cdot\mu\left[E+\rho\cdot\cos(\alpha+\psi_0)-\cos\theta_0\right]\left[C\cdot\tan\alpha-\rho\cdot\sin(\alpha+\psi_0)-\sin\theta_0\right]\cdot\left[E\cdot\sin(\alpha+\psi_0)+C\cdot\tan\alpha\cos(\alpha+\psi_0)-\sin(\alpha+\psi_0+\theta_0)\right]/\underline{R}_{35}^4 + K\left[-E\cdot\cos(\alpha+\psi_0)+C\cdot\sin(\alpha+\psi_0)\cdot\tan\alpha-\rho+\cos(\theta_0+\alpha+\psi_0)\right]/\underline{R}_{35}^2\right\}$$

$$KIII_{35} = \left\{-M\cdot 4\cdot\mu\left[E+\rho\cdot\cos(\alpha+\psi_0)-\cos\theta_0\right]\left[C\cdot\tan\alpha-\rho\cdot\sin(\alpha+\psi_0)-\sin\theta_0\right]\cdot\left[E\cdot\sin(\alpha+\psi_0)+C\cdot\tan\alpha\cos(\alpha+\psi_0)-\sin(\alpha+\psi_0+\theta_0)\right]/\underline{R}_{35}^4 - K\left[-E\cdot\cos(\alpha+\psi_0)+C\cdot\sin(\alpha+\psi_0)\cdot\tan\alpha-\rho+\cos(\theta_0+\alpha+\psi_0)\right]/\underline{R}_{35}^2\right\}$$

$$KIV_{35} = \left\{\left[K-M\cdot 4\cdot\mu\ \frac{(C\cdot\tan\alpha-\rho\cdot\sin(\alpha+\psi_0)-\sin\theta_0)^2}{\underline{R}_{35}^2}\right]\cdot\left[E\cdot\sin(\alpha+\psi_0)+C.\tan\alpha\cos(\alpha+\psi_0)-\sin(\alpha+\psi_0+\theta_0)\right]/\underline{R}_{35}^2\right\}$$

Ker 41

$$\underset{\sim}{R}_{41}^2 = (E+\rho\cdot\cos(\alpha-\psi_0)-B_2)^2+ (C\cdot\tan\alpha-\rho\cdot\sin(\alpha-\psi_0)+C\cdot\tan\psi_0)^2$$

$$KI_{41} = \left\{\left[K-M\cdot 4\cdot\mu\ \frac{(E+\rho\cdot\cos(\alpha-\psi_0)-B_2)^2}{\underset{\sim}{R}_{41}^2}\right]\left[(E+\rho\cdot\cos(\alpha-\psi_0)-B_2)(-\sin(\alpha-\psi_0))\right.\right.$$
$$\left.\left.+(C\cdot\tan\alpha-\rho\cdot\sin(\alpha-\psi_0)+C\cdot\tan\psi_0)(-\cos(\alpha-\psi_0))\right]\right\}/\underset{\sim}{R}_{41}^2$$

$$KII_{41} = \left\{-M\cdot 4\cdot\mu\left[E+\rho\cdot\cos(\alpha-\psi_0)-B_2\right]\left[C\cdot\tan\alpha-\rho\cdot\sin(\alpha-\psi_0)+C\cdot\tan\psi_0\right]\cdot\right.$$
$$\left[(E+\rho\cdot\cos(\alpha-\psi_0)-B_2)(-\sin(\alpha-\psi_0))\right.$$
$$\left.+(C\cdot\tan\alpha-\rho\cdot\sin(\alpha-\psi_0)+C\cdot\tan\psi_0)(-\cos(\alpha-\psi_0))\right]/\underset{\sim}{R}_{41}^4$$
$$+\frac{K}{\underset{\sim}{R}_{41}^2}\left[(E+\rho\cdot\cos(\alpha-\psi_0)-B_2)(\cos(\alpha-\psi_0))\right.$$
$$\left.\left.+(C\cdot\tan\alpha-\rho\cdot\sin(\alpha-\psi_0)+C\cdot\tan\psi_0)(-\sin(\alpha-\psi_0))\right]\right\}$$

$$KIII_{41} = \left\{-M\cdot 4\cdot\mu\left[E+\rho\cdot\cos(\alpha-\psi_0)-B_2\right]\left[C\cdot\tan\alpha-\rho\cdot\sin(\alpha-\psi_0)+C\cdot\tan\psi_0\right]\right.$$
$$\left[(E+\rho\cdot\cos(\alpha-\psi_0)-B_2)(-\sin(\alpha-\psi_0))\right.$$
$$\left.+(C\cdot\tan\alpha-\rho\cdot\sin(\alpha-\psi_0)+C\cdot\tan\psi_0)(-\cos(\alpha-\psi_0))\right]/\underset{\sim}{R}_{41}^4$$
$$-\frac{K}{\underset{\sim}{R}_{41}^2}\left[(E+\rho\cdot\cos(\alpha-\psi_0)-B_2)(\cos(\alpha-\psi_0))\right.$$
$$\left.\left.+(C\cdot\tan\alpha-\rho\cdot\sin(\alpha-\psi_0)+C\cdot\tan\psi_0)(-\sin(\alpha-\psi_0))\right]\right\}$$

$$KIV_{41} = \left\{\left[K - M\cdot 4\cdot\mu\ \frac{(C\cdot\tan\alpha-\rho\cdot\sin(\alpha-\psi_0)+C\cdot\tan\psi_0)^2}{\underset{\sim}{R}_{41}^2}\right]\right.$$
$$\left[(E+\rho\cdot\cos(\alpha-\psi_0)-B_2)(-\sin(\alpha-\psi_0))\right.$$
$$\left.\left.+(C\cdot\tan\alpha-\rho\cdot\sin(\alpha-\psi_0)+C\cdot\tan\psi_0)(-\cos(\alpha-\psi_0))\right]\right\}/\underset{\sim}{R}_{41}^2$$

Ker 42

$$\underset{\sim}{R}^2_{42} = \left\{ (\overline{X1}-B_2)^2 + (2\cdot C\cdot \tan\psi_0)^2 \right\}$$

$$KI_{42} = \left\{ \left[K - \frac{M\cdot 4\cdot \mu (\overline{X1}-B_2)^2}{\underset{\sim}{R}^2_{42}} \right] \left[\frac{-2\cdot C\cdot \tan\psi_0}{\underset{\sim}{R}^2_{42}} \right] \right\}$$

$$KII_{42} = \left\{ +M\cdot 4\cdot \mu (\overline{X1}-B_2)(2\cdot C\cdot \tan\psi_0)^2/\underset{\sim}{R}^4_{42} + K\left[\frac{\overline{X1} - B_2}{\underset{\sim}{R}^2_{42}} \right] \right\}$$

$$KIII_{42} = \left\{ +M\cdot 4\cdot \mu (\overline{X1}-B_2)(2\cdot C\cdot \tan\psi_0)^2/\underset{\sim}{R}^4_{42} - K\left[\frac{\overline{X1} - B_2}{\underset{\sim}{R}^2_{42}} \right] \right\}$$

$$KIV_{42} = \left\{ \left[K - M\cdot 4\cdot \mu \frac{(2\cdot C\cdot \tan\psi_0)^2}{\underset{\sim}{R}^2_{42}} \right] \left[\frac{-2\cdot C\cdot \tan\psi_0}{\underset{\sim}{R}^2_{42}} \right] \right\}$$

Ker 43

$$\underset{\sim}{R}^2_{43} = (\cos\Theta - B_2)^2 + (\sin\Theta + C\cdot\tan\psi_0)^2$$

$$KI_{43} = \left\{ \left[K - M\cdot 4\cdot\mu \frac{(\cos\Theta - B_2)^2}{\underset{\sim}{R}^2_{43}} \right] \left[\frac{1 - B_2\cdot\cos\Theta + C\cdot\tan\psi_0\cdot\sin\Theta}{\underset{\sim}{R}^2_{43}} \right] \right\}$$

$$KII_{43} = \left\{ -M\cdot 4\cdot\mu(\cos\Theta - B_2)(\sin\Theta + C\cdot\tan\psi_0) \frac{(1 - B_2\cdot\cos\Theta + C\cdot\tan\psi_0\cdot\sin\Theta)}{\underset{\sim}{R}^4_{43}} + K\left[B_2\cdot\sin\Theta + C\cdot\tan\psi_0\cdot\cos\Theta\right] / \underset{\sim}{R}^2_{43} \right\}$$

$$KIII_{43} = \left\{ -M\cdot 4\cdot\mu(\cos\Theta - B_2)(\sin\Theta + C\cdot\tan\psi_0) \frac{(1 - B_2\cdot\cos\Theta + C\cdot\tan\psi_0\cdot\sin\Theta)}{\underset{\sim}{R}^4_{43}} - K\left[B_2\cdot\sin\Theta + C\cdot\tan\psi_0\cdot\cos\Theta\right] / \underset{\sim}{R}^2_{43} \right\}$$

$$KIV_{43} = \left\{ \left[K - M\cdot 4\cdot\mu \frac{(\sin\Theta + C\cdot\tan\psi_0)^2}{\underset{\sim}{R}^2_{43}} \right] \left[\frac{1 - B_2\cdot\cos\Theta + C\cdot\tan\psi_0\cdot\sin\Theta}{\underset{\sim}{R}^2_{43}} \right] \right\}$$

Ker 44

$$\underline{R}^2_{44} = (\overline{X1} - B_2)^2$$

$$KI_{44} = 0$$

$$KII_{44} = \frac{-K}{\overline{X1} - B_2}$$

$$KIII_{44} = \frac{K}{\overline{X1} - B_2}$$

$$KIV_{44} = 0$$

Ker 45

$$R_{45}^2 = (E+\rho\cdot\cos(\alpha+\psi_0)-B_2)^2 + (C\cdot\tan\alpha-\rho\cdot\sin(\alpha+\psi_0)+C\cdot\tan\psi_0)^2$$

$$KI_{45} = \left\{\left[K-M\cdot 4\cdot\mu\frac{(E+\rho\cdot\cos(\alpha+\psi_0)-B_2)^2}{R_{45}^2}\right]\left[(E+\rho\cdot\cos(\alpha+\psi_0)-B_2)\sin(\alpha+\psi_0)\right.\right.$$

$$\left.\left.+(C\cdot\tan\alpha-\rho\cdot\sin(\alpha+\psi_0)+C\cdot\tan\psi_0)(\cos(\alpha+\psi_0))\right]/R_{45}^2\right.$$

$$KII_{45} = \left\{-M\cdot 4\cdot\mu(E+\rho\cdot\cos(\alpha+\psi_0)-B_2)(C\cdot\tan\alpha-\rho\cdot\sin(\alpha+\psi_0)+C\cdot\tan\psi_0)/R_{45}^4\right.$$

$$\cdot\left[(E+\rho\cdot\cos(\alpha+\psi_0)-B_2)\sin(\alpha+\psi_0)\right.$$

$$\left.+(C\cdot\tan\alpha-\rho\cdot\sin(\alpha+\psi_0)+C\cdot\tan\psi_0)(\cos(\alpha+\psi_0))\right]$$

$$+\frac{K}{R_{45}^2}\left[(E+\rho\cdot\cos(\alpha+\psi_0)-B_2)(-\cos(\alpha+\psi_0))\right.$$

$$\left.\left.+(C\cdot\tan\alpha-\rho\cdot\sin(\alpha+\psi_0)+C\cdot\tan\psi_0)\sin(\alpha+\psi_0)\right]\right\}$$

$$KIII_{45} = \left\{-M\cdot 4\cdot\mu(E+\rho\cdot\cos(\alpha+\psi_0)-B_2)(C\cdot\tan\alpha-\rho\cdot\sin(\alpha+\psi_0)+C\cdot\tan\psi_0)/R_{45}^4\right.$$

$$\cdot\left[(E+\rho\cdot\cos(\alpha+\psi_0)-B_2)\sin(\alpha+\psi_0)\right.$$

$$\left.+(C\cdot\tan\alpha-\rho\cdot\sin(\alpha+\psi_0)+C\cdot\tan\psi_0)\cos(\alpha+\psi_0)\right]$$

$$-\frac{K}{R_{45}^2}\left[(E+\rho\cdot\cos(\alpha+\psi_0)-B_2)(-\cos(\alpha+\psi_0))\right.$$

$$\left.\left.+(C\cdot\tan\alpha-\rho\cdot\sin(\alpha+\psi_0)+C\cdot\tan\psi_0)\sin(\alpha+\psi_0)\right]\right\}$$

$$KIV_{45} = \left\{\left[K-M\cdot 4\cdot\mu\frac{(C\cdot\tan\alpha-\rho\cdot\sin(\alpha+\psi_0)+C\cdot\tan\psi_0)^2}{R_{45}^2}\right]\cdot\right.$$

$$\left[(E+\rho\cdot\cos(\alpha+\psi_0)-B_2)\sin(\alpha+\psi_0)\right.$$

$$\left.\left.+(C\cdot\tan\alpha-\rho\cdot\sin(\alpha+\psi_0)+C\cdot\tan\psi_0)\cdot\cos(\alpha+\psi_0)\right]/R_{45}^2\right\}$$

Ker 51

$$\underline{R}_{51}^2 = \rho^2+B^2 -2\cdot\rho B\cdot\cos 2\psi_0$$

$$KI_{51} = \left\{\left[K-M\cdot 4\cdot\mu\,\frac{(\rho\cdot\cos(\alpha-\psi_0)-B\cdot\cos(\alpha+\psi_0))^2}{\underline{R}_{51}^2}\right]\left[\frac{-B\cdot\sin 2\psi_0}{\underline{R}_{51}^2}\right]\right\}$$

$$KII_{51} = \left\{+M\cdot 4\cdot\mu\left[\rho\cdot\cos(\alpha-\psi_0)-B\cdot\cos(\alpha+\psi_0)\right]\right.$$
$$\left.\cdot\left[\rho\cdot\sin(\alpha-\psi_0)-B\cdot\sin(\alpha+\psi_0)\right]\cdot\left[\frac{-B\cdot\sin 2\psi_0}{\underline{R}_{51}^4}\right] + K\cdot\left[\frac{\rho-B\cdot\cos 2\psi_0}{\underline{R}_{51}^2}\right]\right\}$$

$$KIII_{51} = \left\{M\cdot 4\cdot\mu\left[\rho\cdot\cos(\alpha-\psi_0) - B\cdot\cos(\alpha+\psi_0)\right]\right.$$
$$\left.\cdot\left[\rho\cdot\sin(\alpha-\psi_0)-B\cdot\sin(\alpha+\psi_0)\right]\cdot\left[\frac{-B\cdot\sin 2\psi_0}{\underline{R}_{51}^4}\right] - K\left[\frac{\rho-B\cdot\cos 2\psi_0}{\underline{R}_{51}^2}\right]\right\}$$

$$KIV_{51} = \left\{\left[K-M\cdot 4\cdot\mu\,\frac{(\rho\cdot\sin(\alpha-\psi_0)-B.\sin(\alpha+\psi_0))^2}{\underline{R}_{51}^2}\right]\left[\frac{-B\cdot\sin 2\psi_0}{\underline{R}_{51}^2}\right]\right\}$$

Ker 52

$$\underline{R}_{52}^2 = \left[\overline{Xl}-E-B\cdot\cos(\alpha+\psi_0)\right]^2 + \left[C\cdot(\tan\psi_0-\tan\alpha)+B\cdot\sin(\alpha+\psi_0)\right]^2$$

$$KI_{52} = \left\{\left[K-\frac{M\cdot 4\cdot\mu(\overline{Xl}-E-B\cdot\cos(\alpha+\psi_0))^2}{\underline{R}_{52}^2}\right]\cdot\left[-C(\tan\psi_0-\tan\alpha)-B\cdot\sin(\alpha+\psi_0)\right]/\underline{R}_{52}^2\right\}$$

$$KII_{52} = \left\{M\cdot 4\cdot\mu\frac{\left[\overline{Xl}-E-B\cdot\cos(\alpha+\psi_0)\right]\cdot\left[C\cdot(\tan\psi_0-\tan\alpha)+B\cdot\sin(\alpha+\psi_0)\right]^2}{\underline{R}_{52}^4} + K\cdot\left[\overline{Xl}-E-B\cdot\cos(\alpha+\psi_0)\right]/\underline{R}_{52}^2\right\}$$

$$KIII_{52} = \left\{M\cdot 4\cdot\mu\frac{\left[\overline{Xl}-E-B\cdot\cos(\alpha+\psi_0)\right]\cdot\left[C\cdot(\tan\psi_0-\tan\alpha)+B\cdot\sin(\alpha+\psi_0)\right]^2}{\underline{R}_{52}^4} - K\cdot\left[\overline{Xl}-E-B\cdot\cos(\alpha+\psi_0)\right]/\underline{R}_{52}^2\right\}$$

$$KIV_{52} = \left\{\left[K - M\cdot 4\cdot\mu\frac{(C\cdot(\tan\psi_0-\tan\alpha)+B\cdot\sin(\alpha+\psi_0))^2}{\underline{R}_{52}^2}\right]\cdot\left[-C\cdot(\tan\psi_0-\tan\alpha)-B\cdot\sin(\alpha+\psi_0)\right]/\underline{R}_{52}^2\right\}$$

Ker 53

$$\underline{R}_{53}^2 = [\cos\Theta - E - B\cdot\cos(\alpha+\psi_0)]^2 + [\sin\Theta - C\cdot\tan\alpha + B\cdot\sin(\alpha+\psi_0)]^2$$

$$KI_{53} = \left\{ \left[K - \frac{M\cdot 4\cdot\mu(\cos\Theta - E - B\cdot\cos(\alpha+\psi_0))^2}{\underline{R}_{53}^2} \right] \cdot [1 - E\cdot\cos\Theta - C\cdot\tan\alpha\cdot\sin\Theta - B\cdot\cos(\Theta+\alpha+\psi_0)]/\underline{R}_{53}^2 \right\}$$

$$KII_{53} = \left\{ -M\cdot 4\cdot\mu[\cos\Theta - E - B\cdot\cos(\alpha+\psi_0)]\cdot[\sin\Theta - C\cdot\tan\alpha + B\cdot\sin(\alpha+\psi_0)] \cdot [1 - E\cdot\cos\Theta - C\cdot\tan\alpha\cdot\sin\Theta - B\cdot\cos(\Theta+\alpha+\psi_0)]/\underline{R}_{53}^4 + K\cdot[E\cdot\sin\Theta - C\cdot\tan\alpha\cdot\cos\Theta + B\cdot\sin(\Theta+\alpha+\psi_0)]/\underline{R}_{53}^2 \right\}$$

$$KIII_{53} = \left\{ -M\cdot 4\cdot\mu[\cos\Theta - E - B\cdot\cos(\alpha+\psi_0)]\cdot[\sin\Theta - C\cdot\tan\alpha + B\cdot\sin(\alpha+\psi_0)] \cdot [1 - E\cdot\cos\Theta - C\cdot\tan\alpha\cdot\sin\Theta - B\cdot\cos(\Theta+\alpha+\psi_0)]/\underline{R}_{53}^4 - K\cdot[E\cdot\sin\Theta - C\cdot\tan\alpha\cdot\cos\Theta + B\cdot\sin(\Theta+\alpha+\psi_0)]/\underline{R}_{53}^2 \right\}$$

$$KIV_{53} = \left\{ \left[K - \frac{M\cdot 4\cdot\mu(\sin\Theta - C\cdot\tan\alpha + B\cdot\sin(\alpha+\psi_0))^2}{\underline{R}_{53}^2} \right] \cdot [1 - E\cdot\cos\Theta - C\cdot\tan\alpha\cdot\sin\Theta - B\cdot\cos(\Theta+\alpha+\psi_0)]/\underline{R}_{53}^2 \right\}$$

Ker 54

$$\underline{R}_{54}^2 = \left[\overline{Xl}-E-B\cdot\cos(\alpha+\psi_0)\right]^2 + \left[-C\cdot\tan\psi_0-C\cdot\tan\alpha+B\cdot\sin(\alpha+\psi_0)\right]^2$$

$$KI_{54} = \left\{\left[K-\frac{M\cdot 4\cdot\mu\left(\overline{Xl}-E-B\cdot\cos(\alpha+\psi_0)\right)^2}{\underline{R}_{54}^2}\right]\cdot\left[\frac{-C\cdot\tan\psi_0-C\cdot\tan\alpha+B\cdot\sin(\alpha+\psi_0)}{\underline{R}_{54}^2}\right]\right\}$$

$$KII_{54} = \left\{-M\cdot 4\cdot\mu\frac{\left[\overline{Xl}-E-B\cdot\cos(\alpha+\psi_0)\right]\cdot\left[-C\cdot\tan\psi_0-C\cdot\tan\alpha+B\cdot\sin(\alpha+\psi_0)\right]^2}{\underline{R}_{54}^4} - K\cdot\left[\overline{Xl}-E-B\cdot\cos(\alpha+\psi_0)\right]/\underline{R}_{54}^2\right\}$$

$$KIII_{54} = \left\{-M\cdot 4\cdot\mu\frac{\left[\overline{Xl}-E-B\cdot\cos(\alpha+\psi_0)\right]\cdot\left[-C\cdot\tan\psi_0-C\cdot\tan\alpha+B\cdot\sin(\alpha+\psi_0)\right]^2}{\underline{R}_{54}^4} + K\cdot\left[\overline{Xl}-E-B\cdot\cos(\alpha+\psi_0)\right]/\underline{R}_{54}^2\right\}$$

$$KIV_{54} = \left\{\left[K-\frac{M\cdot 4\cdot\mu\left[-C\cdot\tan\psi_0-C\cdot\tan\alpha+B\cdot\sin(\alpha+\psi_0)\right]^2}{\underline{R}_{54}^2}\right]\cdot\left[\frac{-C\cdot\tan\psi_0-\tan\alpha+B\cdot\sin(\alpha+\psi_0)}{\underline{R}_{54}^2}\right]\right\}$$

Ker 55

$$\underline{R}_{55}^2 = (\rho-B)^2$$

$$KI_{55} = 0 \qquad KIII_{55} = \frac{K}{\rho-B}$$

$$KII_{55} = \frac{-K}{\rho-B} \qquad KIV_{55} = 0$$

APPENDIX B

GOVERNING B.I.E. FOR CLOSED BENT CRACK

This appendix contains Eq. set (3.2), the governing B.I.E. for the closed bent crack ($\psi_0 = 0$). Section B.1 presents the full set of equations. Section B.2 presents algebraic formulas inserted into these equations depending on the assumed displacement model. Section B.3 contains the detailed forcing function formula necessary for general traction loading.

Appendix B.1

Full I.E. Set (System 3.2)

Define:

$$R_{12}^2 \equiv \left[\overline{X1} - E - B \cdot \cos\alpha\right]^2 + \left[-C \cdot \tan\alpha + B \cdot \sin\alpha\right]^2$$

$$R_{13}^2 \equiv \left[\sin\theta - E - B \cdot \cos\alpha\right]^2 + \left[\sin\theta - C \cdot \tan\alpha + B \cdot \sin\alpha\right]^2$$

$$R_{21}^2 \equiv \left[E + \rho \cdot \cos\alpha - B_2\right]^2 + \left[C \cdot \tan\alpha - \rho \cdot \sin\alpha\right]^2$$

$$R_{23}^2 \equiv \left[1 - 2 \cdot B_2 \cdot \cos\theta + B_2\right]$$

$$R_{31}^2 \equiv \left[E + \rho \cdot \cos\alpha - \cos\theta_0\right]^2 + \left[C \cdot \tan\alpha - \rho \cdot \sin\alpha - \sin\theta_0\right]^2$$

$$R_{32}^2 \equiv \left[1 - 2 \cdot \overline{X1} \cdot \cos\theta_0 + \overline{X1}^2\right]$$

$$- \frac{1}{\underline{\lambda}} \left[u_{1(B)}\right] + \int_F^1 u_{2(\overline{X1})} \left\{ \left[K - \frac{M \cdot 4 \cdot \mu (\overline{X1} - E - B \cdot \cos\alpha)^2}{R_{12}^2} \right] \cdot \left[\frac{C \cdot \tan\alpha - B \cdot \sin\alpha}{R_{12}^2} \right] \right\} d\overline{X1} + \int_0^{2\pi} u_{3(\theta)} \left\{ \left[K - M \cdot 4 \cdot \mu \frac{(\cos\theta - E - B \cdot \cos\alpha)^2}{R_{13}^2} \right] \cdot \left[1 - E \cdot \cos\theta - C \cdot \tan\alpha \cdot \sin\theta - B \cdot \cos(\theta + \alpha) \right] / R_{13}^2 \right\} d\theta$$

$$- \int_F^1 u_{4(\overline{X1})} \left\{ \left[K - \frac{M \cdot 4 \cdot \mu \left[\overline{X1} - E - B \cdot \cos\alpha\right]^2}{R_{12}^2} \right] \left[\frac{C \cdot \tan\alpha - B \cdot \sin\alpha}{R_{12}^2} \right] \right\} d\overline{X1}$$

$$- \frac{1}{\underline{\lambda}} \cdot \left[u_{5(B)}\right] + \int_0^{B-H} v_{1(\rho)} \cdot \frac{K}{\rho - B} \, d\rho$$

$$+ v_{1(B-H)} \cdot (\mathrm{AlVMH}) + v_{1(B)} \cdot (\mathrm{AlVB}) + v_{1(B+H)} \cdot (\mathrm{AlVPH})$$

$$+ \int_{B+H}^{\underline{C}} v_{1(\rho)} \cdot \frac{K}{\rho - B} \, d\rho$$

$$+ \int_F^1 v_{2(\overline{X1})} \left\{ M \cdot 4 \cdot \mu \frac{\left[\overline{X1} - E - B \cdot \cos\alpha\right] \left[-C \cdot \tan\alpha + B \cdot \sin\alpha\right]^2}{R_{12}^4} + K \left[\overline{X1} - E - B \cdot \cos\alpha\right] / R_{12}^2 \right\} d\overline{X1}$$

3.2.A.1

$$+\int_0^{2\pi} v_{3(\Theta)} \left\{ -M\cdot 4\cdot\mu\left[\cos\Theta-E-B\cdot\cos\alpha\right]\cdot\left[\sin\Theta-C\cdot\tan\alpha+B\cdot\sin\alpha\right] \right.$$

$$\cdot \left[1-E\cdot\cos\Theta-C\cdot\tan\alpha\cdot\sin\Theta-B\cdot\cos(\Theta+\alpha)\right]/R_{13}^4$$

$$\left. + K \cdot \left[E\cdot\sin\Theta-C\cdot\tan\alpha\cdot\cos\Theta+B\cdot\sin(\Theta+\alpha)\right]/R_{13}^2 d\Theta \right\}$$

$$-\int_F^1 v_{4(\overline{X1})} \left\{ +M\cdot 4\cdot\mu \frac{\left[\overline{X1}-E-B\cdot\cos\alpha\right]\cdot\left[+B\cdot\sin\alpha-C\cdot\tan\alpha\right]^2}{R_{12}^4} \right.$$

$$\left. + K \left[\overline{X1}-E-B\cdot\cos\alpha\right] /R_{12}^2 \right\} d\overline{X1} \quad -\int_0^{B-H} v_{5(\rho)}\cdot\frac{K}{\rho-B}\, d\rho$$

$$\cdot v_{5(B-H)} \cdot (AlVMH) - v_{5(B)} \cdot (AlVB) - v_{(B+H)} \cdot (AlVPH)$$

$$-\int_{B+H}^{\underline{C}} v_{5(\rho)}\cdot\frac{K}{\rho-B}\, d\rho = \frac{1}{\underline{\lambda}} \cdot FAl_{(B)}$$

3.2.A.1 Cont.

$$\int_0^{\underline{C}} u_{1(\rho)} \left\{ \left[K - \frac{M\cdot 4\cdot \mu (E+\rho\cdot\cos\alpha - B_2)^2}{R_{21}^2} \right] \cdot \left[(E+\rho\cdot\cos\alpha - B_2)(-\sin\alpha) \right.\right.$$

$$\left.\left. + (C\cdot\tan\alpha - \rho\cdot\sin\alpha)(-\cos\alpha) \right] / R_{21}^2 \right\} d\rho$$

$$- \frac{u_{2(B_2)}}{\underline{\lambda}} + \int_0^{2\pi} u_{3(\theta)} \left\{ \left[K \frac{-M\cdot 4\cdot \mu (\cos\theta - B_2)^2}{R_{23}^2} \right] \cdot \left[\frac{1 - B_2\cos\theta}{R_{23}^2} \right] \right\} d\theta$$

$$- \frac{u_{4(B_2)}}{\underline{\lambda}} + \int_0^{\underline{C}} u_{5(\rho)} \left\{ \left[K - \frac{M\cdot 4\cdot \mu (E+\rho\cdot\cos\alpha - B_2)^2}{R_{21}^2} \right] \left[E+\rho\cdot\cos\alpha - B_2 \right) \sin\alpha \right.$$

$$\left. + (C\cdot\tan\alpha - \rho\cdot\sin\alpha)\cos\alpha \right] / R_{21}^2 \right\} d\rho$$

$$+ \int_0^{\underline{C}} v_{1(\rho)} \left\{ \left\{ \left[+ M\cdot 4\cdot \mu \left[E+\rho\cdot\cos\alpha - B_2 \right] \left[C\cdot\tan\alpha - \rho\cdot\sin\alpha \right] \right.\right.\right.$$

$$\left.\left.\left. \left[(E+\rho\cdot\cos\alpha - B_2)(+\sin\alpha) + (C\cdot\tan\alpha - \rho\cdot\sin\alpha)(+\cos\alpha) \right] \right] / R_{21}^4 \right.$$

$$\left. + K \cdot \left[(E+\rho\cdot\cos\alpha - B_2)\cos\alpha + (C\cdot\tan\alpha - \rho\cdot\sin\alpha)(-\sin\alpha) \right] / R_{21}^2 \right\} d\rho$$

$$+ \int_F^{B_2 - H_2} v_{2(\overline{X1})} \left\{ \frac{K}{\overline{X1} - B} \right\} d\overline{X1} + v_{2(B-H)} \cdot (A2VMH)$$

$$+ v_{2(B)} \cdot (A2VB) + v_{2(B+H)} \cdot (A2VPH)$$

3.2.A.2

$$+\int_{B_2+H_2}^{1} v_{2(\overline{X1})} \left\{\frac{K}{\overline{X1}-B_2}\right\} d\overline{X1} \quad + \int_{0}^{2\pi} v_{3(\Theta)} \left\{-M\cdot 4\cdot\mu\left[\cos\Theta - B_2\right]\right.$$

$$\left.\cdot\left[\sin\Theta\right]\cdot\left[\frac{1-B_2\cdot\cos\Theta}{R_{23}^4}\right] + K\cdot\left[B_2\cdot\sin\Theta\right]/R_{23}^2\right\} d\Theta$$

$$+\int_{F}^{B_2-H_2} v_{4(\overline{X1})} \left\{\frac{-K}{\overline{X1}-B_2}\right\} d\overline{X1} - v_{4(B-H)}\cdot(A2VMH) - v_{4(B)}\cdot(A2VB)$$

$$-v_{4(B)}\cdot(A2VPH) + \int_{B_2+H_2}^{1} v_{4(\overline{X1})} \left\{\frac{-K}{\overline{X1}-B_2}\right\} d\overline{X1}$$

$$+ \int_{0}^{\underline{C}} v_{5(\rho)} \left\{\left[-M\cdot 4\cdot\mu\left[E+\rho\cdot\cos\alpha-B_2\right]\cdot\left[C\cdot\tan\alpha-\rho\cdot\sin\alpha\right]\right.\right.$$

$$\cdot\left[(E+\rho\cdot\cos\alpha-B_2)\sin\alpha + (C\cdot\tan\alpha-\rho\cdot\sin\alpha)\cos\alpha\right]/R_{21}^4$$

$$\left.\left.+ K\left[(E+\rho\cdot\cos\alpha-B_2)(-\cos\alpha)+(C\cdot\tan\alpha-\rho\cdot\sin\alpha)\sin\alpha\right]/R_{21}^2\right\} d\rho = \frac{1}{\underline{\lambda}}\cdot FA2_{(B_2)}$$

3.2.A.2 Cont.

$$\int_0^{\underline{C}} u_{1(\rho)} \left\{ \left[K - \frac{M \cdot 4 \cdot \mu (E+\rho \cdot \cos\alpha - \cos\Theta_0)^2}{R_{31}^2} \right] \right.$$

$$\left. \cdot \left[-E \cdot \sin\alpha - C \cdot \sin\alpha + \sin(\Theta_0+\alpha) \right] / R_{31}^2 \right\} d\rho$$

$$+ \int_F^1 u_{2(\overline{X1})} \left\{ \left[K - \frac{M \cdot 4 \cdot \mu (\overline{X1} - \cos\Theta_0)^2}{R_{32}^2} \right] \cdot \left[\frac{\sin\Theta_0}{R_{32}^2} \right] \right\} d\overline{X1}$$

$$+ \int_0^{2\pi} u_{3(\Theta)} \left\{ \frac{K}{2} - \frac{M \cdot 4 \cdot \mu}{2} \cdot \sin^2 \left(\frac{\Theta + \Theta_0}{2} \right) \right\} d\Theta \quad - \frac{1}{\underline{\lambda}} \; u_{3(\Theta_0)}$$

$$+ \int_F^1 u_{4(\overline{X1})} \left\{ \left[K - \frac{M \cdot 4 \cdot \mu (\overline{X1} - \cos\Theta_0)^2}{R_{32}^2} \right] \cdot \left[\frac{-\sin\Theta_0}{R_{32}^2} \right] \right\} d\overline{X1}$$

$$+ \int_0^{\underline{C}} u_{5(\rho)} \left\{ \left[K - \frac{M \cdot 4 \cdot \mu (E+\rho \cdot \cos\alpha - \cos\Theta_0)^2}{R_{31}^2} \right] \right.$$

$$\left. \cdot \left[E \cdot \sin\alpha + C \cdot \sin\alpha - \sin(\alpha+\Theta_0) \right] / R_{31}^2 \right\} d\rho$$

$$+ \int_0^{\underline{C}} v_{1(\rho)} \left\{ -M \cdot 4 \cdot \mu \left[E+\rho \cdot \cos\alpha - \cos\Theta_0 \right] \cdot \left[C \cdot \tan\alpha - \rho \cdot \sin\alpha - \sin\Theta_0 \right] \right.$$

$$\cdot \left[-E \cdot \sin\alpha - C \cdot \sin\alpha + \sin(\Theta_0+\alpha) \right] / R_{31}^4$$

$$\left. + K \cdot \left[E \cdot \cos\alpha - C \cdot \tan\alpha \cdot \sin\alpha + \rho - \cos(\Theta_0+\alpha) \right] / R_{31}^2 \right\} d\rho \qquad \text{3.2.A.3}$$

$$+\int_F^1 v_{2(\overline{X1})} \left\{ M\cdot 4\cdot\mu\left[\overline{X1}-\cos\theta_0\right]\frac{\left[\sin\theta_0\right]^2}{R_{32}^4} + K\cdot\frac{\left[\overline{X1}-\cos\theta_0\right]}{R_{32}^2} \right\} d\overline{X1}$$

$$+\int_0^{2\pi} v_{3(\theta)} \left\{ \frac{M\cdot 4\cdot\mu}{4}\cdot\sin(\theta+\theta_0) \right\} d\theta$$

$$+\int_0^{\theta_0-H_3} v_{3(\theta)} \left\{ \frac{K}{2}\cdot\frac{\cos(\frac{\theta-\theta_0}{2})}{\sin(\frac{\theta-\theta_0}{2})} \right\} d\theta + K\cdot\left\{ v_{3(\theta_0+H_3)} - v_{3(\theta_0-H_3)} \right\}$$

$$+\int_{\theta_0+H_3}^{2\pi} v_{3(\theta)} \frac{K}{2}\left\{ \frac{\cos(\frac{\theta-\theta_0}{2})}{\sin(\frac{\theta-\theta_0}{2})} \right\} d\theta +$$

$$+\int_F^1 v_{4(\overline{X1})} \left\{ -M\cdot 4\cdot\mu\left[\overline{X1}-\cos\theta_0\right]\frac{\left[\sin\theta_0\right]^2}{R_{32}^4} - K\cdot\frac{\left[\overline{X1}-\cos\theta_0\right]}{R_{32}^2} \right\} d\overline{X1}$$

$$\int_0^{\underline{C}} v_{5(\rho)} \left\{ -M\cdot 4\cdot\mu\left[E+\rho\cdot\cos\alpha-\cos\theta_0\right]\cdot\left[C\cdot\tan\alpha-\rho\cdot\sin\alpha-\sin\theta_0\right] \right.$$

$$\left.\cdot\left[E\cdot\sin\alpha+C\cdot\sin\alpha-\sin(\alpha+\theta_0)\right]/R_{31}^4 \right.$$

$$\left. + K\cdot\left[-E\cdot\cos\alpha+C\cdot\sin\alpha\cdot\tan\alpha-\rho+\cos(\theta_0+\alpha)\right]/R_{31}^2 \right\} d\rho$$

$$= \frac{1}{\underline{\lambda}}\cdot FA3_{(\theta_0)}$$

3.2.A.3 Cont.

$$\int_0^{\underline{C}} u_{1(\rho)} \left\{ \left[M\cdot 4\cdot\mu (E+\rho\cdot\cos\alpha - B_2)^2 \cdot (C\cdot\tan\alpha - \rho\cdot\sin\alpha)(-4C) \frac{(B_2-E-C)\sin\alpha}{R_{21}^6} \right] \right.$$

$$+ \left[\left[K - M\cdot 4\cdot\mu \frac{(E+\rho\cdot\cos\alpha - B_2)^2}{R_{21}^2} \right] \cdot \left[\frac{2\cdot C}{R_{21}^2} \cdot \cos\alpha \right. \right.$$

$$\left. \left. + (B_2-E-C) \cdot \sin\alpha \cdot (C\cdot\tan\alpha - \rho\cdot\sin\alpha) \cdot \frac{4\cdot C}{R_{21}^4} \right] \right] \left. \right\} d\rho$$

$$+ \int_F^{B_2-H_2} u_{2(\overline{X1})} \cdot \frac{2\cdot C\cdot (K-M\cdot 4\cdot\mu)}{(\overline{X1} - B_2)^2} \, d\overline{X1} + u_{2(B-H)} \cdot (A4UMH)$$

$$+ u_{2(B)} \cdot (A4UB) + u_{2(B+H)} \cdot (A4UPH)$$

$$+ \int_{B_2+H_2}^{1} u_{2(\overline{X1})} \cdot \frac{2\cdot C\cdot (K-M\cdot 4\cdot\mu)}{(\overline{X1} - B_2)^2} \, d\overline{X1}$$

$$+ \int_0^{2\pi} u_{3(\Theta)} \left\{ \left[M\cdot 4\cdot\mu (\cos\theta - B_2)^2 (1-B_2\cdot\cos\theta)(-4C) \sin\theta / R_{23}^6 \right] \right.$$

$$\left. + \left[\left[K - \frac{M\cdot 4\cdot\mu(\cos\theta - B_2)^2}{R_{23}^2} \right] \left[\frac{-2\cdot C\cdot\sin\theta}{R_{23}^2} + \frac{(1-B_2\cos\theta)4C\cdot\sin\theta}{R_{23}^4} \right] \right] \right\} d\theta$$

$$+ \int_F^{B_2-H_2} u_{4(\overline{X1})} \cdot \frac{(-2C)(K-M\cdot 4\cdot\mu)}{(\overline{X1}-B_2)^2} \, d\overline{X1} - u_{4(B-H)} \cdot (A4^{U}MH)$$

$$-u_{4(B)} \cdot (A4UB) - u_{4(B+H)} \cdot (A4UPH)$$

$$+ \int_{B_2+H_2}^{1} u_{4(\overline{X1})} \cdot \frac{(-2C)(K-M\cdot 4\cdot\mu)}{(\overline{X1}-B_2)^2} \, d\overline{X1} \qquad 3.2.A.4$$

$$- \int_0^{\underline{C}} u_{5(\rho)} \left\{ \left[+M \cdot 4 \cdot \mu (E+\rho \cdot \cos\alpha - B_2)^2 (C \cdot \tan\alpha - \rho \cdot \sin\alpha)(-4C) \frac{(B_2-E-C)\sin\alpha}{R_{21}^6} \right] \right.$$

$$+ \left[\left[K - M \cdot 4 \cdot \mu \frac{(E+\rho \cdot \cos\alpha - B_2)^2}{R_{21}^2} \right] \cdot \left[\frac{2 \cdot C}{R_{21}^2} \cdot \cos\alpha \right. \right.$$

$$\left. \left. + (B_2-E-C) \cdot \sin\alpha \cdot (C \cdot \tan\alpha - \rho \cdot \sin\alpha) \cdot \frac{4 \cdot C}{R_{21}^4} \right] \right] \left. \right\} d\rho$$

$$+ \int_0^{\underline{C}} v_{1(\rho)} \left\{ \left[M \cdot 4 \cdot \mu \cdot 2 \cdot C (E+\rho \cdot \cos\alpha - B_2) \cdot \frac{\sin\alpha}{R_{21}^4} \right. \right.$$

$$\cdot \left[\rho \cdot \cos\alpha - (E+2C-B_2) + 4 \cdot (C \cdot \tan\alpha - \rho \cdot \sin\alpha)^2 \frac{(E+C-B_2)}{R_{21}^2} \right] \Big]$$

$$+ K \cdot \left[\frac{2 \cdot C}{R_{21}^2} \cdot \sin\alpha + \left[\rho + (E-B_2)\cos\alpha - C \cdot \tan\alpha \cdot \sin\alpha \right] \right.$$

$$\left. \left. \cdot \left[C \cdot \tan\alpha - \rho \cdot \sin\alpha \right] (4C) / R_{21}^4 \right] \right\} d\rho + v_{2(B-H)} \cdot (A4VMH)$$

$$+ v_{2(B)} \cdot (A4VB) + v_{2(B+H)} \cdot (A4VPH)$$

$$+ \int_0^{2\pi} v_{3(\theta)} \left\{ M \cdot 4 \cdot \mu 2 \cdot C \cdot \frac{(\cos\theta - B_2)}{R_{23}^4} \cdot \left[(1 - B_2 \cdot \cos\theta + \sin^2\theta) \right. \right.$$

$$\left. \left. -4 \cdot (1 - B_2 \cdot \cos\theta) \cdot \frac{\sin^2\theta}{R_{23}^2} \right] + K \cdot \frac{2C}{R_{23}^2} \cdot \left[\frac{2 \cdot B_2 \sin^2\theta}{R_{23}^2} - \cos\theta \right] \right\} d\theta$$

$$+ v_{4(B-H)} \cdot (A4VBH) + v_{2(B)} \cdot (A4VB) + v_{4(B-H)} \cdot (A4VPH)$$

3.2.A.4 Cont.

$$- \int_0^{\underline{C}} v_{5(\rho)} \left\{ \left[+M \cdot 4 \cdot \mu \cdot 2 \cdot C(E+\rho \cdot \cos\alpha - B_2) \cdot \frac{\sin\alpha}{R_{21}^4} \right.\right.$$

$$\left. \cdot \left[\rho \cdot \cos\alpha - (E+2C-B_2) + 4 \cdot (C \cdot \tan\alpha - \rho \cdot \sin\alpha)^2 \frac{(E+C-B_2)}{R_{21}^2} \right] \right]$$

$$+ K \cdot \left[\frac{2 \cdot C}{R_{21}^2} \cdot \sin\alpha + \left[\rho + (E-B_2)\cos\alpha - C \cdot \tan\alpha \cdot \sin\alpha \right] \right.$$

$$\left. \left. \cdot \left[C \cdot \tan\alpha - \rho \cdot \sin\alpha \right] (4C)/R_{21}^4 \right] \right\} d\rho = \frac{1}{\underline{\lambda}} \cdot FA4_{(B_2)}$$

3.2.A.4 Cont.

$$2\cdot B\cdot\left[K-M\cdot 4\cdot\mu\cos^2\alpha\right]\int_0^{B-H}\frac{u_{1(\rho)}}{(\rho-B)^2}\,d\rho$$

$$+\,u_{1(B-H)}\cdot(A5UMHP+A5UMHN)+u_{1(B)}\cdot(A5UBP+A5UBN)$$

$$+\,u_{1(B)}\cdot(A5UPHP+A5UPHP)$$

$$+\,2\cdot B\cdot\left[K-M\cdot 4\cdot\mu\cos^2\alpha\right]\int_{B+H}^{C}\frac{u_{1(\rho)}}{(\rho-B)^2}\,d\rho$$

$$+\int_F^1 u_{2(\overline{X1})}\left\{\left[M\cdot 4\cdot\mu 4\cdot\frac{(\overline{X1}-E-B\cdot\cos\alpha)}{R_{12}^2}\cdot B\cdot\sin\alpha\right.\right.$$

$$\left.+\frac{M\cdot 4\cdot\mu(\overline{X1})-E-B\cdot\cos\alpha)^2}{R_{12}^4}\left(4\cdot\sin\alpha\cdot\left[(E-\overline{X1}+C)B\right]\right)\right]\cdot\left[\frac{C.\tan\alpha-B\cdot\sin\alpha}{R_{12}^2}\right]$$

$$+\left[K-M\cdot 4\cdot\mu\frac{(\overline{X1}-E-B\cos\alpha)}{R_{12}^2}\right]^2\cdot\left[\frac{2\cdot B\cdot\cos\alpha}{R_{12}^2}-\frac{(C\cdot\tan\alpha-B\cdot\sin\alpha)}{R_{12}^4}\right.$$

$$\left.\left.\cdot\,4\cdot\sin\alpha\,(E-\overline{X1}+C)B)\right]\right\}d\overline{X1}$$

$$+\int_0^{2\pi}u_{3(\theta)}\left\{\left[\frac{1-E\cdot\cos\theta-C\cdot\tan\alpha\cdot\sin\theta-B\cdot\cos(\theta+\alpha)}{R_{13}^2}\right]\cdot\left[4\cdot M\cdot 4\cdot\mu\right]\right.$$

$$\cdot\left[\frac{(\cos\theta-E-B\cdot\cos\alpha)B\cdot\sin\alpha}{R_{13}^2}+\frac{(\cos\theta-E-B\cdot\cos\alpha)^2(-B\cdot\sin(\theta+\alpha)+B(E+C)\sin\alpha)}{R_{13}^4}\right]$$

$$+\left[K-\frac{M\cdot 4\cdot\mu(\cos\theta-E-B\cdot\cos\alpha)^2}{R_{13}^2}\right]\cdot\left[\frac{-2\cdot B\cdot\sin(\theta+\alpha)}{R_{13}^2}\right.$$

$$\left.\left.-(1-E\cdot\cos\theta-C\cdot\tan\alpha\cdot\sin\theta-B\cdot\cos(\theta+\alpha))\cdot 4\cdot\frac{(B\cdot(E+C)\sin\alpha-B\cdot\sin(\theta+\alpha))}{R_{13}^4}\right]\right\}d\theta$$

3.2.A.5

$$
- \int_{F}^{1} u_{4(\overline{X1})} \left\{ \left[+M \cdot 4 \cdot \mu \frac{4(\overline{X1}) - E - B \cdot \cos\alpha)}{R_{12}^2} \cdot B \cdot \sin\alpha \right.\right.
$$

$$
+ \frac{M \cdot 4 \cdot \mu (\overline{X1} - E - B \cdot \cos\alpha)^2}{R_{12}^4} (4 \cdot \sin\alpha \cdot [(E - \overline{X1} + C) B]) \left.\right] \cdot \left[\frac{C \cdot \tan\alpha - B \cdot \sin\alpha}{R_{12}^2} \right]
$$

$$
+ \left[K - M \cdot 4 \cdot \mu \frac{(\overline{X1} - E - B \cdot \cos\alpha)^2}{R_{12}^2} \right] \cdot \left[\frac{2 \cdot B \cdot \cos\alpha}{R_{12}^2} - \frac{(C \cdot \tan\alpha - B \cdot \sin\alpha)}{R_{12}^4} \right.
$$

$$
\left.\left. \cdot 4 \cdot \sin\alpha (E - \overline{X1} + C) B) \right] \right\} d\overline{X1}
$$

$$
+ \int_{0}^{B-H} \frac{-2 \cdot B \left[K - M \cdot 4 \cdot \mu \cdot \cos^2\alpha \right]}{(\rho - B)^2} \cdot u_{5(\rho)} \, d\rho
$$

$$
+ u_{5(B-H)} \cdot (A5UMHP - A5UMHN) + u_{5(B)} \cdot (A5UBP - A5UBN)
$$

$$
+ u_{5(B+H)} \cdot (A5UPHP - A5UPHN)
$$

$$
+ \int_{B+H}^{C} \frac{-2 \cdot B \cdot \left[K - M \cdot 4 \cdot \mu \cos^2\alpha \right]}{(\rho - B)^2} \cdot u_{5(\rho)} \, d\rho
$$

$$
+ \int_{0}^{B-H} v_{1(\rho)} \cdot \frac{M \cdot 4 \cdot \mu \cdot B \cdot \sin^2\alpha}{(\rho - B)^2} \, d\rho
$$

$$
+ v_{1(B-H)} \cdot (A5VMHP + A5VMHN) + v_{1(B)} \cdot (A5VBP + A5VBN)
$$

$$
+ v_{1(B+H)} \cdot (A5VPHP + A5VPHN)
$$

3.2.A.5 Cont.

$$+\int_{B+H}^{C} v_{1(\rho)} \cdot \frac{M \cdot 4 \cdot \mu B \cdot \sin 2\alpha}{(\rho - B)^2} \, d\rho$$

$$+\int_{F}^{1} v_{2(\overline{X1})} \left\{ 2 \cdot M \cdot 4 \cdot \mu \left[-B \cdot \sin\alpha \frac{(-C \cdot \tan\alpha + B \cdot \sin\alpha)^2}{R_{12}^4} \right.\right.$$

$$-2 \cdot B \cdot \cos\alpha \, (-C \cdot \tan\alpha + B \cdot \sin\alpha)(\overline{X1} - E - B \cdot \cos\alpha)/R_{12}^4$$

$$\left. -(\overline{X1} - E - B \cdot \cos\alpha)(-C \cdot \tan\alpha + B \cdot \sin\alpha)^2 \cdot 4 \cdot B(E - \overline{X1} + C) \cdot \sin\alpha / R_{12}^6 \right]$$

$$\left. + 2 \cdot K \left[\frac{-B \cdot \sin\alpha}{R_{12}^2} - \frac{(\overline{X1} - E - B \cdot \cos\alpha) \cdot 2 \cdot B \cdot (E - \overline{X1} + C) \cdot \sin\alpha}{R_{12}^4} \right] \right\} d\overline{X1}$$

$$+\int_{0}^{2\pi} v_{3(\theta)} \left\{ 2 \cdot M \cdot 4 \cdot \mu \left[B \cdot \sin\alpha (\sin\theta - C \cdot \tan\alpha + B \cdot \sin\alpha) \right.\right.$$

$$\cdot (1 - E \cdot \cos\theta - C \cdot \tan\alpha \cdot \sin\theta - B \cdot \cos(\theta + \alpha)/R_{13}^4$$

$$+B \cdot \cos\alpha \cdot (\cos\theta - E - B \cdot \cos\alpha) \cdot (1 - E \cdot \cos\theta - C \cdot \tan\alpha \cdot \sin\theta - B \cdot \cos(\theta + \alpha))/R_{13}^4$$

$$+(\cos\theta - E - B \cdot \cos\alpha)(\sin\theta - C \cdot \tan\alpha + B \cdot \sin\alpha) B \cdot \sin(\theta + \alpha)/R_{13}^4$$

$$+ \left[(\cos\theta - E - B \cdot \cos\alpha)(\sin\theta - C \cdot \tan\alpha + B \cdot \sin\alpha)(1 - E \cdot \cos\theta - C \cdot \tan\alpha \sin\theta - B \cdot \cos(\theta + \alpha)) \right.$$

$$\left. \cdot 4 \cdot (-B \cdot \sin(\theta + \alpha) + B(E + C) \cdot \sin\alpha) \right] / R_{13}^6 \Big]$$

$$-2 \cdot K \cdot \left[\frac{B \cdot \cos(\theta + \alpha)}{R_{13}^2} + (E \cdot \sin\theta - C \cdot \tan\alpha \cdot \cos\theta + B \cdot \sin(\theta + \alpha)) \right.$$

$$\left. \left. \cdot 2 \cdot (-B \cdot \sin(\theta + \alpha) + B \cdot (E + C) \cdot \sin\alpha)/R_{13}^4 \right] \right\} d\theta$$

3.2.A.5 Cont.

$$
-\int_{F}^{1} v_{4(\overline{X1})} \left\{ +2\cdot M\cdot 4\cdot \mu \left[-B\cdot \sin\alpha \frac{(-C\cdot\tan\alpha + B\cdot\sin\alpha)^2}{R_{12}^4} \right.\right.
$$

$$
-2\cdot B\cdot\cos\alpha(-C\cdot\tan\alpha+B\cdot\sin\alpha)(\overline{X1}-E-B\cdot\cos\alpha)/R_{12}^4
$$

$$
\left.\left. -(\overline{X1}-E-B\cdot\cos\alpha)(-C\cdot\tan\alpha+B\cdot\sin\alpha)^2\cdot 4\cdot B(E-\overline{X1}+C)\cdot\sin\alpha/R_{12}^6 \right]
$$

$$
\left. + 2\cdot K\cdot \left[\frac{-B\cdot\sin\alpha}{R_{12}^2} - \frac{(\overline{X1}-E-B\cdot\cos\alpha)\cdot 2\cdot B\cdot(E-\overline{X1}+C)\cdot\sin\alpha}{R_{12}^4} \right] \right\} d\overline{X1}
$$

$$
+\int_{0}^{B-H} v_{5(\rho)}\cdot \frac{(-M\cdot 4\cdot \mu B\cdot \sin 2\alpha)}{(\rho-B)^2}\, d\rho
$$

$$
+ v_{5(B-H)}\cdot (A5VMHP - A5VMHN) + v_{5(B)}\cdot (A5VBP - A5VBN)
$$

$$
+ v_{5(B+H)}\cdot (A5VPHP - A5VPHN)
$$

$$
+\int_{B+H}^{\underline{C}} v_{5(\rho)}\cdot \frac{(-M\cdot 4\cdot \mu\cdot B\cdot \sin 2\alpha)}{(\rho-B)^2}\, d\rho = \frac{1}{\underline{\lambda}}\cdot FA5_{(B)}
$$

3.2.A.5 Cont.

$$-\int_{0}^{B-H} u_{1(\rho)} \left\{\frac{K}{\rho-B}\right\} d\rho + u_{1(B-H)} \cdot (B1UMH) + u_{1(B)} \cdot (B1UB)$$

$$+ u_{1(B+H)} \cdot (B1UPH)$$

$$-\int_{B+H}^{\underline{C}} u_{1(\rho)} \left\{\frac{+K}{\rho-B}\right\} d\rho + \int_{F}^{1} u_{2(\overline{X1})} \left\{M\cdot 4\cdot\mu\left[\overline{X1}-E-B\cdot\cos\alpha\right]\right.$$

$$\left. \cdot \frac{\left[B\cdot\sin\alpha-C\cdot\tan\alpha\right]^2}{R^4_{12}} - K \cdot \frac{\left[\overline{X1}-E-B\cdot\cos\alpha\right]}{R^2_{12}}\right\} d\overline{X1}$$

$$+\int_{0}^{2\pi} u_{3(\theta)} \left\{-M\cdot 4\cdot\mu\left[\cos\theta-E-B\cdot\cos\alpha\right]\cdot\left[\sin\theta-C\cdot\tan\alpha+B\cdot\sin\alpha\right]\right.$$

$$\cdot\left[1-E\cdot\cos\theta-C\cdot\tan\alpha\cdot\sin\theta-B\cdot\cos(\theta+\alpha)\right]/R^4_{13}$$

$$\left.-K\cdot\left[E\cdot\sin\theta-C\cdot\tan\alpha\cdot\cos\theta+B\cdot\sin(\theta+\alpha)\right]/R^2_{13}\right\} d\theta$$

$$+\int_{F}^{1} u_{4(\overline{X1})} \left\{-M\cdot 4\cdot\mu\left[\overline{X1}-E-B\cdot\cos\alpha\right]\cdot\left[B\cdot\sin\alpha-C\cdot\tan\alpha\right]^2/R^4_{12}\right.$$

$$\left. + K\cdot\left[\overline{X1}-E-B\cdot\cos\alpha\right]/R^2_{14}\right\} d\overline{X1}$$

$$+\int_{0}^{B-H} u_{5(\rho)} \left\{\frac{K}{\rho-B}\right\} d\rho - u_{5(B-H)} \cdot (B1UMH) - u_{5(B)} \cdot (B1UB)$$

$$-u_{5(B+H)} \cdot (B1UPH) + \int_{B+H}^{\underline{C}} u_{5(\rho)} \left\{\frac{K}{\rho-B}\right\} d\rho$$

3.2.B.1

$$- \frac{v_{1(B)}}{\underline{\lambda}} + \int_F^1 v_{2(\overline{X1})} \left\{ \left[K - \frac{M \cdot 4 \cdot \mu \left[B \cdot \sin\alpha - C \cdot \tan\alpha \right]^2}{R_{12}^2} \right] \right.$$

$$\left. \cdot \left[-B \cdot \sin\alpha + C \cdot \tan\alpha \right] / R_{12}^2 \right\} d\overline{X1}$$

$$+ \int_0^{2\pi} v_{3(\theta)} \left\{ \left[K - M \cdot 4 \cdot \mu \frac{\left[\sin\theta - C \cdot \tan\alpha + B \cdot \sin\alpha \right]^2}{R_{13}^2} \right] \right.$$

$$\left. \cdot \left[1 - E \cdot \cos\theta - C \cdot \tan\alpha \cdot \sin\theta - B \cdot \cos(\theta + \alpha) \right] / R_{13}^2 \right\} d\theta$$

$$+ \int_F^1 v_{4(\overline{X1})} \left\{ \left[K - M \cdot 4 \cdot \mu \frac{\left[B \cdot \sin\alpha - C \cdot \tan\alpha \right]^2}{R_{12}^2} \right] \left[\frac{B \cdot \sin\alpha - C \cdot \tan\alpha}{R_{12}^2} \right] \right\} d\overline{X1}$$

$$- \frac{v_{5(B)}}{\underline{\lambda}} = \frac{1}{\underline{\lambda}} \cdot FB1_{(B)}$$

3.2.B.1 Cont.

$$\int_0^{\underline{C}} u_{1(\rho)} \left\{ -M\cdot 4\cdot\mu\left[E+\rho\cdot\cos\alpha-B_2\right]\cdot\left[C\cdot\tan\alpha-\rho\cdot\sin\alpha\right] \right.$$

$$\cdot\left[(E+\rho\cdot\cos\alpha-B_2)(-\sin\alpha)+(C\cdot\tan\alpha-\rho\cdot\sin\alpha)(-\cos\alpha)\right] /R_{21}^4$$

$$\left. -K\cdot\left[(E+\rho\cdot\cos\alpha-B_2)(\cos\alpha)+ (C\cdot\tan\alpha-\rho\cdot\sin\alpha)(-\sin\alpha)\right]/R_{21}^2 \right\} d\rho$$

$$+\int_F^{B_2-H_2} u_{2(\overline{X1})} \left\{\frac{-K}{\overline{X1}-B_2}\right\} d\overline{X1} \quad + u_{2(B-H)}\cdot(B2UMH) + u_{2(B)}\cdot(B2UB)$$

$$+ u_{2(B+H)}\cdot(B2UPH) + \int_{B_2+H_2}^{1} u_{2(\overline{X1})} \left\{\frac{-K}{\overline{X1}-B_2}\right\} d\overline{X1}$$

$$+\int_0^{2\pi} u_{3(\theta)} \left\{ -M\cdot 4\cdot\mu(\cos\theta-B_2)(\sin\theta)(1-B_2\cos\theta)/R_{23}^4 \right.$$

$$\left. -K\left[B_2\cdot\sin\theta\right] /R_{23}^2 \right\} d\theta$$

$$+\int_F^{B_2-H_2} u_{4(\overline{X1})} \left\{\frac{K}{\overline{X1}-B_2}\right\} d\overline{X1} \quad - u_{4(B-H)}\cdot(B2UMH) - u_{4(B)}\cdot(B2UB)$$

$$- u_{4(B+H)}\cdot(B2UPH) + \int_{B_2+H_2}^{1} u_{4(\overline{X1})} \left\{\frac{K}{\overline{X1}-B_2}\right\} d\overline{X1}$$

$$+\int_0^{\underline{C}} u_{5(\rho)} \left\{ -M\cdot 4\cdot\mu\left[E+\rho\cdot\cos\alpha-B_2\right]\cdot\left[C\cdot\tan\alpha-\rho\cdot\sin\alpha\right] \right.$$

$$+ \left[(E+\rho\cdot\cos\alpha-B_2)(+\sin\alpha) + (C\cdot\tan\alpha-\rho\cdot\sin\alpha)(+\cos\alpha)\right] /R_{21}^4$$

$$\left. + K\left[(E+\rho\cdot\cos\alpha-B_2)\cos\alpha +(C\cdot\tan\alpha-\rho\cdot\sin\alpha)(-\sin\alpha)\right]/R_{21}^2 \right\} d\rho$$

3.2.B.2

$$+\int_0^{\underline{C}} v_{1(\rho)} \left\{\left[K-M\cdot 4\cdot\mu\ \frac{(C\cdot\tan\alpha-\rho\cdot\sin\alpha)^2}{R_{21}^2}\right]\right.$$

$$\left.\cdot\ \left[(E+\rho\cdot\cos\alpha-B_2)(-\sin\alpha)\ +\ (C\cdot\tan\alpha-\rho\cdot\sin\alpha)(-\cos\alpha)\right]/R_{21}^2\right\}d\rho$$

$$-\frac{1}{\underline{\lambda}}\cdot v_{2(B_2)}\quad +\quad \int_0^{2\pi} v_{3(\theta)}\left\{\left[K-\frac{M\cdot 4\cdot\mu\ (\sin^2\theta)}{R_{23}^2}\right]\cdot\left[\frac{1-B_2\cos\theta}{R_{23}^2}\right]\right\}\ d\theta$$

$$-\frac{1}{\underline{\lambda}}\cdot v_{4(B_2)}$$

$$+\int_0^{\underline{C}} v_{5(\rho)}\left\{\left[K-\ M\cdot 4\cdot\mu\ \frac{(C\cdot\tan\alpha-\rho\cdot\sin\alpha)^2}{R_{21}^2}\right]\right.$$

$$\left.\cdot\left[(E+\rho\cdot\cos\alpha-B_2)\sin\alpha\ +(C\cdot\tan\alpha-\rho\cdot\sin\alpha)\cos\alpha\right]/R_{21}^2\right\}d\rho$$

$$=\ \frac{1}{\underline{\lambda}}\cdot FB2_{(B_2)}$$

3.2.B.2 Cont.

$$\int_0^{\underline{C}} u_{1(\rho)} \left\{ -M\cdot 4\cdot\mu\left[E+\rho\cdot\cos\alpha-\cos\theta_0\right]\cdot\left[C\cdot\tan\alpha-\rho\cdot\sin\alpha-\sin\theta_0\right] \right.$$

$$\cdot\left[-E\cdot\sin\alpha-C\cdot\sin\alpha+\sin(\theta_0+\alpha)\right]/R_{31}^4$$

$$\left. -K\cdot\left[E\cdot\cos\alpha-C\cdot\tan\alpha\cdot\sin\alpha+\rho-\cos(\theta_0+\alpha)\right]/R_{31}^2 \right\} d\rho$$

$$+\int_F^1 u_{2(\overline{X1})} \left\{ M\cdot 4\cdot\mu\left[\overline{X1}-\cos\theta_0\right]\cdot\left[\sin^2\theta_0\right]/R_{32}^4 - K\left[\overline{X1}-\cos\theta_0\right]/R_{32}^2 \right\} d\overline{X1}$$

$$+\int_0^{2\pi} u_{3(\theta)} \left\{ \frac{M\cdot 4\cdot\mu}{4} \cdot \sin(\theta+\theta_0) \right\} d\theta$$

$$-\int_0^{\theta_0-H_3} u_{3(\theta)} \left\{ \frac{K}{2} \frac{\cos(\frac{\theta-\theta_0}{2})}{\sin(\frac{\theta-\theta_0}{2})} \right\} d\theta - K\cdot\left\{ u_{3(\theta_0+H_3)} - u_{3(\theta_0-H_3)} \right\}$$

$$-\int_{\theta_0+H_3}^{2\pi} u_{3(\theta)} \left\{ \frac{K}{2} \cdot \frac{\cos(\frac{\theta-\theta_0}{2})}{\sin(\frac{\theta-\theta_0}{2})} \right\} d\theta$$

$$+\int_F^1 u_{4(\overline{X1})} \left\{ -M\cdot 4\cdot\mu\left[\overline{X1}-\cos\theta_0\right]\cdot\left[\sin^2\theta_0\right]/R_{32}^4 + K\cdot\left[\overline{X1}-\cos\theta_0\right]/R_{32}^2 \right\} d\overline{X1}$$

$$+\int_0^{\underline{C}} u_{5(\rho)} \left\{ -M\cdot 4\cdot\mu\left[E+\rho\cdot\cos\alpha-\cos\theta_0\right]\cdot\left[C\cdot\tan\alpha-\rho\cdot\sin\alpha-\sin\theta_0\right] \right.$$

$$\cdot\left[E\cdot\sin\alpha+C\cdot\sin\alpha-\sin(\alpha+\theta_0)\right]/R_{31}^4$$

$$\left. -K\cdot\left[-E\cdot\cos\alpha+C\cdot\sin\alpha\cdot\tan\alpha-\rho+\cos(\theta_0+\alpha)\right]/R_{31}^2 \right\} d\rho \qquad 3.2.B.3$$

$$+\int_0^{\underline{C}} v_{1(\rho)} \left\{\left[K-M\cdot 4\cdot\mu\frac{(C\cdot\tan\alpha-\rho\cdot\sin\alpha-\sin\theta_0)^2}{R_{31}^2}\right]\right.$$

$$\left.\cdot\left[-E\cdot\sin\alpha-C\cdot\sin\alpha+\sin(\theta_0+\alpha)\right]/R_{31}^2\right\} d\rho$$

$$+\int_F^1 v_{2(\overline{X1})} \left\{\left[K\frac{-M\cdot 4\cdot\mu(\sin^2\theta_0)}{R_{32}^2}\right]\cdot\left[\frac{\sin\theta_0}{R_{32}^2}\right]\right\} d\overline{X1}$$

$$+\int_0^{2\pi} v_{3(\Theta)} \left\{\left\{\frac{K}{2}-\frac{M\cdot 4\cdot\mu}{2}\cdot\cos^2\left(\frac{\Theta+\theta_0}{2}\right)\right\} d\Theta\right\} - \frac{1}{\underline{\lambda}}\cdot v_{3(\theta_0)}$$

$$+\int_F^1 v_{4(\overline{X1})} \left\{\left[K\frac{M\cdot 4\cdot\mu(\sin^2\theta_0)}{R_{32}^2}\right]\cdot\left[\frac{-\sin\theta_0}{R_{32}^2}\right]\right\} d\overline{X1}$$

$$+\int_0^{\underline{C}} v_{5(\rho)} \left\{\left[K-M\cdot 4\cdot\mu\frac{(C\cdot\tan\alpha-\rho\cdot\sin\alpha-\sin\theta_0)^2}{R_{31}^2}\right]\right.$$

$$\left.\cdot\left[E\cdot\sin\alpha+C\cdot\sin\alpha-\sin(\alpha+\theta_0)\right]/R_{31}^2\right\} d\rho$$

$$= \frac{1}{\underline{\lambda}}\cdot FB3_{(\theta_0)}$$

3.2.B.3 Cont.

$$\int_0^{\underline{C}} u_{1(\rho)} \left\{ \left[M \cdot 4 \cdot \mu 2 \cdot C (E+\rho \cdot \cos\alpha - B_2) \frac{\sin\alpha}{R_{21}^4} \right.\right.$$

$$\left. \cdot \left[\rho \cdot \cos\alpha - (E+2 \cdot C - B_2) + 4 \cdot (C \cdot \tan\alpha - \rho \cdot \sin\alpha)^2 \cdot \frac{(E+C-B_2)}{R_{21}^2} \right] \right]$$

$$-K \left[\frac{2 \cdot C}{R_{21}^2} \cdot \sin\alpha + \left[\rho + (E-B_2) \cdot \cos\alpha - C \cdot \tan\alpha \cdot \sin\alpha \right] \right.$$

$$\left. \left. \cdot \left[C \cdot \tan\alpha - \rho \cdot \sin\alpha \right] (4C) / R_{21}^4 \right] \right\} d\rho$$

$$+ u_{2(B-H)} \cdot (B4UMH) + u_{2(B)} \cdot (B4UB) + u_{2(B+H)} \cdot (B4UPH)$$

$$+ \int_0^{2\pi} u_{3(\theta)} \left\{ M \cdot 4 \cdot \mu \cdot (2C) \cdot \frac{(\cos\theta - B_2)}{R_{23}^4} \cdot \left[1 - B_2 \cos\theta + \sin^2\theta \right) \right.$$

$$\left. -4 \cdot (1 - B_2 \cdot \cos\theta) \frac{\sin^2\theta}{R_{23}^2} \right] - K \cdot \frac{2 \cdot C}{R_{23}^2} \cdot \left[\frac{2 \cdot B_2 \cdot \sin^2\theta}{R_{23}^2} - \cos\theta \right] \Bigg\} d\theta$$

$$+ u_{4(B-H)} \cdot (B4UMH) + u_{4(B)} \cdot (B4UB) + u_{4(B+H)} \cdot (B4UPH)$$

$$- \int_0^{\underline{C}} u_{5(\rho)} \left\{ \left[M \cdot 4 \cdot \mu 2 \cdot C (E+\rho \cdot \cos\alpha - B_2) \frac{\sin\alpha}{R_{21}^4} \right.\right.$$

$$\left. \cdot \left[\rho \cdot \cos\alpha - (E+2 \cdot C - B_2) + 4 \cdot (C \cdot \tan\alpha - \rho \cdot \sin\alpha)^2 \cdot \frac{(E+C-B_2)}{R_{21}^2} \right] \right]$$

$$-K \left[\frac{2 \cdot C}{R_{21}^2} \cdot \sin\alpha + \left[\rho + (E-B_2) \cdot \cos\alpha - C \cdot \tan\alpha - \sin\alpha \right] \right.$$

$$\left. \left. \cdot \left[C \cdot \tan\alpha - \rho \cdot \sin\alpha \right] (4 \cdot C) / R_{21}^4 \right] \right\} d\rho$$

3.2.B.4

$$+\int_0^{\underline{C}} v_{1(\rho)} \left\{ \left[\left[M\cdot 4\cdot \mu\cdot (B_2-E-C)\cdot \sin\alpha\cdot \ (C\cdot\tan\alpha-\rho\cdot\sin\alpha)\ (4C) \right] \cdot \frac{1}{R_{21}^4} \right.\right.$$

$$\left.\left. \cdot \left[1 - \frac{(C\cdot\tan\alpha-\rho\cdot\sin\alpha)^2}{R_{21}^2} \right] \right]$$

$$+ \left[\left[K - M\cdot 4\cdot\mu \frac{(C\cdot\tan\alpha-\rho\cdot\sin\alpha)^2}{R_{21}^2} \right] \right.$$

$$\left. \cdot \left[\frac{2C}{R_{21}^2} + (B_2-E-C)\cdot\sin\alpha\cdot(C\cdot\tan\alpha-\rho\cdot\sin\alpha)\frac{(4C)}{R_{21}^4} \right] \right] \Bigg\} \ d\rho$$

$$+\int_F^{B_2-H_2} v_{2(\overline{X1})} \cdot \frac{(+K\cdot 2\cdot C)}{(\overline{X1}-B_2)^2} \ d\overline{X1} + v_{2(B-H)}\cdot (B4VMH) + v_{2(B)}\cdot(B4VB)$$

$$+v_{2(B+H)}\cdot(B4VPH) + \int_{B_2+H_2}^{1} v_{2(\overline{X1})} \cdot \frac{(+K\cdot 2\cdot C)}{(\overline{X1}-B_2)^2} \ d\overline{X1}$$

$$+\int_0^{2\pi} v_{3(\theta)} \left\{ M\cdot 4\cdot\mu\cdot \frac{4\cdot C\cdot\sin\theta}{R_{23}^4} \cdot \left[1 - \frac{\sin^2\theta}{R_{23}^2} \right] \cdot \left[1 - B_2\cdot\cos\theta \right] \right.$$

$$\left. + \frac{2\cdot C\cdot\sin\theta}{R_{23}^2} \cdot \left[K \frac{-M\cdot 4\cdot\mu\cdot\sin^2\theta}{R_{23}^2} \right] \cdot \left[-1 + \frac{2\cdot(1-B_2\cdot\cos\theta)}{R_{23}^2} \right] \right\} \ d\theta$$

$$+\int_F^{B_2-H_2} v_{4(\overline{X1})} \cdot \frac{(-K\cdot 2\cdot C)}{(\overline{X1}-B_2)^2} \ d\overline{X1} - v_{4(B-H)}\cdot (B4VMH)$$

$$- v_{4(B)}\cdot(B4VB) - v_{4(B+H)}\cdot (B4VPH)$$

3.2.B.4 Cont.

$$+\int_{B_2+H_2}^{1} v_{4(\overline{X1})} \cdot \frac{(-K \cdot 2 \cdot C)}{(\overline{X1}-B_2)^2} \cdot d\overline{X1}$$

$$-\int_{0}^{\underline{C}} v_{5(\rho)} \left\{ \left[\left[M \cdot 4 \cdot \mu (B_2-E-C) \cdot \sin\alpha \cdot (C \cdot \tan\alpha - \rho \cdot \sin\alpha)(4C) \right] \cdot \frac{1}{R_{21}^4} \right.\right.$$

$$\cdot \left[1 - \frac{(C \cdot \tan\alpha - \rho \cdot \sin\alpha)^2}{R_{21}^2} \right] \Bigg]$$

$$+ \left[\left[K-M \cdot 4 \cdot \mu \frac{(C \cdot \tan\alpha - \rho \cdot \sin\alpha)^2}{R_{21}^2} \right] \right.$$

$$\left.\left. \cdot \left[\frac{2C}{R_{21}^2} + (B_2-E-C) \cdot \sin\alpha \cdot (C \cdot \tan\alpha - \rho \cdot \sin\alpha) \frac{(4C)}{R_{21}^4} \right] \right] \right\} d\rho$$

$$= \frac{1}{\underline{\lambda}} \cdot FB4_{(B_2)}$$

3.2.B.4 Cont.

$$\int_0^{B-H} u_{1(\rho)} \quad \frac{M\cdot 4\mu B\cdot \sin 2\alpha}{(\rho-B)^2} \quad d\rho$$

$$+ u_{1(B-H)}\cdot (B5UMHP + B5UMHN) + u_{1(B)}\cdot (B5UBP + B5UBN)$$

$$+ u_{1(B+H)}\cdot (B5UPHP + B5UPHN)$$

$$+\int_{B+H}^{\underline{C}} u_{1(\rho)}\cdot \frac{M\cdot 4\cdot\mu\cdot B\cdot \sin 2\alpha}{(\rho-B)^2} \quad d\rho$$

$$+\int_F^1 u_{2(\overline{X1})} \quad \left\{ 2\cdot M\cdot 4\cdot\mu \left[-B\cdot\sin\alpha \frac{(-C\cdot\tan\alpha+B\cdot\sin\alpha)^2}{R_{12}^4} \right.\right.$$

$$-2\cdot B\cdot\cos\alpha(-C\cdot\tan\alpha+B\cdot\sin\alpha)(\overline{X1}-E-B\cdot\cos\alpha)\ /R_{12}^4$$

$$\left.\left. -(\overline{X1}-E-B\cdot\cos\alpha)(-C\cdot\tan\alpha+B\cdot\sin\alpha)^2 4\cdot B(E-\overline{X1}+C)\cdot\sin\alpha/R_{12}^6 \right]\right.$$

$$\left. -2\cdot K \left[\frac{-B\cdot\sin\alpha}{R_{12}^2} - \frac{(\overline{X1}-E-B\cdot\cos\alpha)\ 2\cdot B(E-\overline{X1}+C)\sin\alpha}{R_{12}^4} \right] \right\} d\overline{X1}$$

$$+\int_0^{2\pi} u_{3(\Theta)} \left\{ 2\cdot M\cdot 4\cdot\mu\cdot \left[B\cdot\sin\alpha(\sin\Theta-C\cdot\tan\alpha+B\cdot\sin\alpha) \right.\right.$$

$$\cdot(1-E\cdot\cos\Theta-C\cdot\tan\alpha\cdot\sin\Theta-B\cdot\cos(\Theta+\alpha)/R_{13}^4$$

$$+ B\cdot\cos\alpha(\cos\Theta-E-B\cdot\cos\alpha)(1-E\cdot\cos\Theta-C\cdot\tan\alpha\cdot\sin\Theta-B\cdot\cos(\Theta+\alpha))/R_{13}^4$$

$$+(\cos\Theta-E-B\cdot\cos\alpha)(\sin\Theta-C\cdot\tan\alpha+B\cdot\sin\alpha)B\cdot\sin(\Theta+\alpha)/R_{13}^4$$

$$+\left[(\cos\Theta-E-B\cdot\cos\alpha)(\sin\Theta-C\cdot\tan\alpha+B\cdot\sin\alpha)(1-E\cdot\cos\Theta-C\cdot\tan\alpha\cdot\sin\Theta-B\cdot\cos(\Theta+\alpha))\right.$$

3.2.B.5

$$\cdot 4(-B\cdot\sin(\theta+\alpha)+B(E+C)\sin\alpha)\Big]/R_{13}^{6}\Big]$$

$$+2\cdot K\Big[\frac{B\cdot\cos(\theta+\alpha)}{R_{13}^{2}} + (E\cdot\sin\theta - C\cdot\tan\alpha\cdot\cos\theta - B\cdot\sin(\theta+\alpha))$$

$$\cdot 2\cdot(-B\cdot\sin(\theta+\alpha) + B\cdot(E+C)\sin\alpha)/R_{13}^{4}\Big\}d\theta$$

$$-\int_{F}^{1} u_{4(\overline{X1})}\Big\{+2\cdot M\cdot 4\cdot\mu\Big[-B\cdot\sin\alpha\frac{(-C\cdot\tan\alpha+B\cdot\sin\alpha)^{2}}{R_{12}^{4}}$$

$$-2\cdot B\cdot\cos\alpha(-C\cdot\tan\alpha+B\cdot\sin\alpha)(\overline{X1}-E-B\cdot\cos\alpha)/R_{12}^{4}$$

$$-(\overline{X1}-E-B\cdot\cos\alpha)(-C\cdot\tan\alpha+B\cdot\sin\alpha)^{2}\cdot 4\cdot B(E-\overline{X1}+C)\cdot\sin\alpha/R_{12}^{6}\Big]$$

$$-2\cdot K\Big[\frac{-B\cdot\sin\alpha}{R_{12}^{2}} - \frac{(\overline{X1}-E-B\cdot\cos\alpha)\cdot 2\cdot B\ (E-\overline{X1}+C)\sin\alpha}{R_{12}^{4}}\Big]\Big\}\ d\overline{X1}$$

$$+\int_{0}^{B-H} u_{5(\rho)}\ \frac{(-M\cdot 4\cdot\mu\cdot B\cdot\sin 2\alpha)}{(\rho-B)^{2}}\ d\rho\ + u_{5(B-H)}\cdot(B5UMHP - B5UMHN)$$

$$+ u_{5(B)}\cdot(B5UBP - B5UBN) + u_{5(B+H)}\cdot(B5UPHP - B5UPHN)$$

$$+\int_{B+H}^{C} u_{5(\rho)}\ \frac{(-M\cdot 4\cdot\mu\cdot B\cdot\sin 2\alpha)}{(\rho-B)^{2}}\ d\rho$$

$$+\int_{0}^{B-H} v_{1(\rho)}\ \Big\{2\cdot B\cdot\Big[K-M\cdot 4\cdot\mu\cdot\sin^{2}\alpha\Big]\ \frac{1}{(\rho-B)^{2}}\Big\}\ d\rho$$

$$+ v_{1(B-H)}\cdot(B5VMHP + B5VMHN) + v_{1(B)}\cdot(B5VBP + B5VBN)$$

$$+ v_{1(B+H)}\cdot(B5VPHP + B5VPHN)$$

3.2.B.5 Cont.

$$+\int_{B+H}^{C} v_{1(\rho)} \left\{2\cdot B\cdot\left[K-M\cdot 4\cdot\mu\cdot\sin^2\alpha\right]\frac{1}{(\rho-B)^2}\right\} d\rho$$

$$+\int_{F}^{1} v_{2(\overline{X1})} \left\{2\cdot M\cdot 4\cdot\mu\cdot\left[(B\cdot\sin\alpha-C\cdot\tan\alpha)\cdot 2\cdot B\cdot\cos\alpha\right.\right.$$

$$\left.+(B\cdot\sin\alpha-C\cdot\tan\alpha)^2\cdot\frac{2\cdot B\cdot\sin\alpha(E+C-\overline{X1})}{R_{12}^2}\right]\cdot\left[\frac{C\cdot\tan\alpha-B\cdot\sin\alpha}{R_{12}^4}\right]$$

$$+\left[K-M\cdot 4\cdot\mu\frac{(B\cdot\sin\alpha-C\cdot\tan\alpha)^2}{R_{12}^2}\right]$$

$$\left.\cdot\left[\frac{2\cdot B\cdot\cos\alpha}{R_{12}^2}+\frac{2\cdot(B\cdot\sin\alpha-C\cdot\tan\alpha)\cdot 2\cdot B\cdot\sin\alpha(E+C-\overline{X1})}{R_{12}^4}\right]\right\} d\overline{X1}$$

$$+\int_{0}^{2\pi} v_{3(\Theta)} \left\{2\cdot M\cdot 4\cdot\mu\left[(\sin\Theta-C\cdot\tan\alpha+B\cdot\sin\alpha)\cdot 2\cdot B\cdot\cos\alpha\right.\right.$$

$$+\left[\sin\Theta-C\cdot\tan\alpha+B\cdot\sin\alpha\right]^2\cdot 2\cdot B\cdot\left[\frac{(E+C)\sin\alpha-\sin(\alpha+\Theta)}{R_{13}^2}\right]$$

$$\cdot\left[1-E\cdot\cos\Theta-C\cdot\tan\alpha\cdot\sin\Theta-B\cdot\cos(\Theta+\alpha)\right]/R_{13}^4$$

$$+\left[K-M\cdot 4\cdot\mu\frac{(\sin\Theta-C\cdot\tan\alpha+B\cdot\sin\alpha)^2}{R_{13}^2}\right]$$

$$\cdot\left[\frac{-2\cdot B\cdot\sin(\Theta+\alpha)}{R_{13}^2}-2\cdot(1-E\cdot\cos\Theta-C\cdot\tan\alpha\cdot\sin\Theta-B\cdot\cos(\Theta+\alpha))\right.$$

$$\left.\left.\cdot 2\cdot B\cdot((E+C)\cdot\sin\alpha-\sin(\alpha+\Theta))/R_{13}^4\right]\right\} d\Theta$$

$$-\int_{F}^{1} v_{4(\overline{X1})} \left\{+2\cdot M\cdot 4\cdot\mu\cdot\left[(B\cdot\sin\alpha-C\cdot\tan\alpha)\cdot 2\cdot B\cdot\cos\alpha\right.\right.$$

$$\left.+(B\cdot\sin\alpha-C\cdot\tan\alpha)^2\cdot\frac{2\cdot B\cdot\sin\alpha(E+C-\overline{X1})}{R_{12}^2}\right]\cdot\left[\frac{C\cdot\tan\alpha-B\cdot\sin\alpha}{R_{12}^4}\right]$$

3.2.B.5 Cont.

$$+\left[K\text{-}M\cdot 4\cdot\mu\cdot\frac{(B\cdot\sin\alpha - C\cdot\tan\alpha)^2}{R_{12}^2}\right]$$

$$\cdot\left[\frac{2\cdot B\cdot\cos\alpha}{R_{12}^2} + \frac{2\cdot(B\cdot\sin\alpha - C\cdot\tan\alpha)\cdot 2\cdot B\cdot\sin\alpha\,(E+C-\overline{X1})}{R_{12}^4}\right]\Bigg\}\; d\overline{X1}$$

$$+\int_0^{B-H} v_{5(\rho)}\left\{-2\cdot B\left[K\text{-}M\cdot 4\cdot\mu\cdot\sin^2\alpha\right]\cdot\frac{1}{(\rho-B)^2}\right\}\; d\rho$$

$$+ v_{5(B-H)}\cdot(B5VMHP - B5VMHN) + v_{5(B)}\cdot(B5VBP - B5VBN)$$

$$+ v_{5(B+H)}\cdot(B5VPHP - B5VPHN)$$

$$+\int_{B+H}^{C} v_{5(\rho)}\left\{-2\cdot B\cdot\left[K\text{-}M\cdot 4\cdot\mu\cdot\sin^2\alpha\right]\cdot\frac{1}{(\rho-B)^2}\right\} d\rho$$

$$= \frac{1}{\lambda}\cdot FB5_{(B)}$$

3.2.B.5 Cont.

Appendix B.2

Algebraic Insert Formula

B. 2 Insert Formulas for Eq. set (3.2)

Insert Formula for Linear Displacement Assumption

$$(u = c_1 \rho + c_2)$$

Linear Insert Eq. A1

$$A1VMH \equiv -K$$

$$A1VB \equiv 0$$

$$A1VPH \equiv +K$$

Linear Insert Eq. A2

$$A2VMH \equiv -K$$

$$A2VB \equiv 0$$

$$A2VPH \equiv K$$

Linear Insert Eq. A4

$$A4UMH \equiv 0$$

$$A4UB \equiv -4 \cdot C \cdot (K - M \cdot 4 \cdot \mu)/H_2$$

$$A4UPH \equiv 0$$

$$A4VMH \equiv \pi \cdot C \cdot (M \cdot 2 \cdot \mu \cdot -K)/H_2$$

$$A4VB \equiv 0$$

$$A4VPH \equiv -\pi \cdot C \cdot (M \cdot 2 \cdot \mu \cdot -K)/H_2$$

Linear Insert Eq. A5

$$A5UMHP \equiv M \cdot 2 \cdot \mu \cdot \sin(2\alpha) \cdot B \cdot \pi/H$$

$$A5UBN \equiv 16 \cdot M \cdot \mu \cdot \frac{B}{H} \cdot \cos^2\alpha - 4 \cdot K \cdot \frac{B}{H}$$

$$A5UPHP \equiv -M \cdot 2 \cdot \mu \cdot \sin(2\alpha) \cdot B \cdot \frac{\pi}{H}$$

$$A5UMHN \equiv A5UBP = A5UPHN = 0$$

$$A5VMHP \equiv (M \cdot 2 \cdot \mu \cdot \cos 2\alpha - K) \cdot \frac{B\pi}{H}$$

$$A5VBN \equiv -M \cdot 8 \cdot \mu \cdot \frac{B}{H} \cdot \sin 2\alpha$$

$$A5VPHP \equiv -(M \cdot 2 \cdot \mu \cdot \cos 2\alpha - K) \cdot \frac{B\pi}{H}$$

$$A5VMHN \equiv A5VBP = A5VPHN = 0$$

Linear Insert Eq. B1

$$B1UMH \equiv K$$

$$B1UB \equiv 0$$

$$B1UPH \equiv -K$$

Linear Insert Eq. B2

$$B2UMH \equiv K$$

$$B2UB \equiv 0$$

$$B2uPH \equiv K$$

Linear Insert Eq. B4

$$B4UMH \equiv \pi \cdot C \cdot (M \cdot 2 \cdot \mu + K)/H_2$$

$$B4UB \equiv 0$$

$$B4UPH \equiv -\Pi \cdot C \cdot (M \cdot 2\mu + K)/H_2$$

$$B4VMH \equiv 0$$

$$B4VB \equiv -4 \cdot C \cdot K/H_2$$

$$B4VPH \equiv 0$$

Linear Insert Eq. B5

$$B5UMHP \equiv (M \cdot 2 \cdot \mu \cdot \cos 2\alpha + K) \cdot \frac{B\pi}{H}$$

$$B5UBN \equiv -M \cdot 8 \cdot \mu \cdot \frac{B}{H} \cdot \sin 2\alpha$$

$$B5UPHP \equiv -(M \cdot 2 \cdot \mu \cdot \cos 2\alpha + K) \cdot \frac{B\pi}{H}$$

$$B5UMHN \equiv B5UBP = B5UPHN = 0$$

$$B5VMHP \equiv -B \cdot M \cdot 2 \cdot \mu \cdot \frac{\pi}{H} \cdot \sin 2\alpha$$

$$B5VBN \equiv 4 \cdot \frac{B}{H} \cdot (M \cdot 4 \cdot \mu \cdot \sin^2\alpha - K)$$

$$B5VPHP \equiv B \cdot M \cdot 2 \cdot \mu \cdot \frac{\pi}{H} \cdot \sin 2\alpha$$

$$B5VMHN \equiv B5VBP = B5VPHN = 0$$

Insert Formula for Square Root Displacement Assumption

$$(u \doteq c_1^{1/2} + c_2)$$

Define:

$$D_1 \equiv \sqrt{B + H} - 2\sqrt{B} + \sqrt{B-H}$$

$$AG \equiv \left[\frac{(\sqrt{B+H} + \sqrt{B})}{\sqrt{B+H} - \sqrt{B}} \cdot \frac{(\sqrt{B-H} - \sqrt{B})}{(\sqrt{B-H} + \sqrt{B})} \right]^2$$

Square Root Insert Eq. A1

$$A1VMH \equiv K \left| 2\sqrt{B} - 2\sqrt{B-H} - .5\sqrt{B} \cdot Ln(AG) \right| \frac{1}{D_1}$$

$$A1VB \equiv K \left| 2\sqrt{B-H} - 2\sqrt{B+H} + \sqrt{B} \cdot Ln(AG) \right| \frac{1}{D_1}$$

$$A1VPH \equiv K \left| -2\sqrt{B} + 2\sqrt{B+H} - .5\sqrt{B} \cdot Ln(AG) \right| \frac{1}{D_1}$$

Square Root Insert Eq. B1

$$B1UMH \equiv -A1VMH$$

$$B1UB \equiv -A1VB$$

$$B1UPH \equiv -A1VPH$$

Square Root Insert Eq. A5

$$A5UMHN \equiv (M \cdot 4 \cdot \mu \cdot \cos^2\alpha - K) \left(\frac{\sqrt{B}}{2D_1} Ln(AG) + \frac{2B}{H} \right)$$

$$A5UBN \equiv (M \cdot 4 \cdot \mu \cdot \cos^2\alpha - K) \left(- \frac{\sqrt{B}}{D_1} Ln(AG) \right)$$

$$A5UPHN \equiv A5UMHN$$

$$A5UMHP \equiv -M \cdot 2\mu \frac{\sqrt{B}\pi}{H \cdot D_1} \cdot \sin 2\alpha (H + 2B - 2\sqrt{B}\sqrt{B+H})$$

$$A5UBP \equiv -M \cdot 4 \cdot \mu \cdot \frac{\sqrt{B}\pi}{H \cdot D_1} \cdot \sin 2\alpha (-H + \sqrt{B}\sqrt{B+H} - \sqrt{B}\sqrt{B-H})$$

$$A5UPHP \equiv -M \cdot 2 \cdot \mu \cdot \frac{\sqrt{B}\pi}{H \cdot D_1} \cdot \sin 2\alpha (H - 2B + 2\sqrt{B}\sqrt{B-H})$$

$$A5VMHN \equiv -M \cdot 4 \cdot \mu \cdot \sin^2 2\alpha \left(\frac{B}{H} + \frac{\sqrt{B}}{4} \cdot Ln(AG) \right)$$

$$A5VBN \equiv M \cdot 4 \cdot \mu \cdot \sin 2\alpha \left(\frac{\sqrt{B}}{2D_1} \cdot Ln(AG) \right)$$

$$A5VPHN \equiv A5VMHN$$

$$A5VMHP \equiv \frac{\pi}{H \cdot D_1}(K - M \cdot 2 \cdot \mu \cdot \cos 2\alpha)(2 \cdot B\sqrt{B} + H\sqrt{B} - 2B\sqrt{B+H}$$

$$A5VBP \equiv \frac{\pi}{H \cdot D_1}(K - M \cdot 2 \cdot \mu \cdot \cos 2\alpha)(2 \cdot B\sqrt{B+H} - 2\sqrt{B} \cdot H - 2 \cdot B\sqrt{B-H})$$

$$A5VPHP \equiv \frac{\pi}{H \cdot D_1}(K - M \cdot 2 \cdot \mu \cdot \cos 2\alpha)(2 \cdot B\sqrt{B-H} - 2 \cdot B\sqrt{B} + H\sqrt{B})$$

Square Root Insert Eq. B5

$$B5UMHN \equiv A5UMHN$$

$$B5UBN \equiv A5UBN$$

$$B5UPHN \equiv A5UPHN$$

$$B5UMHP \equiv \frac{-\pi}{H \cdot D_1}(K + M \cdot 2 \cdot \mu \cdot \cos 2\alpha)(2 \cdot B\sqrt{B} - 2 \cdot B\sqrt{B+H} + H\sqrt{B})$$

$$B5UBP \equiv \frac{-\pi}{H \cdot D_1}(K + M \cdot 2 \cdot \mu \cdot \cos 2\alpha)(2 \cdot B\sqrt{B+H} - 2\sqrt{B} \cdot H - 2 \cdot B\sqrt{B-H})$$

$$B5UPHP \equiv \frac{-\pi}{H \cdot D_1}(K + M \cdot 2 \cdot \mu \cdot \cos 2\alpha)(2 \cdot B\sqrt{B-H} - 2 \cdot B\sqrt{B} + H\sqrt{B})$$

$$B5VMHN \equiv (M \cdot 4 \cdot \mu \cdot \sin^2\alpha - K)\left(\frac{\sqrt{B}}{2D_1} \cdot \mathrm{Ln}(AG) + \frac{2B}{H}\right)$$

$$B5VBN \equiv (M \cdot 4 \cdot \mu \cdot \sin^2\alpha - K)\left(-\frac{\sqrt{B}}{D_1} \cdot \mathrm{Ln}(AG)\right.$$

$$B5VPHN \equiv B5VMHN$$

$$B5VMHP \equiv M \cdot 2\mu \cdot \frac{\sqrt{B} \cdot \pi}{H \cdot D_1} \sin 2\alpha (H + 2 \cdot B - 2\sqrt{B}\sqrt{B+H})$$

$$B5VBP \equiv M \cdot 4\mu \cdot \frac{\sqrt{B} \cdot \pi}{H \cdot D_1} \sin 2\alpha (-H + \sqrt{B}\sqrt{B+H} = \sqrt{B}\sqrt{B-H})$$

$$B5VPHP \equiv M \cdot 2 \cdot \mu \cdot \frac{\sqrt{B} \cdot \pi}{H \cdot D_1} \sin 2\alpha (H - 2 \cdot B + 2\sqrt{B}\sqrt{B-H})$$

Insert Formula for General Non-Linear Displacement Assumption

$(u \doteq \rho r + c_2)$

Solution of the following transcendental equation

$$\sin \gamma[\pi + \alpha]) + \gamma \cdot \sin [\pi + \alpha] = 0$$

Define:

$$D_2 \quad [\underline{C} - B + H]^{\gamma} - [\underline{C} - B - H]^{\gamma}$$

$$D_{11} \quad \frac{\gamma(\gamma - 1)(C - B)^{\gamma-2}}{2 \cdot D_2}$$

$$D_{21} \quad \frac{-\gamma(C - B)^{\gamma-1} - B \cdot \gamma(\gamma - 1)(C - B)^{\gamma-2}}{D_2}$$

γ- Insert Eq. A1

$$A1VMH \equiv -D_{11} \cdot K \cdot 4 \cdot B \cdot H - D_{21} \cdot K \cdot 2 \cdot H$$

$$A1VB \equiv 0$$

$$A1VPH \equiv -A1VMH$$

γ- Insert Eq. B1

$$B1VMH \equiv -A1VMH$$

$$B1VB \equiv 0$$

$$B1VPH \equiv -A1VPH$$

γ- Insert Eq. A5

$$A5UMHP \equiv -D_{11}(B \cdot M \cdot 4 \cdot \mu[4 \cdot \cos^2\alpha \cdot H - 2 \cdot B \cdot \pi \cdot \sin 2\alpha] - K \cdot B \cdot 4 \cdot H) + D_{21} \cdot M \cdot 4 \cdot \mu \cdot \pi \cdot B \cdot \sin 2\alpha$$

$$A5UBP \equiv -M \cdot 4 \cdot \mu \cdot \frac{B}{H} \cdot \cos^2 \alpha + K \cdot \frac{B}{H} \cdot 4$$

$$A5UPHP \equiv -A5UMHP$$

$$A5UMHN \equiv A5UBN = A5UPHN = 0$$

$$A5VMHP \equiv D_{21}\cdot(M\cdot 4\cdot\mu\cdot B\cdot\pi\cdot\cos 2\alpha - 2\cdot K\cdot\pi\cdot B) + D_{11}\cdot(M\cdot 8\cdot\mu\cdot B(H\cdot\sin 2\alpha + B\cdot\pi\cdot\cos 2\alpha) - 2\cdot\pi\cdot B^2\cdot K)$$

$$A5VBP \equiv M\cdot 8\cdot\mu\cdot\frac{B}{H}\sin 2\alpha$$

$$A5VPHP \equiv -A5VMHP$$

$$A5VMHN \equiv A5VBN = A5VPHN = 0$$

Insert Eq. B5

$$B5UMHP \equiv D_{21}\cdot(M\cdot 4\cdot\mu\cdot B\cdot\pi\cdot\cos 2\alpha + 2\cdot K\cdot\pi\cdot B) + D_{11}\cdot(M\cdot 8\cdot\mu\cdot B(H\cdot\sin 2\alpha + B\cdot\pi\cdot\cos 2\alpha) + 2\cdot\pi\cdot B^2\cdot K)$$

$$B5UBP \equiv M\cdot 8\cdot\mu\cdot\frac{B}{H}\cdot\sin 2\alpha$$

$$B5UPHP \equiv -B5UMHP$$

$$B5UMHN \equiv B5UBN = B5UPHN = 0$$

$$B5VMHP \equiv -D_{11}\cdot(B\cdot M\cdot 4\cdot\mu(4\cdot\sin^2\alpha\cdot H + 2\cdot B\cdot\pi\cdot\sin 2\alpha - K\cdot B\cdot 4\cdot H) - D_{21}\cdot M\cdot 4\cdot\mu\cdot\pi\cdot B\cdot\sin 2\alpha$$

$$B5VBP \equiv -M\cdot 16\cdot\mu\cdot\frac{B}{H}\cdot\sin^2\alpha + 4\cdot B\cdot\frac{K}{H}$$

$$B5VPHP \equiv -B5VMHP$$

$$B5VMHN \equiv B5VBN = B5VPHN = 0$$

Define:

$$D_3 \quad [B_2 + H_2 - F]^{\gamma} - [B_2 - H_2 - F]^{\gamma}$$

$$C_{11} \quad \frac{-\gamma(\gamma-1)(B_2 - F)^{\gamma-2}}{2D_3}$$

$$C_{21} \quad \frac{-\gamma(B_2 - F)^{\gamma-1} + B_2\cdot\gamma\cdot(-1)(B_2-F)^{\gamma-2}}{D_3}$$

γ-Insert Eq. A2

$$A2BMH \equiv C_{11} \cdot K \cdot 4 \cdot B_2 \; H_2 + C_{21} \cdot K \cdot 2 \cdot H_2$$

$$A2VB \equiv 0$$

$$A2VPH \equiv -A2VMH$$

γ-Insert Eq. B2

$$B2UMH \equiv -A2VMH$$

$$B2UB \equiv 0$$

$$B2UPH \equiv -B2UMH$$

γ-Insert Eq. A4

$$A4UMH \equiv +C_{11} \cdot 4 \cdot C(K - 4 \cdot M \cdot \mu) H_2$$

$$A4UB \equiv -4 \cdot C(K - M \cdot 4 \cdot \mu)/H_2$$

$$A4UPH \equiv -A4UMH$$

$$A4VMH \equiv (C_{11} \cdot 2 \cdot B_2 + C_{21}) 2 \cdot \pi \cdot C(K - 2 \cdot M \cdot \mu)$$

$$A4VB \equiv 0$$

$$A4VPH \equiv -A4VMH$$

γ-Insert Eq. B4

$$B4UMH \equiv -(C_{11} \cdot 2 \cdot B_2 + C_{21}) 2 \cdot \pi \cdot C(K + 2 \cdot \mu \cdot M)$$

$$B4UB \equiv 0$$

$$B4UPH \equiv -B4UHM$$

$$B4VMH \equiv C_{11} \cdot K \cdot 4 \cdot C \cdot H_2$$

$$B4VB \equiv -K \cdot 4 \cdot C/H_2$$

$$B4VPH \equiv -B4VMH$$

Appendix B.3

Forcing Functions

$$\int_0^{\underline{C}} (t_{x1(\rho)} - t_{x1(B)}) \cdot \frac{1}{2} \cdot \mathrm{Ln}(\rho-B)^2 d\rho + t_{x1(B)} \cdot \frac{1}{2} \int_0^{B-H} \mathrm{Ln}(\rho-B)^2 d\rho$$

$$+ t_{x1(B)} \left[2 \cdot H \cdot \mathrm{Ln}H - 2 \cdot H\right] + t_{x1(B)} \cdot \frac{1}{2} \cdot \int_{B+H}^{\underline{C}} \mathrm{Ln}(\rho-B)^2 \, d\rho$$

$$+ \int_0^{\underline{C}} \left[t_{x1(\rho)} \cdot M \cdot \cos^2(\alpha) - t_{y1(\rho)} \cdot M \cdot \sin\alpha \cdot \cos\alpha \right] d\rho$$

$$+ \int_F^1 \{ t_{x2(\overline{X1})} \cdot \frac{1}{2} \cdot \mathrm{Ln}(R^2_{12}) + t_{x2(\overline{X1})} \cdot M \cdot (\overline{X1}-E-B \cdot \cos\alpha)^2 / R^2_{12}$$

$$+ t_{y2(\overline{X1})} \cdot M \cdot (\overline{X1}-E-B \cdot \cos\alpha)(B \cdot \sin\alpha - C \cdot \tan\alpha)/R^2_{12} \} \, d\overline{X1}$$

$$+ \int_0^{2\pi} \{ t_{x3} \cdot \frac{1}{2} \cdot \mathrm{Ln} \cdot R^2_{13} + t_{x3(\Theta)} \cdot M \cdot (\cos\theta - E - B \cdot \cos\alpha)^2 / R^2_{13}$$

$$+ t_{y3} \cdot M \cdot (\cos\theta - E - B \cdot \cos\alpha)(\sin\theta - C \cdot \tan\alpha + B \cdot \sin\alpha)/R^2_{13} \} \, d\theta$$

$$+ \int_F^1 \{ t_{x4(\overline{X1})} \cdot \frac{1}{2} \cdot \mathrm{Ln} \, R^2_{12} + t_{x4(\overline{X1})} \cdot M \cdot (\overline{X1}-E-B \cdot \cos\alpha)^2 / R^2_{12}$$

$$+ t_{y4(\overline{X1})} \cdot M \cdot (\overline{X1}-E-B \cdot \cos\alpha)(B \cdot \sin\alpha - C \cdot \tan\alpha)/R^2_{12} \} \, d\overline{X1}$$

$$+ \int_0^{\underline{C}} (t_{x5(\rho)} - t_{x5(B)}) \cdot \frac{1}{2} \cdot \mathrm{Ln}(\rho-B)^2 d\rho + t_{x5(B)} \cdot \frac{1}{2} \cdot \int_0^{B-H} \mathrm{Ln}(\rho-B)^2 \, d\rho$$

$$+ t_{x5(B)} \left[2 \cdot H \cdot \mathrm{Ln}H - 2 \cdot H\right] + t_{x5(B)} \cdot \frac{1}{2} \cdot \int_{B+H}^{\underline{C}} \mathrm{Ln}(\rho-B)^2 \, d\rho$$

FA1(B)

$$+ \int_0^{\underline{C}} \left[t_{x5(\rho)} \cdot M \cdot \cos^2\alpha - t_{y5(\rho)} \cdot M \cdot \sin\alpha \cdot \cos\alpha \right] d\rho$$

$$\int_0^{\underline{C}} \{t_{x1(\rho)} \cdot \frac{1}{2} \cdot \mathrm{Ln}\, R_{21}^2 + t_{x1(\rho)} \cdot M \cdot (E+\rho\cdot\cos\alpha-B_2)^2/R_{21}^2$$

$$+ t_{y1(\rho)} \cdot M \cdot (E+\rho\cdot\cos\alpha-B_2)(C\cdot\tan\alpha-\rho\cdot\sin\alpha)/R_{21}^2 \}\, d\rho$$

$$+ \int_F^1 \{(t_{x2(\overline{X1})} - t_{x2(B_2)}) \cdot \frac{1}{2} \cdot \mathrm{Ln}(\overline{X1}-B_2)^2 + t_{x2(\overline{X1})} \cdot M \}\, d\overline{X1}$$

$$+ t_{x2(B_2)} \int_F^{B_2-H} \frac{1}{2} \cdot \mathrm{Ln}(\overline{X1}-B_2)^2\, d\overline{X1} + t_{x2(B_2)} \cdot 2\,(H\cdot\mathrm{Ln}\, H-H)$$

$$+ t_{x2(B_2)} \int_{B_2+H}^1 \frac{1}{2}\cdot\mathrm{Ln}(\overline{X1}-B_2)^2\, d\overline{X1}$$

$$+ \int_0^{2\pi} \{t_{x3(\Theta)} \cdot \frac{1}{2}\cdot\mathrm{Ln}\, R_{23}^2 + t_{x3(\Theta)} \cdot M\cdot(\mathrm{Cos}\Theta-B_2)^2/R_{23}^2$$

$$+ t_{y3} \cdot M\cdot(\cos\Theta-B_2)(\sin\Theta)/R_{23}^2 \}\, d\Theta$$

$$+ \int_F^1 \{(t_{x4(\overline{X1})} - t_{x4(B_2)}) \cdot \frac{1}{2} \cdot \mathrm{Ln}(\overline{X1}-B_2)2 + t_{x4(\overline{X1})} \cdot M\}\, d\overline{X1}$$

$$+ t_{x4(B_2)} \int_F^{B_2-H} \frac{1}{2} \cdot \mathrm{Ln}(\overline{X1}-B_2)^2\, d\overline{X1} + t_{x4(B_2)} \cdot 2\cdot(H\cdot\mathrm{Ln}H-H)$$

$$+ t_{x4(B_2)} \int_{B_2+H}^1 \frac{1}{2}\cdot\mathrm{Ln}(\overline{X1}-B_2)2\, d\overline{X1}$$

$$+ \int_0^{\underline{C}} \{t_{x5} \cdot \frac{1}{2} \cdot \mathrm{Ln}\, R_{21}^2 + t_{x5}\cdot M\,(E+\rho\cdot\cos\alpha-B_2)2/R_{21}^2 \quad FA2(B_2)$$

$$+ t_{y5} \cdot M\cdot(E+\rho\cdot\cos\alpha-B_2)(C\cdot\tan\alpha-\rho\cdot\sin\alpha)/R_{21}^2 \}\, d\rho$$

$$\int_0^{\underline{C}} \{t_{xl(\rho)} \cdot \frac{1}{2} \cdot \mathrm{Ln}\, R_{31}^2 + t_{xl(\rho)} \cdot M \cdot (E+\rho \cdot \cos\alpha - \cos\theta_0)^2 / R_{31}^2$$

$$+ t_{yl(\rho)} \cdot M \cdot (E+\rho \cdot \cos\alpha - \cos\theta_0)(C \cdot \tan\alpha - \rho \cdot \sin\alpha - \sin\theta_0)/R_{31}^2 \}\, d\rho$$

$$+ \int_F^1 \{t_{x2(\overline{Xl})} \cdot \frac{1}{2} \cdot \mathrm{Ln}\, R_{32}^2 + t_{x2(\overline{Xl})} \cdot M \cdot (\overline{Xl} - \cos\theta_0)^2 / R_{32}^2$$

$$+ t_{y2} \cdot (\overline{Xl} - \cos\theta_0)(-\sin\theta_0)/R_{32}^2 \}\, d\overline{Xl}$$

$$+ \int_0^{2\pi} \{t_{x3(\theta)} \cdot M \cdot \sin^2 \frac{(\theta+\theta_0)}{2} - t_{y3(\theta)} \cdot \frac{M}{2} \cdot \sin(\theta+\theta_0)\}\, d\theta$$

$$+ \int_0^{2\pi} \left\{ \frac{t_{x3(\theta)} - t_{x3(\theta_0)}}{2} \cdot Ln(2-2 \cdot \cos(\theta-\theta_0)) \right\} d\theta +$$

$$t_{x3(\theta_0)} \cdot \frac{1}{2} \cdot \int_0^{\theta_0-\Delta\theta} \mathrm{Ln}(2-2 \cdot \cos(\theta-\theta_0)\, d\theta + t_{x3(\theta_0)} \cdot \frac{1}{2} \cdot \int_{\theta_0+\Delta\theta}^{2\pi} \mathrm{Ln}(2-2 \cdot \cos(\theta-\theta_0))\, d\theta$$

$$+ t_{x3(\theta_0)} \cdot \frac{\Delta\theta}{2} \cdot \left[4 \cdot \mathrm{Ln}(\Delta\theta) - 2 \cdot \mathrm{Ln} \cdot 4 - 4 - \frac{(\Delta\theta)^2}{18}\right]$$

$$+ \int_F^1 \{t_{x4(\overline{Xl})} \cdot \frac{1}{2} \cdot \mathrm{Ln}\, R_{32}^2 + t_{x4(\overline{Xl})} \cdot M \cdot \frac{(\overline{Xl} - \cos\theta_0)^2}{R_{32}^2}$$

$$+ t_{y4(\overline{Xl})} \cdot M \cdot (\overline{Xl} - \cos\theta_0)(-\sin\theta_0)/R_{32}^2 \}\, d\overline{Xl}$$

$$+ \int_0^{\underline{C}} \{t_{x5(\rho)} \cdot \frac{1}{2} \cdot \mathrm{Ln}\, R_{31}^2 + t_{x5(\rho)} \cdot M \cdot (E+\rho \cdot \cos\alpha - \cos\theta_0)/R_{31}^2$$

$$+ t_{y5(\rho)} \cdot M \cdot (E+\rho \cdot \cos\alpha - \cos\theta_0)(C \cdot \tan\alpha - \rho \cdot \sin\alpha - \sin\theta_0)/R_{31}^2 \}\, d\rho$$

$$FA3_{(\theta_0)}$$

$$\int_0^{\underline{C}} \Big\{ t_{x1(\rho)} \quad (-2\ C)(C\cdot\tan\alpha-\rho\cdot\sin\alpha)/R_{21}^2$$

$$+t_{x1(\rho)}\cdot M\cdot(E+\rho\cdot\cos\alpha-B_2)^2\ (+4C)(C\cdot\tan\alpha-\rho\cdot\sin\alpha)/R_{21}^4$$

$$+ t_{y1(\rho)}\cdot M\cdot\left[(E+\rho\cdot\cos\alpha-B_2)\right]\left[\frac{(-2C)}{R_{21}^2} + \frac{(C\cdot\tan\alpha-\rho\cdot\sin\alpha)^2(+4C)}{R_{21}^4}\right]\Big\}\ d\rho$$

$$+\int_F^{B_2-H} t_{y2(\overline{X1})}\left[\frac{-M\cdot 2\cdot C}{\overline{X1}-B_2}\right]\ d\overline{X1} + \int_{B_2+H}^{1} t_{y2(\overline{X1})}\ \frac{-M\cdot 2\cdot C}{\overline{X1}-B_2}\ d\overline{X1}$$

$$+ t_{x2(B_2)}\ \left[2\cdot C\ (M-1)\cdot\pi\right]$$

$$+\int_0^{2\pi}\Big\{t_{x3(\theta)}\left[\frac{-2\cdot C\cdot\sin\theta}{R_{23}^2}\right] + t_{x3(\theta)}\cdot M\cdot\frac{(\cos\theta-B_2)^2(4\cdot C\cdot\sin\theta)}{R_{23}^4}$$

$$+ t_{y3}\cdot M\cdot(\cos\theta-B_2)\left[\frac{-2\cdot C}{R_{23}^2} + \frac{\sin^2\theta\ (4C)}{R_{23}^4}\right]\Big\}\ d\theta$$

$$- t_{x4(B_2)}\ \left[2\cdot C\ (M-1)\cdot\pi\right]$$

$$+\int_F^{B_2-H} t_{y4(\overline{X1})}\ \left[\frac{-M\cdot 2\cdot C}{\overline{X1}-B_2}\right]\ d\overline{X1} + \int_{B_2+H}^{1} t_{y4(\overline{X1})}\left[\frac{-M\cdot 2\cdot C}{\overline{X1}-B_2}\right]\ d\overline{X1}$$

$$+\int_0^{\underline{C}}\Big\{t_{x5(\rho)}\ \frac{-2\cdot C\cdot(C\cdot\tan\alpha-\rho\cdot\sin\alpha)}{R_{21}^2}$$

$$FA4(B_2)$$

$$+ t_{x5(\rho)} \cdot M \cdot (E+\rho \cdot \cos\alpha - B_2)^2 \ (4C) \ (C \cdot \tan\alpha - \rho \cdot \sin\alpha)/R_{21}^4$$

$$+ t_{y5(\rho)} \cdot M \cdot (E+\rho \cdot \cos\alpha - B_2) \left[\frac{-2C}{R_{21}^2} + \frac{4 \cdot C \cdot (C \cdot \tan\alpha - \rho \cdot \sin\alpha)^2}{R_{21}^4} \right] \Bigg\} d\rho$$

FA4(B_2) Cont.

$$- t_{xl(B)} \cdot 2 \cdot B \cdot \pi + \int_0^{\underline{C}} t_{xl(\rho)} \cdot M \cdot \sin 2\alpha \; d\rho$$

$$- \int_{0,B+H}^{B-H,\underline{C}} t_{xl(\rho)} \cdot M \cdot \sin 2\alpha \cdot \frac{(\rho+B)}{\rho-B} \; d\rho - t_{xl(B)} \cdot M \cdot 2 \cdot B \cdot \pi \cdot \sin^2\alpha$$

$$+ \int_0^{\underline{C}} t_{yl(\rho)} \cdot M \cdot \cos 2\alpha \; d\rho - \int_{0,B+H}^{B-H,\underline{C}} t_{yl(\rho)} \cdot M \cdot \cos 2\alpha \cdot \frac{(\rho+B)}{\rho-B} \; d\rho$$

$$- t_{yl(B)} \cdot M \cdot 2 \cdot B \cdot \pi \cdot \sin 2\alpha$$

$$+ \int_F^1 t_{x2(\overline{Xl})} \left\{ \cdot 2 \cdot B \cdot \sin\alpha \frac{(C+E-\overline{Xl})}{R_{12}^2} + \frac{M \cdot (\overline{Xl}-E-B\cdot\cos\alpha)^2 (\overline{Xl}-E-C) 4 \cdot B \cdot \sin\alpha}{R_{12}^4} \right.$$

$$\left. -4 \cdot M \cdot (+B \cdot \sin\alpha)(\overline{Xl}-E-B\cdot\cos\alpha)/R_{12}^2 \right\} d\overline{Xl}$$

$$+ \int_F^1 t_{y2(\overline{Xl})} \left\{ -M \cdot 2 \cdot B \cdot \sin\alpha \; \frac{(B\cdot\sin\alpha - C\cdot\tan\alpha)}{R_{12}^2} + 2 \cdot M \frac{(\overline{Xl}-E-B\cdot\cos\alpha)}{R_{12}^2} \; (-B\cdot\cos\alpha) \right.$$

$$\left. + M \cdot (\overline{Xl}-E-B\cdot\cos\alpha)(B\cdot\sin\alpha - C\cdot\tan\alpha) \; \frac{4\cdot B\cdot\sin\alpha\cdot(\overline{Xl}-E-C)}{R_{12}^4} \right\} \; d\overline{Xl}$$

$$+ \int_0^{2\pi} t_{x3(\Theta)} \left\{ 2 \cdot B \cdot \frac{(\lceil E+C \rceil \sin\alpha - \sin(\alpha+\Theta))}{R_{13}^2} \right.$$

$$-4 \cdot B \cdot M \cdot \sin\alpha (\cos\Theta - E - B\cdot\cos\alpha)/R_{13}^2$$

$$\left. + M \cdot (\cos\Theta - E - B\cdot\cos\alpha)^2 \cdot 4 \cdot B \cdot (\sin(\alpha+\Theta) - (E+C)\sin\alpha)/R_{13}^4 \right\} d\Theta$$

$$+ \int_0^{2\pi} t_{y3(\Theta)} \left\{ -2 \cdot M \cdot B \cdot \sin\alpha \cdot (\sin\Theta - C\cdot\tan\alpha + B\cdot\sin\alpha)/R_{13}^2 \right.$$

FA5(B)

$$- 2\cdot M\cdot(\cos\theta - E - B\cdot\cos\alpha)\cdot B\cdot\cos\alpha \,/R_{13}^2$$

$$+4\cdot B\cdot M\cdot(\cos\theta - E - B\cdot\cos\alpha)(\sin\theta - C\cdot\tan\alpha + B\cdot\sin\alpha)\frac{(\sin(\alpha+\theta)-(E+C)\sin\alpha)}{R_{13}^4}\Bigg\}\, d\theta$$

$$+\int_F^1 t_{x4(\overline{X1})}\left\{\frac{+2\cdot B\cdot\sin\alpha\,(C+E-\overline{X1})}{R_{12}^2} - M\cdot(4\cdot B\cdot\sin\alpha)\frac{(\overline{X1}-E-B\cdot\cos\alpha)}{R_{12}^2}\right.$$

$$\left. + M\,(\overline{X1}-E-B\cdot\cos\alpha)^2\cdot 4\cdot B\cdot\sin\alpha\,(\overline{X1}-E-C)/R_{12}^4\right\} d\overline{X1}$$

$$+\int_F^1 t_{y4(\overline{X1})}\left\{2\cdot M\cdot(-B\cdot\sin\alpha)\frac{(B\cdot\sin\alpha - C\cdot\tan\alpha)}{R_{12}^2}\right.$$

$$+ 2\cdot M\cdot(\overline{X1}-E-B\cdot\cos\alpha)(-B\cdot\cos\alpha)/R_{12}^2$$

$$\left. + M\,(\overline{X1}-E-B\cdot\cos\alpha)(B\cdot\sin\alpha - C\cdot\tan\alpha)(4\cdot B\cdot\sin\alpha)\frac{(\overline{X1}-E-C)}{R_{12}^4}\right\} d\overline{X1}$$

$$+t_{x5(B)}\cdot 2\cdot B\cdot\pi\cdot + \int_{0,B+H}^{B-H,\underline{C}} t_{x5(\rho)}\cdot M(-1)\cdot\sin 2\alpha\,\frac{(\rho+B)}{\rho-B}\, d\rho$$

$$+\int_0^{\underline{C}} t_{x5(\rho)}\cdot M\cdot\sin 2\alpha\; d\rho \;+ t_{x5(B)}\cdot M\cdot 2\cdot B\cdot\pi\cdot\sin^2\alpha$$

$$+\int_{0,B+H}^{B-H,\underline{C}} t_{y5(\rho)}\left\{-M\cdot\cos 2\alpha\;\frac{\rho+B}{\rho-B}\right\} d\rho + t_{y5(B)}\left[M\cdot 2\cdot\pi B\cdot\sin 2\alpha\right]$$

$$+\int_0^{\underline{C}} t_{y5(\rho)}\left\{M\,(\cos 2\alpha\,)\right\} d\rho$$

FA5(B) Cont.

$$\int_{0,B+H}^{B-H,\underline{C}} t_{y1(\rho)} \cdot \frac{1}{2} \cdot \mathrm{Ln}(\rho-B)^2 \, d\rho + t_{y1(B)} \cdot 2 \cdot (H \cdot \mathrm{Ln}H - H)$$

$$+ \int_{0}^{\underline{C}} t_{y1(\rho)} \cdot M \cdot \sin^2(\alpha) \, d\rho + \int_{0}^{\underline{C}} t_{x1(\rho)} \cdot M \cdot (-\frac{1}{2} \sin 2\alpha) \, d\rho$$

$$+ \int_{F}^{1} \left\{ t_{y2(\overline{X1})} \cdot \frac{1}{2} \mathrm{Ln}R_{12}^2 + t_{y2(\overline{X1})} \cdot M \cdot (B \cdot \sin\alpha - C \cdot \tan\alpha)^2 / R_{12}^2 \right.$$

$$\left. + t_{x2(\overline{X1})} \cdot M \cdot (\overline{X1} - E - B \cdot \cos\alpha)(B \cdot \sin\alpha - C \cdot \tan\alpha) / R_{12}^2 \right\} d\overline{X1}$$

$$+ \int_{0}^{2\pi} \left\{ t_{y3(\Theta)} \cdot \frac{1}{2} \cdot \mathrm{Ln} \, R_{13}^2 + t_{y3(\Theta)} \cdot M \cdot (\sin\Theta - C \cdot \tan\alpha + B \cdot \sin\alpha)^2 / R_{13}^2 \right.$$

$$\left. + t_{x3(\Theta)} \cdot M \cdot (\cos\Theta - E - B \cdot \cos\alpha)(\sin\Theta - C \cdot \tan\alpha + B \cdot \sin\alpha) / R_{13}^2 \right\} d\Theta$$

$$+ \int_{F}^{1} \left\{ t_{y4(\overline{X1})} \cdot \frac{1}{2} \cdot \mathrm{Ln} \, R_{12}^2 + t_{y4(\overline{X1})} \cdot M \cdot (B \cdot \sin\alpha - C \cdot \tan\alpha)^2 / R_{12}^2 \right.$$

$$\left. + t_{x4(\overline{X1})} \cdot M \cdot (\overline{X1} - E - B \cdot \cos\alpha)(B \cdot \sin\alpha - C \cdot \tan\alpha) / R_{12}^2 \right\} d\overline{X1}$$

$$+ \int_{0,B+H}^{B-H,\underline{C}} t_{y5(\rho)} \cdot \frac{1}{2} \cdot \mathrm{Ln}(\rho-B)^2 \, d\rho + t_{y5(B)} \cdot 2 \cdot (H \cdot \mathrm{Ln}H - H)$$

$$+ \int_{0}^{\underline{C}} t_{y5(\rho)} \cdot M \cdot \sin^2\alpha \, d\rho + \int_{0}^{\underline{C}} t_{x5(\rho)} \cdot M \cdot (-\frac{1}{2} \sin 2\alpha) \, d\rho$$

FB1(B)

$$\int_0^{\underline{C}} \left\{ t_{y1(\rho)} \cdot \frac{1}{2} \cdot \mathrm{Ln}\ R_{21}^2 + t_{y1(\rho)} \cdot M \cdot (C \cdot \tan\alpha - \rho \cdot \sin\alpha)^2 / R_{21}^2 \right.$$

$$\left. + t_{x1(\rho)} \cdot M \cdot (E + \rho \cdot \cos\alpha - B_2)(C \cdot \tan\alpha - \rho \cdot \sin\alpha) / R_{21}^2 \right\} d\rho$$

$$+ \int_{F,B+H}^{B-H,1} t_{y2(\overline{X1})} \cdot \frac{1}{2} \cdot \mathrm{Ln}(\overline{X1} - B_2)^2\ d\overline{X1} + t_{y2(B_2)} \cdot 2 \cdot (H \cdot \mathrm{Ln}H - H)$$

$$+ \int_0^{2\pi} \left\{ t_{y3(\Theta)} \cdot \frac{1}{2} \cdot \mathrm{Ln}\ R_{23}^2 + t_{y3(\Theta)} \cdot M \cdot (\sin^2\Theta) / R_{23}^2 \right.$$

$$\left. + t_{x3(\Theta)} \cdot M \cdot (\cos\Theta - B_2)(\sin\Theta) / R_{23}^2 \right\} d\Theta$$

$$+ \int_{F,B+H}^{B-H,1} t_{y4(\overline{X1})} \cdot \frac{1}{2} \cdot \mathrm{Ln}(\overline{X1} - B_2)^2\ d\overline{X1} + t_{y4(B_2)} \cdot 2 \cdot (H \cdot \mathrm{Ln}H - H)$$

$$+ \int_0^{\underline{C}} \left\{ t_{y5(\rho)} \cdot \frac{1}{2} \cdot \mathrm{Ln}\ R_{21}^2 + t_{y5(\rho)} \cdot M \cdot (C \cdot \tan\alpha - \rho \cdot \sin\alpha)^2 / R_{21}^2 \right.$$

$$\left. + t_{x5(\rho)} \cdot M \cdot (E + \rho \cdot \cos\alpha - B_2)(C \cdot \tan\alpha - \rho \cdot \sin\alpha) / R_{21}^2 \right\} d\rho$$

$$FB2(B_2)$$

$$\int_0^{\underline{C}} \left\{ t_{y1(\rho)} \cdot \frac{1}{2} \cdot \mathrm{Ln}\ R_{31}^2 + t_{y1(\rho)} \cdot M \cdot (C \cdot \tan\alpha - \rho \cdot \sin\alpha - \sin\Theta_0)^2 / R_{31}^2 \right.$$

$$\left. + t_{x1(\rho)} \cdot M \cdot (E + \rho \cdot \cos\alpha - \cos\Theta_0)(C \cdot \tan\alpha - \rho \cdot \sin\alpha - \sin\Theta_0)/R_{31}^2 \right\} d\rho$$

$$+ \int_F^1 \left\{ t_{y2(\overline{Xl})} \cdot \frac{1}{2} \cdot \mathrm{Ln}\ R_{32}^2 + t_{y2(\overline{Xl})} \cdot M \cdot \sin^2\Theta_0 / R_{31}^2 \right.$$

$$\left. + t_{x2(\overline{Xl})} \cdot M \cdot (-\sin\Theta_0)(\overline{Xl} - \cos\Theta_0)/R_{31}^2 \right\} d\overline{Xl}$$

$$+ \int_0^{2\pi} \left\{ t_{y3(\Theta)} \cdot M \cdot \cos^2\left(\frac{\Theta + \Theta_0}{2}\right) - t_{x3(\Theta)} \cdot \frac{M}{2} \cdot \sin(\Theta + \Theta_0) \right\} d\Theta$$

$$+ \int_0^{2\pi} \left\{ \frac{(t_{y3(\Theta)} - t_{y3(\Theta_0)})}{2} \cdot \mathrm{Ln}(2 - 2 \cdot \cos(\Theta - \Theta_0)) \right\} d\Theta +$$

$$\frac{t_{y3(\Theta_0)}}{2} \int_0^{\Theta_0 - \Delta\Theta} \mathrm{Ln}(2 - 2 \cdot \cos(\Theta - \Theta_0))\ d\Theta + \frac{t_{y3(\Theta_0)}}{2} \int_{\Theta_0 + \Delta\Theta}^{2\pi} \mathrm{Ln}(2 - 2\cos(\Theta - \Theta_0))\, d\Theta$$

$$+ \frac{t_{y3(\Theta_0)}}{2} (\Delta\Theta) \left[4 \cdot \mathrm{Ln}(\Delta\Theta) - 2 \cdot \mathrm{Ln}\ 4 - 4 - \frac{(\Delta\Theta)^2}{18} \right]$$

$$+ \int_F^1 \left\{ t_{y4} \cdot \frac{1}{2} \cdot \mathrm{Ln}\ R_{32}^2 + t_{y4(\overline{Xl})} \cdot M \cdot (\sin^2\Theta_0)/R_{32}^2 \right.$$

$$\left. + t_{x4(\overline{Xl})} \cdot M \cdot (\overline{Xl} - \cos\Theta_0)(-\sin\Theta_0)/R_{32}^2 \right\} d\overline{Xl}$$

$$+ \int_0^{\underline{C}} \left\{ t_{y5(\rho)} \cdot \frac{1}{2} \cdot \mathrm{Ln}\ R_{31}^2 + t_{y5(\rho)} \cdot M \cdot (C \cdot \tan\alpha - \rho \cdot \sin\alpha - \sin\Theta_0)^2 / R_{31}^2 \right.$$

$$\left. + t_{x5(\rho)} \cdot M \cdot (E + \rho \cdot \cos\alpha - \cos\Theta_0)(C \cdot \tan\alpha - \rho \cdot \sin\alpha - \sin\Theta_0)/R_{31}^2 \right\} d\rho$$

$$FB3(\theta_o)$$

$$\int_0^{\underline{C}} \left\{ t_{y1(\rho)} \cdot (-2C)(C\cdot\tan\alpha-\rho\cdot\sin\alpha)(1+2M)/R_{21}^2 \right.$$

$$+ t_{y1(\rho)} \cdot M \cdot (C\cdot\tan\alpha-\rho\cdot\sin\alpha)^3(4\cdot C)/R_{21}^4$$

$$\left. + t_{x1(\rho)} \cdot M \cdot \left[E+\rho\cdot\cos\alpha-B_2\right]\cdot\left[\frac{(-2C)}{R_{21}^2} + \frac{(C\cdot\tan\alpha-\rho\cdot\sin\alpha)^2(4C)}{R_{21}^4}\right] \right\} d\rho$$

$$+\int_{F,B_2+H}^{B_2-H,\,1} t_{x2(\overline{X1})} \cdot M \cdot \left(\frac{-2\cdot C}{\overline{X1}-B_2}\right) d\overline{X1} + t_{y2(B_2)}(-2\cdot C(M+1)\pi)$$

$$+\int_0^{2\pi} \left\{ t_{y3(\Theta)} \left[\frac{-2\cdot C\cdot\sin\Theta}{R_{23}^2}\right] + t_{y3(\Theta)} \left[\frac{-\sin\Theta\cdot 4\cdot C}{R_{23}^2} + \frac{\sin^3\Theta\cdot 4\cdot C}{R_{23}^4}\right]\cdot M \right.$$

$$\left. + t_{x3(\Theta)} \cdot M \cdot \left[(-2\cdot C)\frac{(\cos\Theta-B_2)}{R_{23}^2} + \frac{(\cos\Theta-B_2)\sin^2\Theta\cdot 4\cdot C}{R_{23}^4}\right] \right\} d\Theta$$

$$+\int_{F,B_2+H}^{B_2-H,1} t_{x4(\overline{X1})} \cdot M \cdot \left(\frac{-2\cdot C}{\overline{X1}-B_2}\right) d\overline{X1} + t_{y4(B_2)} \cdot (2\cdot C\ (M+1)\pi)$$

$$+\int_0^{\underline{C}} \left\{ t_{y5(\rho)} \left[\frac{-2\cdot C\ (C\cdot\tan\alpha-\rho\cdot\sin\alpha)}{R_{21}^2}\right]\cdot\left[1 + 2M - 2M\cdot\frac{(C\cdot\tan\alpha-\rho\cdot\sin\alpha)^2}{R_{21}^2}\right] d\rho \right.$$

$$\left. +\int_0^{\underline{C}} t_{x5(\rho)} \cdot M \cdot (E+\rho\cdot\cos\alpha-B_2)\left[\frac{-2\cdot C}{R_{21}^2} + C\cdot 4\cdot\frac{(C\cdot\tan\alpha-\rho\cdot\sin\alpha)^2}{R_{21}^4}\right] d\rho \right.$$

$$FB4(B_2)$$

$$t_{yl(B)}\ (-2\cdot B\cdot\pi)(1+M\cdot\cos 2\alpha)$$

$$+\ t_{xl(B)}\ (-2\cdot B\cdot\pi)(M\cdot\sin 2\alpha)$$

$$+\int_0^{\underline{C}} t_{yl(\rho)}\cdot M\cdot(-\sin 2\alpha)\ d\rho\ +\ \int_0^{\underline{C}} t_{xl(\rho)}\cdot M\cdot(\cos 2\alpha)\ d\rho$$

$$+\int_{0,B+H}^{B-H,\underline{C}} t_{yl(\rho)}\cdot M\cdot\left(\frac{\rho+B}{\rho-B}\right)\sin 2\alpha\ d\rho\ -\int_{0,B+H}^{B-H,\underline{C}} t_{xl(\rho)}\cdot M\left(\frac{\rho+B}{\rho-B}\right)\cos 2\alpha\ \ d\rho$$

$$+\int_F^1 t_{y2(\overline{Xl})}\ (-2\cdot B\cdot\sin\alpha)\frac{(\overline{Xl})-E-C)}{R_{12}^2}\ \ d\overline{Xl}$$

$$+\int_F^1 t_{y2(\overline{Xl})}\cdot M\cdot(B\cdot\sin\alpha-C\cdot\tan\alpha)(-4B)(\cos\alpha)/R_{12}^2$$

$$+\int_F^1 t_{y2(\overline{Xl})}\cdot M\cdot(B\cdot\sin\alpha-C\cdot\tan\alpha)^2(4B)\sin\alpha(\overline{Xl}-E-C)/R_{12}^4$$

$$+\int_F^1 t_{x2(\overline{Xl})}\left\{-M\cdot 2\cdot B\cdot\sin\alpha(B\cdot\sin\alpha-C\cdot\tan\alpha)/R_{12}^2\right.$$

$$-2\cdot B\cdot M\cdot\frac{(\overline{Xl}-E-B\cdot\cos\alpha)}{R_{12}^2}\cos\alpha$$

$$\left.+M(\overline{Xl}-E-B\cdot\cos\alpha)(B\cdot\sin\alpha-C\cdot\tan\alpha)(4\cdot B\cdot\sin\alpha(\overline{Xl}-E-C))/R_{12}^4\right\}\ d\overline{Xl}$$

$$+\int_0^{2\pi}\left\{t_{y3(\theta)}\ \cdot 2B(-\sin(\alpha+\theta)+(E+C)\cdot\sin\alpha)/R_{13}^2\right.$$

FB5(B)

$$+ t_{x3(\theta)} \cdot M \cdot (\cos\theta - E - B\cdot\cos\alpha)(\sin\theta - C\cdot\tan\alpha + B\cdot\sin\alpha)$$

$$\cdot 4\cdot B\cdot(\sin(\alpha+\theta) - (E+C)\cdot\sin\alpha)/R_{13}^4$$

$$+ t_{x3(\theta)} \cdot M \cdot \Big[(\sin\theta - C\cdot\tan\alpha + B\cdot\sin\alpha)(-2\cdot B\cdot\sin\alpha)/R_{13}^2$$

$$+ (\cos\theta - E - B\cdot\cos\alpha)(-2\cdot B\cdot\cos\alpha)/R_{13}^2\Big]$$

$$+ t_{y3(\theta)} \cdot M \cdot \Big[-4\cdot B\cdot(\sin\theta - C\cdot\tan\alpha + B\cdot\sin\alpha)(\cos\alpha)/R_{13}^2$$

$$+4\cdot B\cdot(\sin\theta - C\cdot\tan\alpha + B\cdot\sin\alpha)^2 \frac{(\sin(\alpha+\theta) - (E+C)\sin\alpha)}{R_{13}^4}\Big]\Big\}\, d\theta$$

$$+\int_F^1 \Big\{ t_{y4(\overline{X1})}\Big[(-2\cdot B\cdot\sin\alpha)(\overline{X1} - E - C)/R_{12}^2 - (4B)\cos\alpha(B\cdot\sin\alpha - C\cdot\tan\alpha)\cdot M/R_{12}^2\Big]$$

$$+ t_{y4(\overline{X1})} \cdot \Big[M\cdot(B\cdot\sin\alpha - C\cdot\tan\alpha)^2 (4B)\sin\alpha(\overline{X1} - E - C)/R_{12}^4\Big]$$

$$+ t_{x4(\overline{X1})} \cdot \Big[M\cdot(-2B)\Big]\cdot\Big[\sin\alpha(B\cdot\sin\alpha - C\cdot\tan\alpha) + \cos\alpha(\overline{X1} - E - B\cdot\cos\alpha)\Big]\cdot\frac{1}{R_{12}^2}$$

$$+ t_{x4(\overline{X1})} \cdot \Big[M\cdot(\overline{X1} - E - B\cdot\cos\alpha)(B\cdot\sin\alpha - C\cdot\tan\alpha)(4B\cdot\sin\alpha)(\overline{X1} - E - C)/R_{12}^4\Big]\Big\} d\overline{X1}$$

$$+ t_{y5(B)} \cdot \Big[(2\cdot B\cdot\pi)(1 + M\cdot\cos 2\alpha)\Big] + t_{x5(B)} \cdot M\cdot 2\cdot B\cdot\pi\cdot \sin 2\alpha$$

$$+\int_{0,B+H}^{B-H,\underline{C}} t_{y5(\rho)} \cdot M\cdot\left(\frac{\rho+B}{\rho-B}\right)\sin 2\alpha\, d\rho - \int_{0,B+H}^{B-H,\underline{C}} t_{x5(\rho)}\cdot M\left(\frac{\rho+B}{\rho-B}\right)\cos 2\alpha\, d\rho$$

$$+\int_0^{\underline{C}} t_{y5(\rho)} \cdot M\cdot\sin 2\alpha\, d\rho + \int_0^{\underline{C}} t_{x5(\rho)} \cdot M\cdot\cos 2\alpha\, d\rho$$

FB5(B) Cont.

Where

$$\Delta\Theta \ll \pi \qquad , H \ll 1$$

$$\int_{0,B+H}^{B-H,\underline{C}} K_{(\xi)}\ d\xi \equiv \int_{0}^{B-H} K_{(\xi)}\ d\xi + \int_{B+H}^{\underline{C}} K_{(\xi)}\ d\xi$$

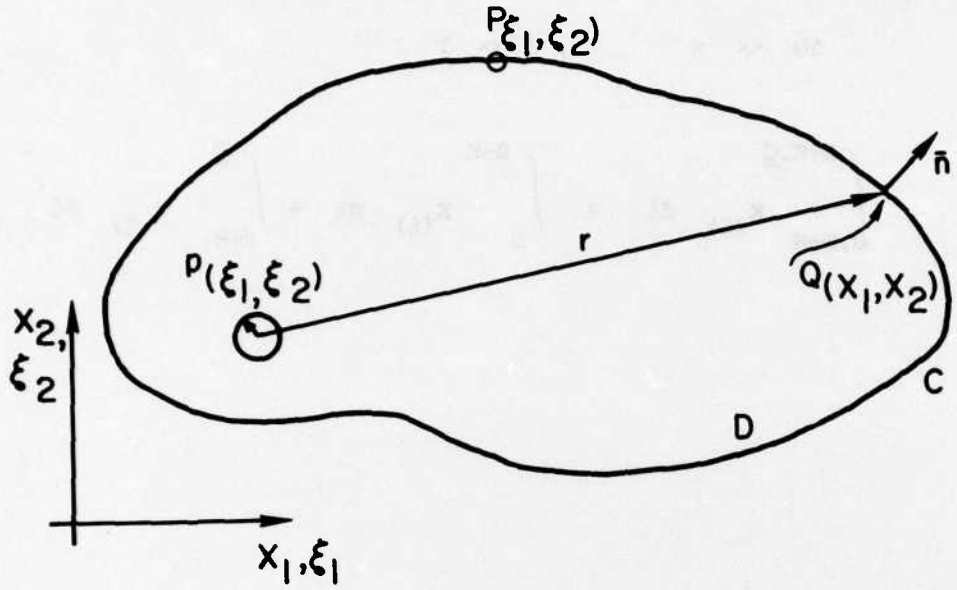

Figure 1. General Elastic Closed Domain.

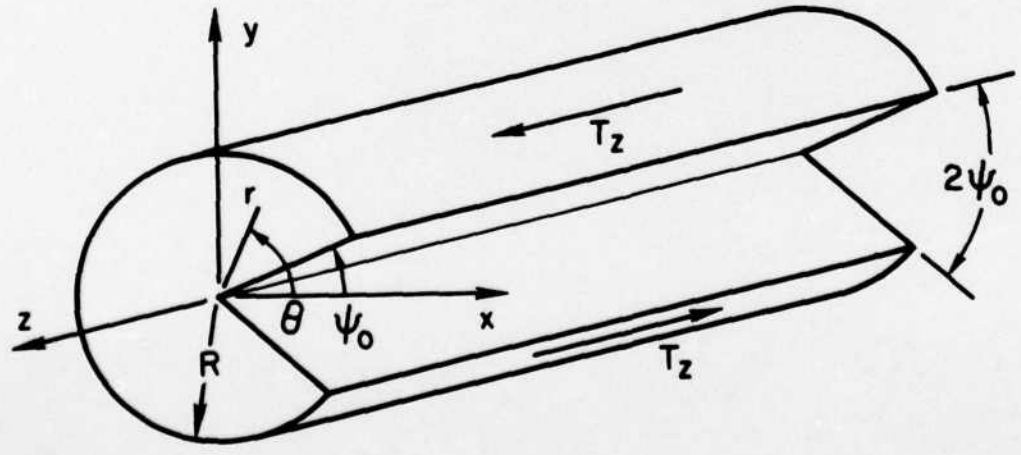

Figure 2. Simple Anti-Plane Geometry.

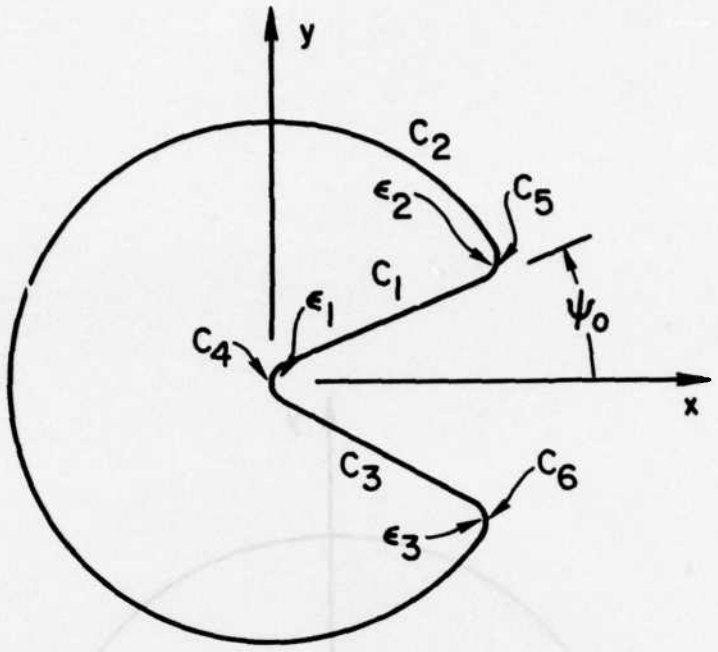

Figure 3. Modified Wedge Cracked Geometry.

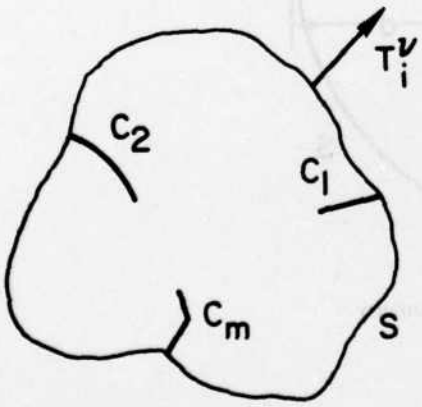

Figure 4a. General Cracked Body.

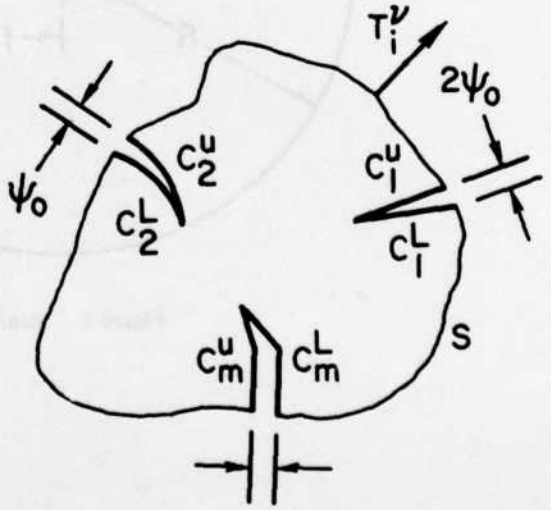

Figure 4b. Modified Cracked Body.

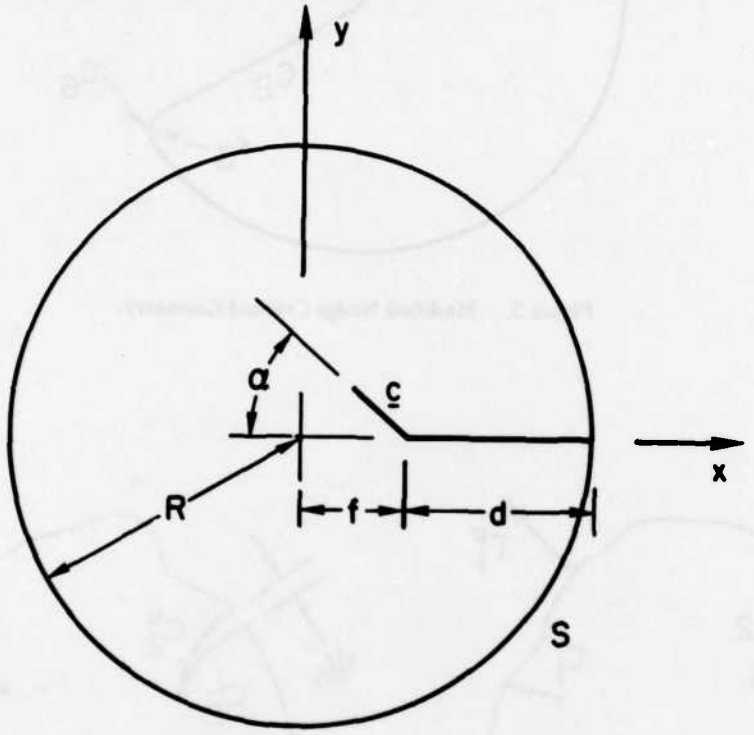

Figure 5. Bent Crack Geometry.

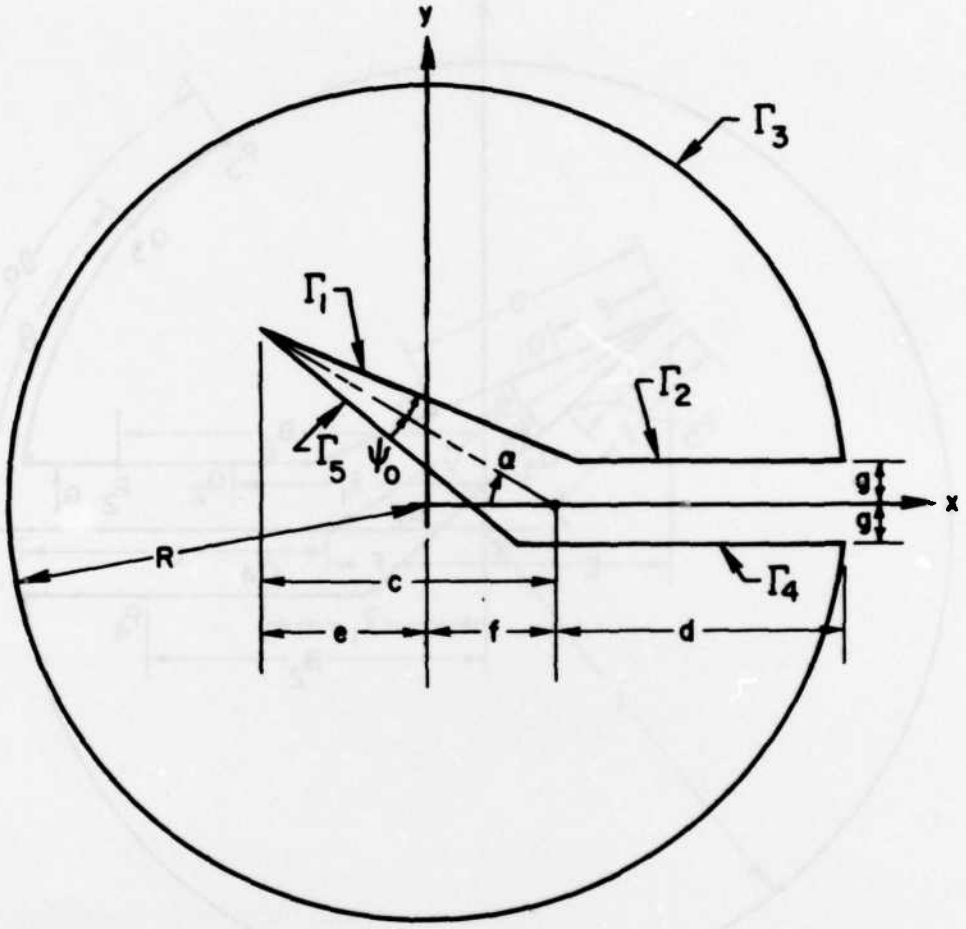

Figure 6. Modified Bent Crack Geometry.

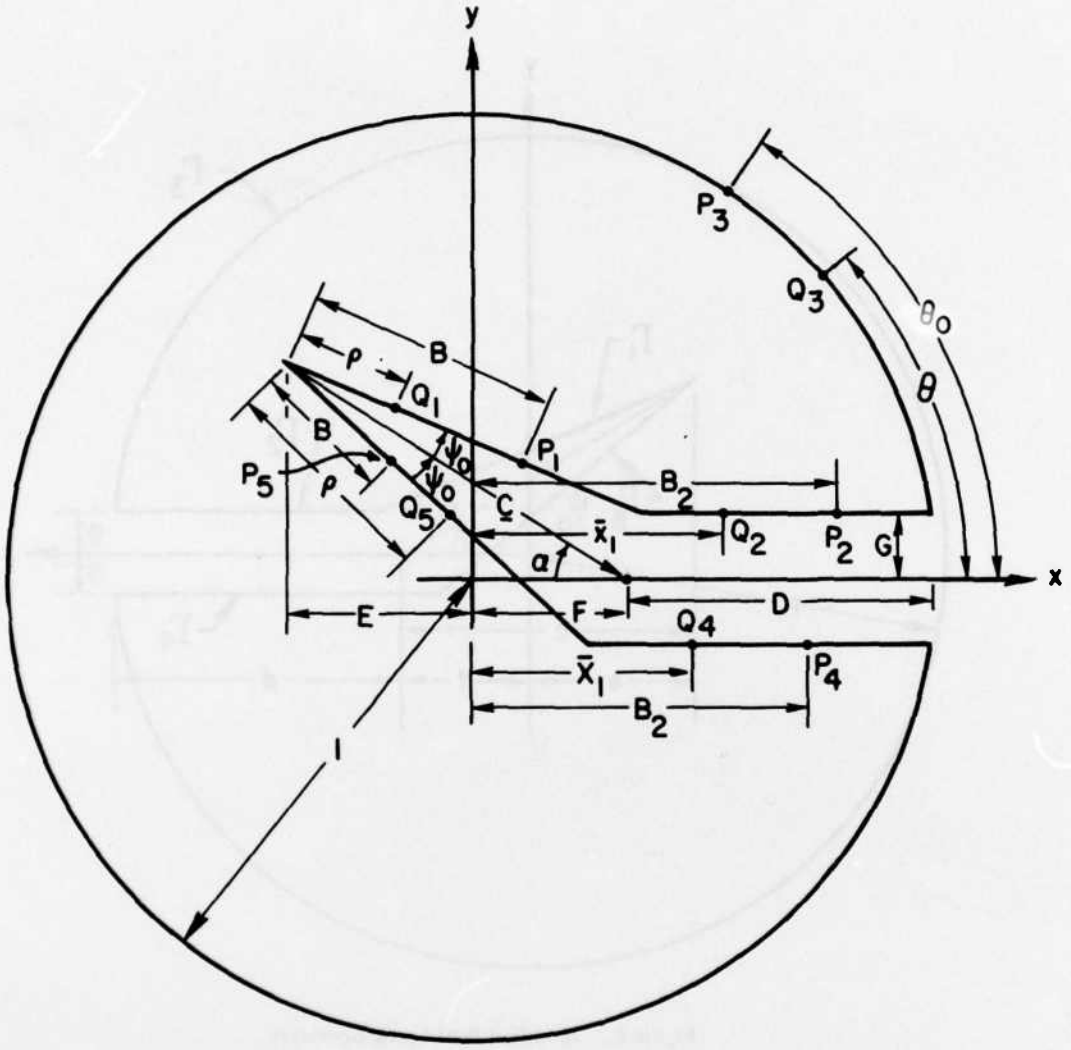

Figure 7. Bent Crack Parametric Variable Definitions Normalized Geometry.

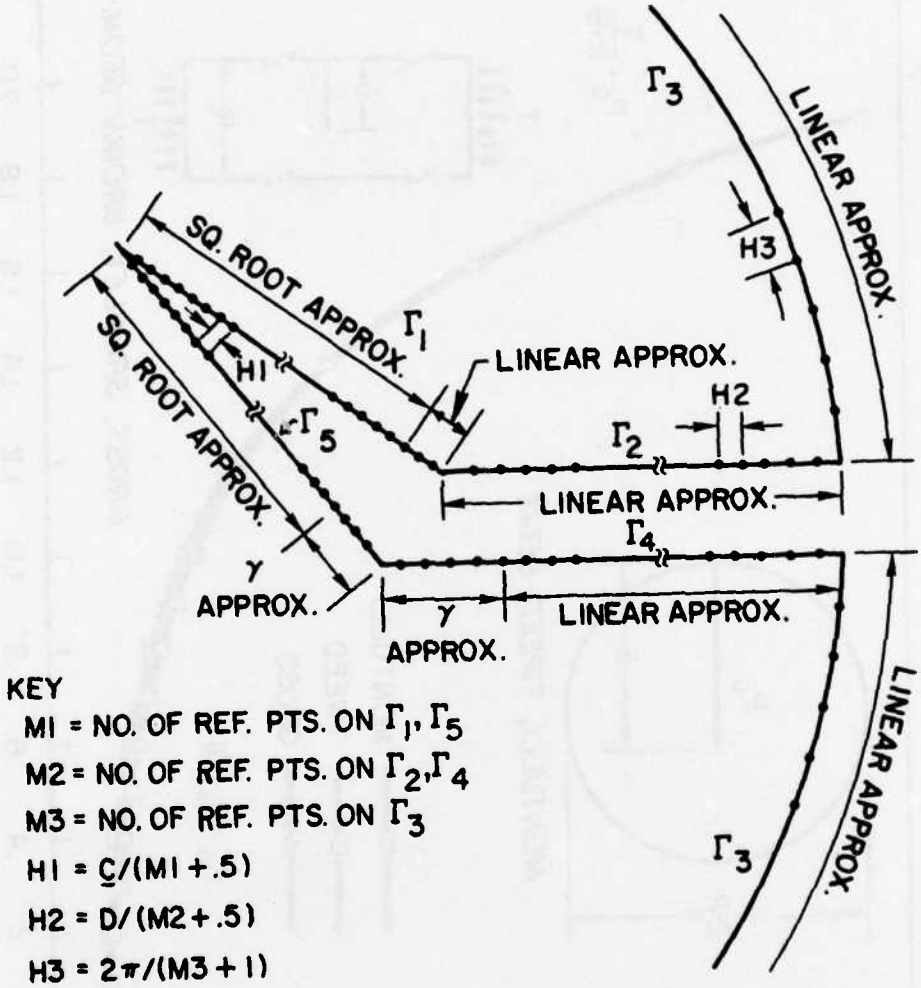

KEY

M1 = NO. OF REF. PTS. ON Γ_1, Γ_5

M2 = NO. OF REF. PTS. ON Γ_2, Γ_4

M3 = NO. OF REF. PTS. ON Γ_3

H1 = C/(M1 + .5)

H2 = D/(M2 + .5)

H3 = 2π/(M3 + 1)

Figure 8. Reference Point Locations for Bent Crack Geometry.

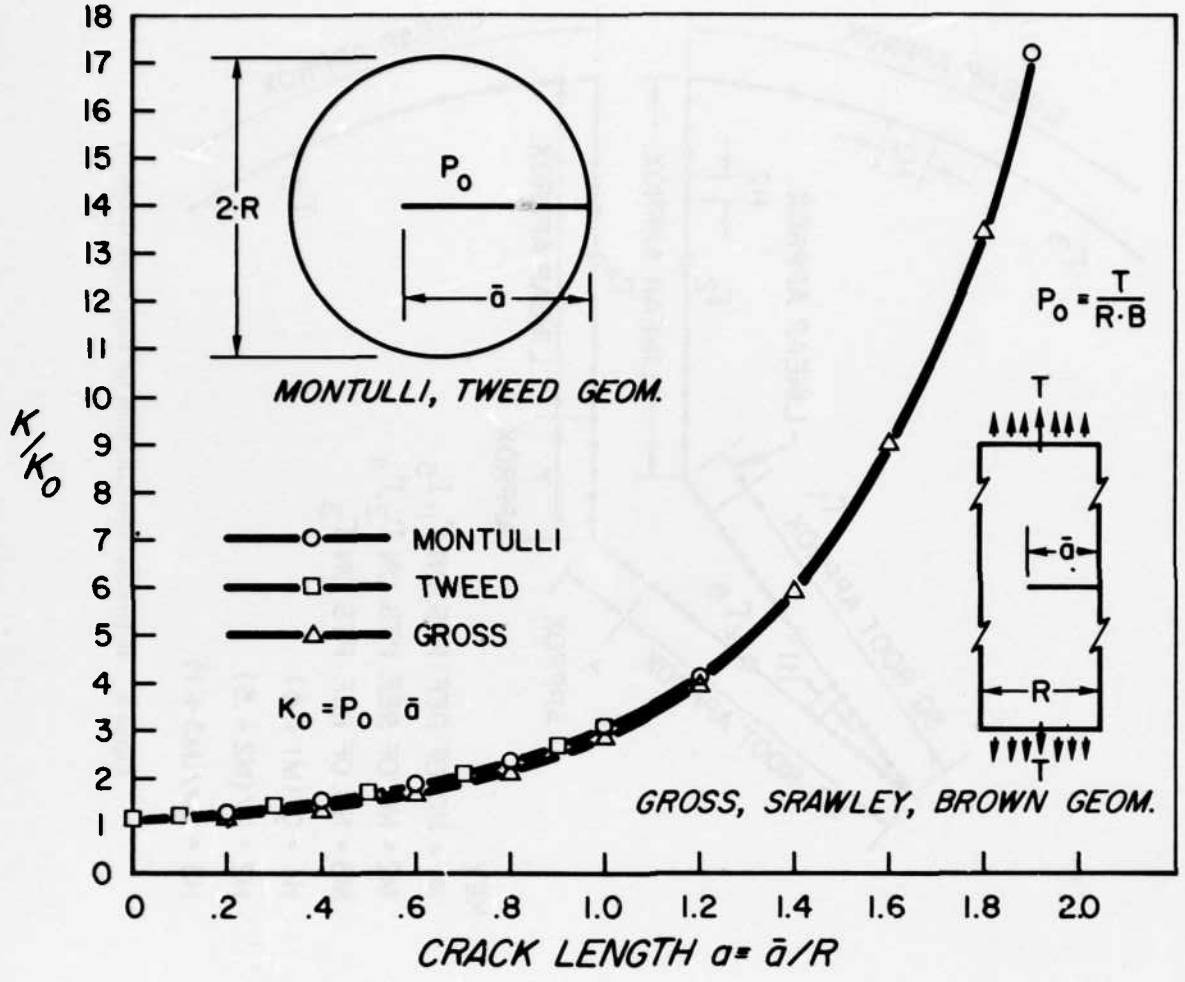

Figure 9. Pressure Loaded Crack.

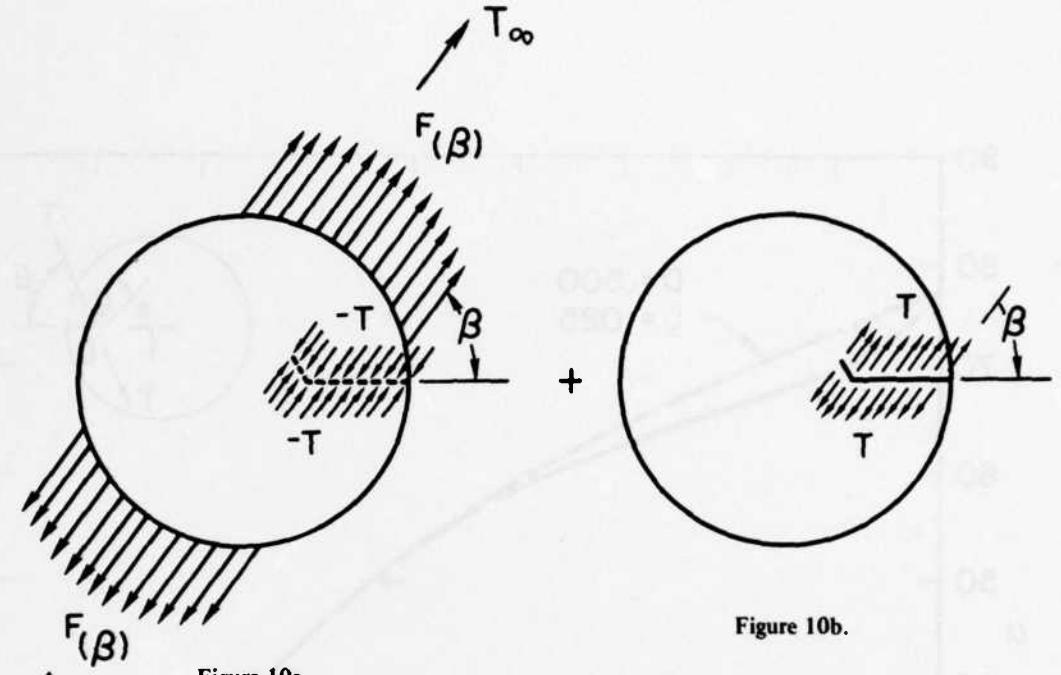

Figure 10a.

Figure 10b.

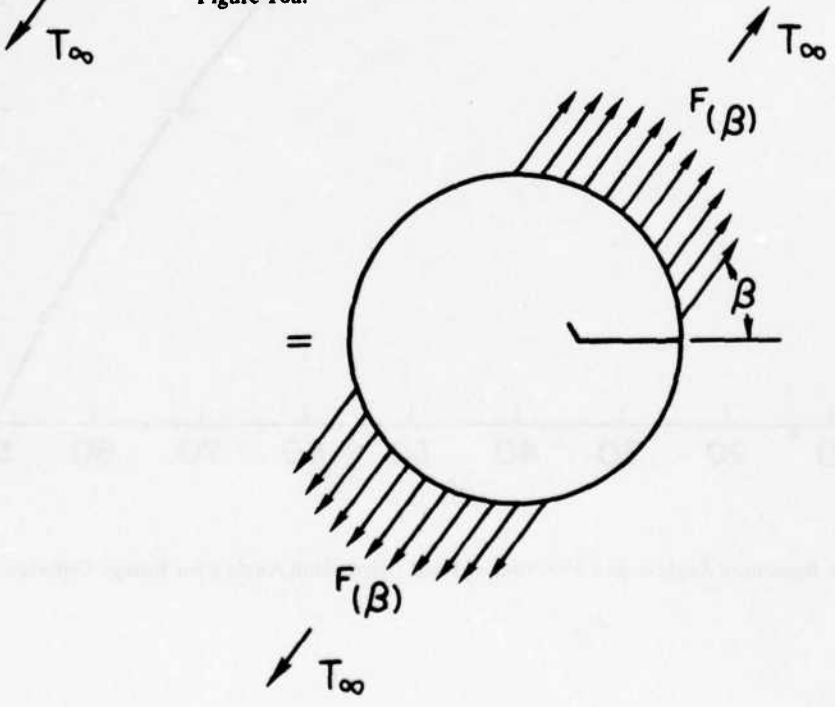

Figure 10c. Traction Loading on Bent Crack.

Figure 10. Principle of Linear Superposition.

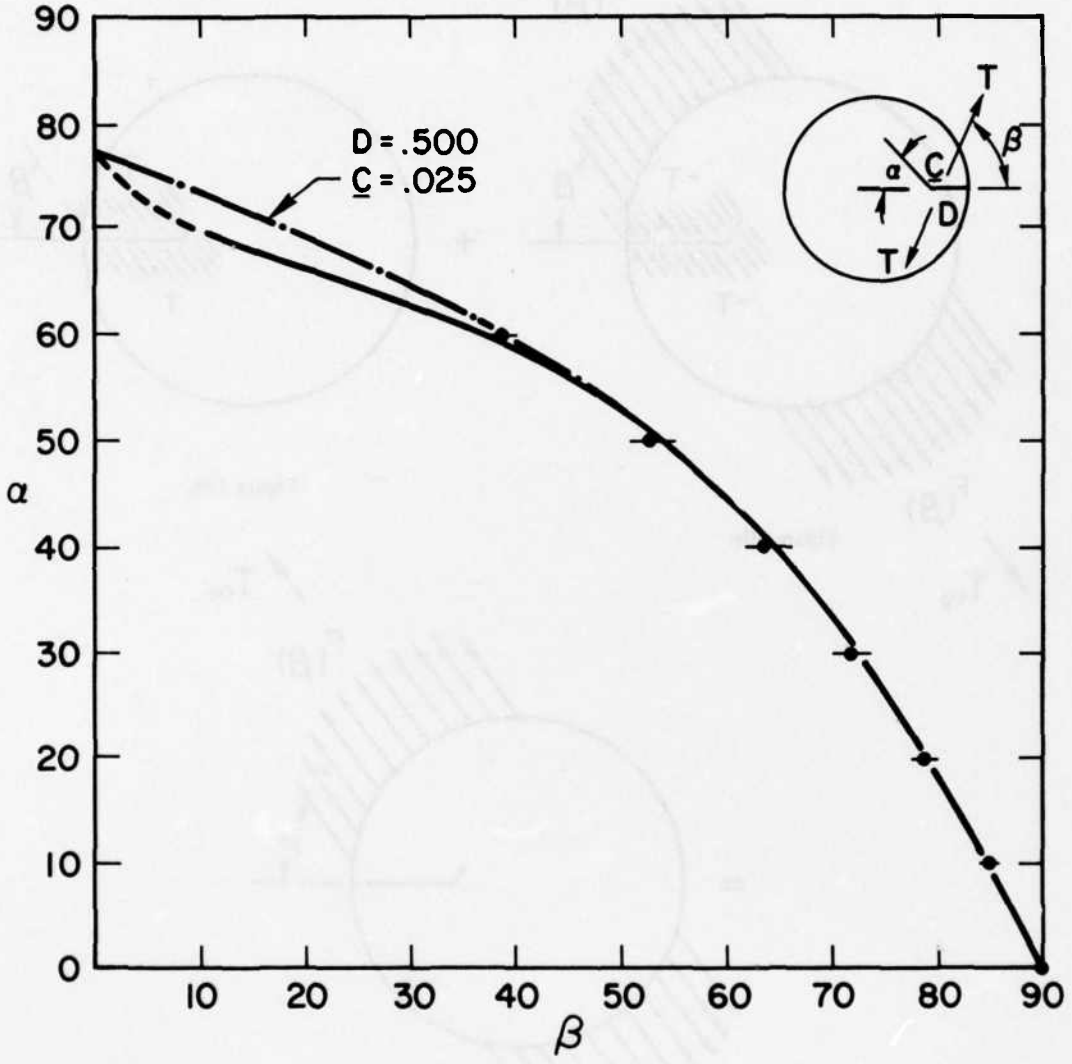

Figure 11. Crack Branching Angle α as a Function of Load Orientation Angle β for Energy Criterion.

☆ U. S. GOVERNMENT PRINTING OFFICE: 1977 — 757-001/246


ATE
LME